Drivers of the carbonate system variability in the southern North Sea: River input, anaerobic alkalinity generation in the Wadden Sea and internal processes

Dissertation zur Erlangung
des Doktorgrades der Naturwissenschaften
an der Fakultät für Mathematik, Informatik und Naturwissenschaften
im Fachbereich Geowissenschaften der Universität Hamburg

Vorgelegt von

Fabian Schwichtenberg

aus Hamburg

Hamburg, im August 2013

- Korrigierte Fassung –

Als Dissertation angenommen vom Fachbereich Geowissenschaften der Universität Hamburg auf Grund der Gutachten von Prof. Dr. Kay-Christian Emeis und Dr. Johannes Pätsch.

Tag der Disputation: 29.11.2013

Prof. Dr. Christian Betzler

Leiter des Fachbereichs Geowissenschaften

Summary

The presented work examines the carbonate system in the southern North Sea and its sensitivity to river input, anaerobic total alkalinity (TA) generation in the Wadden Sea and internal processes by using the ecosystem model ECOHAM. Furthermore, it is aimed to reproduce observations of high TA concentrations in the German Bight that could not be reproduced in former model studies. The study consists of three main parts that examine the TA production in the southern North Sea, the impact of riverine inputs on TA in the southern North Sea and the impact of TA and DIC exported from the Wadden Sea.

The TA production in the southern North Sea was examined in the first main chapter. A prognostic treatment of TA was implemented into ECOHAM that enables the calculation of TA concentration changes due to the uptake and release of nutrients into the water column as well as calcification and decalcification. It was shown that the internal processes that produced TA irreversibly were mainly driven by the uptake of allochthonous nitrate and its subsequent denitrification. In the year 2008, about 76 Gmol TA yr^{-1} (228 mmol TA m^{-2} yr^{-1}) was produced in the entire model domain (332,050 km²). Thereof, 13 Gmol TA yr^{-1} (221 mmol m^{-2} yr^{-1}) were produced in the validation area (59,338 km²). TA production in shelf seas on annual scales was also derived from denitrification rates in former studies. Therefore, the internal turnover of TA calculated in the study at hand was compared to simulated denitrification in the validation area and in the whole model domain in 2008. A total amount of 80 Gmol N yr^{-1} (241 mmol N m^{-2} yr^{-1}) was denitrified in the whole model domain, whereas 22 Gmol N yr^{-1} (370 mmol N m^{-2} yr^{-1}) was denitrified in the southern North Sea. The deviation of denitrification from TA production was also examined for the years 1977 – 2009. Denitrification exceeded the TA production in the whole model domain / southern North Sea by 13 Gmol yr^{-1} / 11 Gmol yr^{-1} on average. Furthermore, it was shown that TA production correlates with nutrient supply from rivers in the southern North Sea but observed high TA concentrations could even not be reproduced in years with high river loads of TA.

In the second main chapter it was examined whether observed high TA concentrations in the German Bight could originate from rivers. River loads of TA and DIC used in former studies were based on daily observations of freshwater discharge and on one concentration for TA and DIC for each river. Thus, these data lacked seasonal variability that can occur due to changes in riverine concentrations. Therefore, new data of river input of TA, DIC and nitrate were introduced for the main continental rivers. The level of TA concentration in the German Bight could be increased due to the increased loads of the river Rhine, but it was not possible to reproduce the observed high TA concentrations in the German Bight. Furthermore, the effective river load (Riv_{eff}) was introduced in this chapter in order to take freshwater discharges of rivers

into account and to obtain a quantity that enables a comparison with TA production in the North Sea. As a result it was shown that concentration changes caused by river inputs in the German Bight were comparable with a TA consumption of 3 Gmol yr^{-1} in 2008. Thus, the effect of dilution due to freshwater discharge dominated there. This was in contrast to the Riv_{eff} of the river Rhine, which was comparable with a TA production of 24 Gmol TA yr^{-1}.

In the third main chapter the impact of Wadden Sea exchange rates of TA and DIC on concentrations in the German Bight was examined. Therefore, sources and sinks of TA and DIC were implemented into the model that indentified the dynamic behaviour of the Wadden Sea as an area of effective production and decomposition of organic material. The respective exchange rates were calculated by using measured pelagic DIC and TA concentrations in the Wadden Sea and modelled tidal water mass exchange. It was possible to bring the simulations significantly closer to observations in summer due to the implementation of the Wadden Sea. About 40 Gmol TA yr^{-1} were exported from the Wadden Sea into the North Sea, which was lower than the first estimate by Thomas et al. (2009) who calculated about 73 Gmol TA yr^{-1} originating from the Wadden Sea. Furthermore, the interannual variabilities of TA and DIC concentrations were examined for the years 2001 – 2009, which was mainly driven by hydrodynamic conditions. It was shown that the occurrence of weak meteorological blocking situations can lead to enhanced accumulation of simulated TA in the German Bight.

In summary, it was found that the Wadden Sea was an important driver of the carbonate system variability in the southern North Sea. 68% of all TA concentration changes in the German Bight were caused by Wadden Sea export of TA, 23% were caused by the internal production of TA in the model and 9% caused by effective river loads.

Zusammenfassung

Die vorliegende Arbeit untersucht den Einfluss von Flusseinträgen, anaerober Produktion von Alkalinität (TA) im Wattenmeer und interner Prozesse auf das Karbonatsystem in der südlichen Nordsee mit Hilfe des Ökosystemmodells ECOHAM. Des Weiteren ist es das Ziel, beobachtete erhöhte TA Konzentrationen in der Deutschen Bucht mit dem Modell zu reproduzieren, was bisher in noch keiner Modellstudie gelang. Die Arbeit gliedert sich in drei Hauptteile, in denen es um die TA Produktion in der südlichen Nordsee geht, sowie um den Einfluss von Flusseinträgen auf die dortigen TA Konzentrationen und TA Exportmengen aus dem Wattenmeer.

Die TA Produktion in der südlichen Nordsee wurde im ersten Hauptkapitel behandelt. Dazu wurde eine prognostische Behandlung der TA in das Modell eingebaut, die die Berechnung von TA Konzentrationsänderungen aufgrund von Aufnahme und Abgabe von Nährstoffen aus der Wassersäule sowie Kalzifizierung und Dekalzifizierung ermöglicht. Es wurde gezeigt, dass die internen Prozesse die irreversibel TA produzieren, hauptsächlich durch die Aufnahme von allochthonem Nitrat und anschließender Denitrifizierung angetrieben werden. Ca. 76 Gmol TA yr^{-1} (228 mmol TA m^{-2} yr^{-1}) wurden im gesamten Modellgebiet (332.050 km²) produziert, davon wurden ca. 13 Gmol TA yr^{-1} (221 mmol m^{-2} yr^{-1}) im Validationsgebiet produziert. Jährliche TA Produktionsraten wurden in früheren Studien auch von Denitrifizierungsraten abgeleitet, daher wurden in der vorliegenden Studie auch die produzierte TA mit simulierten Denitrifizierungsraten im Validationsgebiet und im gesamten Modellgebiet in 2008 verglichen. Eine Gesamtmenge von 80 Gmol N yr^{-1} (241 mmol N m^{-2} yr^{-1}) wurde im gesamten Modellgebiet denitrifiziert, wohingegen 22 Gmol N yr^{-1} (370 mmol N m^{-2} yr^{-1}) im Validationsgebiet denitrifiziert wurden. Die Abweichung der Denitrifizierung von der produzierten TA wurde auch für die Jahre 1977 bis 2009 untersucht. Die Denitrifizierung überstieg die TA Produktion im gesamten Modellgebiet / im Validationsgebiet im Durchschnitt um 13 Gmol yr^{-1} / 11 Gmol yr^{-1}. Des Weiteren wurde gezeigt, dass die TA Produktion mit der Menge an Nährstoffen korreliert, die über die Flüsse in die südliche Nordsee eingetragen werden. Allerdings konnten die beobachteten hohen TA Konzentrationen auch in Jahren mit hohem Nährstoffeintrag nicht reproduziert werden.

Im zweiten Hauptkapitel wurde untersucht, ob die beobachteten hohen TA Konzentrationen in der Deutschen Bucht von Flüssen stammen können. Flussfrachten, die in früheren Studien verwendet wurden, basierten auf täglichen Beobachtungen von Abflussmengen und jeweils einem Wert für TA und DIC Konzentrationen für jeden Fluss. Daher werden Variationen der Flussfrachten auf Grundlage von Konzentrationsänderungen in diesen Studien vernachlässigt. Aus diesem Grund wurden in diesem Kapitel neue Flussfrachten für die größten kontinentalen

Flüsse eingeführt. Das Niveau der TA Konzentration in der Deutschen Bucht wurde mit den neuen Flussfrachten des Rheins erhöht, allerdings war es nicht möglich die beobachteten hohen TA Konzentrationen in der Deutschen Bucht zu reproduzieren. Des Weiteren wurden die effektiven Flussfrachten (Riv_{eff}) in diesem Kapitel eingeführt, um auch Abflussmengen von Süßwasser aus den Flüssen zu berücksichtigen, und um eine Größe zu erhalten mit der es möglich ist die internen Prozesse mit Flussfrachten von TA zu vergleichen. Es konnte für das Jahr 2008 gezeigt werden, dass der Einfluss von Flusseinträgen in der Deutschen Bucht vergleichbar ist mit einer Abnahme von TA um 3 Gmol yr^{-1} und damit der Verdünnungseffekt durch den Abfluss von Süßwasser dominiert. Im Gegensatz dazu ist der Einfluss des effektiven Flusseintrags von TA des Rheins vergleichbar mit einer TA Produktion von 24 Gmol yr^{-1}.

Im dritten Hauptkapitel wurde der Einfluss von TA und DIC Exportraten aus dem Wattenmeer auf die Deutsche Bucht untersucht. Dazu wurden Quellen und Senken von TA und DIC in das Modell eingebaut, die das dynamische Verhalten des Wattenmeeres als ein Gebiet von effektiver Produktion und Abbau von organischem Material darstellen. Die entsprechenden Austauschraten wurden auf Grundlage von gemessenen pelagischen TA und DIC Konzentrationen im Wattenmeer und modellierten Tidenprismen berechnet. Es war möglich die Simulationen signifikant näher an die beobachteten TA Konzentrationen zu bringen. Ca. 40 Gmol TA yr^{-1} wurden aus dem Wattenmeer in die Nordsee exportiert, weniger als die erste Abschätzung über 73 Gmol TA yr^{-1} von Thomas et al. (2009). Weiterhin wurden die zwischenjährlichen Variabilitäten von TA und DIC Konzentrationen für die Jahre 2001 – 2009 untersucht, die hauptsächlich aufgrund von unterschiedlichen hydrodynamischen Bedingungen hervorgerufen wurden. Es wurde in den Modellrechnungen gezeigt, dass das Aufkommen von schwachen meteorologischen Blocksituationen zu einer erhöhten Akkumulierung von TA in der Deutschen Bucht führt.

Zusammengefasst wurde herausgefunden, dass das Wattenmeer eine wichtige Triebkraft des Karbonatsystems in der südlichen Nordsee war. 68% aller Änderungen in den TA Konzentrationen in der Deutschen Bucht wurden durch das Wattenmeer hervorgerufen, 23% durch interne Prozesse im Modell und 9% durch effektive Flusseinträge.

Contents

1 Introduction

Since the industrial revolution the consumption of fossil fuels increases steadily. The additional release of CO_2 into the atmosphere might lead to changes in the global heat budget und hence in the climate system of the earth (IPCC, 2001). Today about 30% of current CO_2 emissions are taken up by the oceans (Sabine et al. 2004), which corresponds to about 2.2 GtC yr^{-1} on an average. Thus, the world's oceans help to moderate climate change but the consequently rising oceanic CO_2 concentrations causes an ongoing acidification of the marine environment (Jacobsen, 2005). Up to now, the pH of surface ocean waters has fallen by approximately 0.1 pH units representing an increase of almost 30% in H^+ concentration. If CO_2 emissions continue to rise, the resulting changes in seawater chemistry, namely in the carbonate system, will expose marine organisms to conditions never experienced before during their evolutionary history (Raven et al., 2005). Especially calcifying organisms like corals or coccolithophores are expected to be affected (Kleypas et al., 2006). Furthermore, it was observed by Ilyina et al. (2010) that the propagation of noise in the ocean is also affected by ocean acidification, because of the ability of seawater to absorb sound decreases with decreasing pH values. This may influence the communication of marine mammals. As a consequence, there is an increasing risk of losses in biodiversity and significant ecological and functional shifts (Fabry et al., 2008; Kroeker et al., 2010). In addition to these ecological threats, recent findings suggested that the ocean's capacity of further CO_2 uptake is weakening (Doney et al., 2009; Sabine & Tanhua, 2010) and thus the ability to mitigate climate change. Therefore, it is essential to understand the biogeochemical processes that affect the further evolution of the carbonate system in the ocean.

1.1 The carbonate system

A detailed description of the carbonate system is given in the textbook of Zeebe & Wolf-Gladrow (2001) but some aspects should be briefly explained here: The carbonate system is defined by six variables: CO_2, HCO_3^-, CO_3^{2-}, H_3O^+, dissolved inorganic carbon (DIC) and total alkalinity (TA). If there are any two variables given (together with temperature and salinity), one may calculate the others (Deffeyes, 1965, Park, 1969). DIC and TA are conservative with respect to mixing and changes in temperature and pressure, and are thus most qualified to calculate the remaining variables of the carbonate system (Wolf-Gladrow, 2007). CO_2 uptake by

seawater depends on the buffering capacity, which is defined as the Revelle factor (Revelle & Suess, 1957). It is linked to the ratio of DIC and TA (Broecker & Peng, 1982). The CO_2 partial pressure (pCO_2) is determined as the balance between DIC and TA (Frankignoulle, 1994; Millero, 2001; Egleston et al., 2010) and the pCO_2 gradient controls the direction of CO_2 flux. In general, CO_2 dissolves in seawater if the partial pressure in the atmosphere is higher than the partial pressure in seawater, which can be reduced by biological drawdown and increased by respiration. The additionally dissolved CO_2 changes the chemical equilibrium of the carbonate system and lowers pH. This is expressed by the two equations describing the equilibrium of the carbonate system:

$$CO_2 + 2H_2O \Leftrightarrow HCO_3^- + H_3O^+$$
$$HCO_3^- + H_2O \Leftrightarrow CO_3^{2-} + H_3O^+$$

The equilibrium is also temperature-, pressure- and salinity-dependent. Altogether, DIC and TA are the most important parameters of the carbonate system with respect to ocean acidification and buffering CO_2 emissions. DIC and TA are also suitable for biogeochemical tracers in numerical models due to their conservative characteristics.

The definition of DIC as the sum of CO_2, HCO_3^- and CO_3^{2-} is easy to understand compared to the definition of TA. The historical development of the TA concept was discussed by Dickson (1992). The alkaline characteristic of seawater and its large amounts of DIC that could be released in the form of CO_2 by titration with a strong acid was already known in the 19th century. A connection between salt and DIC was already supposed e.g. by Jacobsen (1873) but a clear concept of TA was still missing due to the lacks of knowledge of the form of salts in aqueous solutions (ions) and of advanced concepts of acids and bases (Bronsted, 1923). Rakestraw (1949) was the first whose expression of TA considered bicarbonate, carbonate ion and borate. Before then, alkalinity was defined operationally without knowledge of the chemical species that are responsible for the observed neutralization during titration. Nevertheless, Rakestraw's expression was only a first estimate of the recent definition given by Dickson (1981). He defined TA as the excess of proton acceptors over proton donors with respect to a certain zero level of protons for each acid-base system (see chapter 2 for a further description). It could be written for seawater as follows:

$$\begin{aligned} TA = {} & [HCO_3^-] + 2[CO_3^{2-}] + [B(OH)_4^-] + [OH^-] + [HPO_4^{2-}] \\ & + 2[PO_4^{3-}] + [H_3SiO_4^-] + [NH_3] + [HS^-] \\ & - [H^+] - [HSO_4^-] - [HF] - [H_3PO_4] \end{aligned}$$

However, several different definitions of TA can still be found in textbooks, which may lead to confusion (Wolf-Gladrow, 2007).

Several processes lead to changes of TA in the ocean. TA is closely related to salinity and the corresponding processes such as precipitation, evaporation, fresh water input and formation and melting of sea ice (Zeebe & Wolf-Gladrow, 2001). Additionally, there are also biogeochemical processes that change TA. The impact of calcium carbonate precipitation and dissolution on alkalinity can be directly explained by Dickson's expression due to changes in carbonate and bicarbonate ions:

$$Ca^{2+} + 2HCO_3^- \Leftrightarrow CaCO_3 + CO_2 + H_2O$$

$$Ca^{2+} + CO_3^{2-} \Leftrightarrow CaCO_3$$

Changes of TA due to the assimilation of nitrate and ammonia by plants were investigated by Brewer & Goldman (1976) and Goldman & Brewer (1980). In contrast to calcium carbonate related processes, the impact of changes in nutrient concentrations on TA has to be explained by the 'nutrient-H^+-compensation principle' that was introduced by Wolf-Gladrow et al. (2007). Although nitrate and ammonium are no part of Dickson's TA definition their uptake or release by algae results in changes of TA in the respective environment. The absorbing cell has to maintain electroneutrality so e.g. an uptake of one molecule of nitrate is accompanied with the uptake of one proton (symport) or a release of one hydroxide ion (antiport) that both are part of Dickson's definition. Wolf-Gladrow et al. (2007) introduced an equivalent expression to Dickson's definition of TA that is called 'the explicit conservative form of total alkalinity' (TA_{ec}). It enables to explain changes of TA due to nutrient assimilation and other biogeochemical processes in a simple way. The foundation of this expression is the assumption of electroneutrality of aqueous solutions, so that the sum of all charges is zero. If the equation of Dickson's expression is rearranged the expression for TA_{ec} reads as follows (see chapter 2 for a further description):

$$\begin{aligned}
&\left[Na^+\right] + 2\left[Mg^{2+}\right] + 2\left[Ca^{2+}\right] + \left[K^+\right] + 2\left[Sr^{2+}\right] + ... \\
&- \left[Cl^-\right] - \left[Br^-\right] - \left[NO_3^-\right] - ...TPO_4 \\
&+ TNH_3 - 2TSO_4 - THF - THNO_2 \\
&= TA_{ec}
\end{aligned}$$

On a global scale, calcium carbonate dissolution and precipitation are the dominant processes with respect to TA inventory (e.g. Chung et al., 2003; Berelson et al., 2007). TA production can be related to carbonate dissolution in shallow and deep sea calcareous sediments (e.g. Jahnke et al., 1994; Berelson et al., 1996; Martin & Sayles, 1996).

1.2 The impact of ocean margin anaerobic processes on alkalinity budget

Shelf seas are highly productive and the interface between the anthropogenically influenced coastal areas and the global ocean. They represent only about 7.6% of the global ocean's area, but current estimates assume that they contribute approximately 21% of total global ocean CO_2 sequestration (Borges, 2011). The uncertainties of these estimates are high due to the lack of data on a global scale but some studies investigated the carbon cycles on regional scales in more detail (Thomas et al., 2009; Artioli et al., 2012; Lorkowski et al., 2012). Besides that, pH variations in coastal- and shelf regions can be up to an order of magnitude higher than in the open ocean (Provoost et al, 2010). The nearshore effects of acidification and CO_2 uptake are difficult to determine, because of the shallow water column and the tight coupling to the benthic environment. Strong variations in fluxes of TA exist in association with inflow of nutrients from rivers and from pore water exchange in sediments.

Berner et al. (1970) were one of the first who investigated elevated TA in anoxic pore water sediments due to sulphate reduction. Further studies were also conducted in the 1990s in Tomales Bay at the Californian coast (Dollar et al., 1991; Smith & Hollibaugh, 1993; Chambers et al., 1994). In this area, the observed enhanced TA export was related to the burial of reduced sulphur compounds (pyrite). Other studies conducted in the Satilla and Altamaha estuaries and the adjacent continental shelf found nonconservative mixing lines of TA versus salinity, which was attributed to anaerobic TA production in nearshore sediments (Wang & Cai, 2004; Cai et al., 2010).

The ocean's ability to buffer ocean acidification and its capacity to absorb atmospheric CO_2 provoked recent discussions about the magnitude of ocean margin TA production due to anaerobic processes. Chen (2002) suggested that TA is produced at a rate of 16 – 31 Tmol yr^{-1} due to anaerobic processes in ocean margins. He also stated that this amount of anaerobically produced TA may contribute to upper ocean excess TA, whereas this was previously related to biology-mediated carbon dissolution (Milliman et al., 1999). Nevertheless, the estimations of Chen (2002) were based on incomplete redox cycles of nitrogen, sulphur and metals and their internal cycling. Hence, it is likely that they overestimated the TA production in global ocean margins. In this context, Hu & Cai (2011) stated that irreversible anaerobic TA production and consumption can only be attributed to the permanent loss of anaerobic remineralisation products. These are nitrogen gas from denitrification and reduced sulphur buried as pyrite. However, denitrification does only contribute to irreversible net TA production if it is fuelled by allochthonous nitrate (Hu & Cai, 2011). Hu & Cai (2011) recalculated the TA production in global ocean margins and estimated about 4 – 5 Tmol yr^{-1} that included continental shelves and

oxygen minimum zones near the continental margins. The latter contribute to net TA production due to anaerobic ammonia oxidation (anammox), which removes fixed nitrogen in addition to the canonical denitrification (Hulth et al., 2005; Lam et al., 2009). Furthermore, pyrite burial in coastal habitats (salt marshes, mangroves, seagrass meadows) contribute another 0.1 – 1.1 Tmol yr^{-1} to the TA production rate calculated by Hu & Cai (2011), resulting in a total TA production of about 4 – 6 Tmol yr^{-1}.

1.3 The North Sea as study site

The focus of the study at hand is on the southern North Sea located on the Northwest European Shelf. The general circulation pattern is shown in Fig. 1.1. Atlantic water enters the North Sea in the northern part and to a lesser extent in the south via the English Channel. The circulation pattern is anticlockwise in general. The shallower southern part of the North Sea is dominated by Channel water, continental coastal water and to a lesser extent by southern North Sea water. A strong tidal forcing (M2 tide) enhances the mixing in the southern North Sea, which is nearly always well mixed (Otto et al., 1990) in contrast to the northern part, which is exposed to seasonal stratification. The Wadden Sea system of the southern North Sea extends from Den Helder (Netherland) in the west to Esbjerg (Denmark) in the north covering an area of about 9500 km^2 (Ehlers, 1994). Barrier islands form a boundary between the Wadden Sea and the open North Sea and deep inlet channels between them enable water and material exchange with the open North Sea. The entire Wadden Sea system is characterised by semidiurnal tides with a tidal range between 1.5 m in the most westerly part and 4 m in the estuaries of the rivers Weser and Elbe (Streif, 1990). The North Sea is intensely used by humans for energy production, as a recreational area or as a food source. Especially the latter economic interest relies on a healthy ecosystem that might be threatened by climate change and ocean acidification.

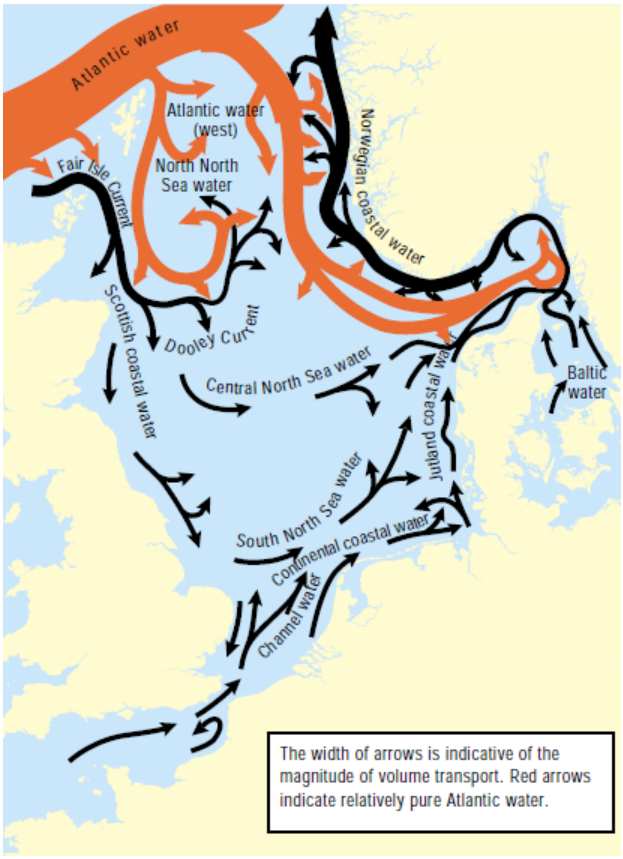

Fig. 1.1: Schematic diagram of general circulation pattern in the North Sea after Turrell et al. (1992). Source: OSPAR (2000).

The North Sea was subject to some recent studies of the carbonate system. Lorkowski et al. (2012) focused on the interannual variability of the air-sea flux of CO_2 between the ocean and atmosphere and on the carbon shelf pump in the North Sea in the period of 1970 to 2006. The latter transports CO_2 that was taken up from the atmosphere into deeper waters of the adjacent ocean via mixing and lateral advection. Lorkowski et al. (2012) stated that the North Sea acts as a sink for atmospheric CO_2 and absorbs in the mean about 1.31 mol C m^{-2} yr^{-1}. Artioli et al. (2012) focused on the sensitivity of the carbonate system in the North Sea and on reproducing pH and pCO_2 observations. They applied a semi-prognostic treatment of TA by calculating a diagnostic, salinity-dependent part of TA and a prognostic part of TA that depended on the uptake and release of nutrients, calcification and decalcification. This model approach was suitable for investigations of sensitivities of the carbonate system in terms of carbon uptake and acidification. Field measurements of the carbonate system in the North Sea were described by Thomas et al. (2009) for 2001 and 2002 and by Salt et al. (subm.) for 2008. Both measurements were part of the CANOBA program, where samples were taken at the same stations covering the whole North Sea. In comparison to the central and northern part of the North Sea, TA concentrations in the German Bight were significantly elevated in summer in both campaigns. Thomas et al. (2009) related the observed high TA concentrations in summer to TA originating

in the Wadden Sea. They calculated the annual TA export from the Wadden Sea into the North Sea to be about 73 Gmol TA yr^{-1} and related it to enhanced anaerobic degradation of organic material in summer. In this context, van Beusekom et al. (2012) recently stated that the eutrophication status of a tidal basin depends on its size. A wider tidal basin (distance between barrier island and mainland) has a lower eutrophication status than a narrower tidal basin due to "dilution" effects of the imported organic material in wider tidal basins.

1.4 Research gaps

The Wadden Sea TA export calculated by Thomas et al. (2009) was defined as closing term in the budget. However, three main inconsistencies arise upon closer inspection of the other TA sources mainly related to denitrification and riverine input of bulk TA.

1. Thomas et al. (2009) considered the fact that only the permanent loss of anaerobic remineralisation products can contribute to net TA production. Thus, they derived annual TA production rates in the North Sea (without Wadden Sea) from simulated denitrification rates (Pätsch & Kühn, 2008). This approach may overestimate the annual TA production rate, because only denitrification of allochthonous nitrate changes net TA (Hu & Cai, 2011). In the North Sea (without the Wadden Sea), benthic denitrification is mainly fuelled by nitrate produced during nitrification in the upper layer of the sediment (Raaphorst et al., 1990; Seitzinger & Giblin, 1996; Pätsch & Kühn, 2008). This coupling of benthic nitrification and denitrification does not change TA in total (Hu & Cai, 2011). Hence, net TA is only produced by denitrification if it is fuelled by allochthonous nitrate either directly by pelagic nitrate invading the sediment or taken up by phytoplankton prior to denitrification. The overestimation of TA production caused by denitrification in the budgeting of Thomas et al. (2009) occurred mainly due to nitrogen entering the study site as total organic nitrogen (TON) e.g. via rivers. Furthermore, they included denitrification of atmospherically deposited nitrogen in their budgeting, which does not change net TA either (Hu & Cai, 2011).

2. Another point is that Thomas et al. (2009) considered river input data that lack seasonal variability in their TA and DIC concentrations (Pätsch & Lenhart, 2008). That implies that temporally resolved riverine input may potentially explain the observed high TA concentrations in the German Bight in summer, because riverine seasonality of TA was neglected.

3. The amount of Wadden Sea export TA calculated by Thomas et al. (2009) was also based on flushing times in the German Bight. They considered a mean value of six

weeks for their calculations (Lenhart et al., 1995) but neglected possible higher times in summer due to weaker currents in the German Bight in that time. Higher flushing times in their calculations would reduce the amount of calculated TA export rates.

Altogether, there are substantial simplifications in the TA budgeting of Thomas et al. (2009) that need further investigations in order to estimate the impact of anaerobic processes on TA production and the carbonate system in the southern North Sea. Subsequent model studies by Lorkowski et al. (2012) and Artioli et al. (2012) could not yet reproduce the high TA concentrations that occurred in the German Bight. The model study of Lorkowski et al. (2012) lacked an appropriate treatment of TA because simulated TA concentrations were restored to prescribed interpolated values from observations in 2001 and 2002 (Thomas et al., 2009) with a relaxation time of two weeks. As a consequence, the impact of biogeochemical processes on TA was missed and thus an important driver of the carbonate system was neglected. Artioli et al. (2012) considered TA changes caused by the uptake and release of nutrients and calcite-related processes but they could not reproduce TA in the German Bight. Both model studies considered riverine TA and DIC loads based on the report of Pätsch & Lenhart (2008). As a consequence, seasonal variations in riverine TA and DIC concentrations were neglected in both studies. Finally, it has to be pointed out that no model study of the North Sea considered Wadden Sea TA and DIC exports yet.

1.5 The contribution of this study

The main aim of this study is to investigate the impact of anaerobic processes on TA in the southern North Sea and to calculate the amount of TA that is exported from the Wadden Sea into the North Sea. The above mentioned research gaps induce the following questions that will be answered in this study:

- Which processes dominate the TA turnover (production – consumption) in the southern North Sea?
- TA production was often derived from denitrification rates (e.g. Chen, 2002; Thomas et al., 2009). What are the temporal and spatial deviations between the amount of denitrification and actually produced TA?
- At which spatial scales is it adequate to use denitrification rates as an estimate for TA production in the North Sea?
- Can enhanced river loads of nutrients induce a significantly higher TA turnover that can explain the high TA concentrations observed in the German Bight?

- Can seasonal variations in river loads of bulk TA be the origin of high TA concentrations observed in the German Bight?

- Do loads of the river Rhine affect TA concentrations or the TA turnover in the German Bight significantly?

- What is the dominant driver of TA concentrations in the southern North Sea and what drives their interannual variability?

- Are there regional differences in TA exported from the Wadden Sea into the North Sea?

The ecosystem model ECOHAM (ECOlogical model HAMburg) (Lorkowski et al., 2012) is used and further developed in this study to answer these questions. The following chapters are stand-alone studies but also aspects of one single study. The first chapter deals with the internal turnover of TA induced by the uptake and release of nutrients out of and into the water column and calcite-related processes. Therefore, a prognostic treatment of TA is introduced in this chapter that enables the calculation of TA due to biogeochemical and physical processes. Denitrification rates are compared with produced TA in the period of 1977 to 2009 and especially in the year 2008. Only the river loads of nutrients and their impact on TA turnover in the German Bight are examined in this chapter. Additionally, an area for validation is introduced in that chapter that is used for validation in every chapter.

River loads of bulk TA and their impact on TA concentrations in the southern North Sea are examined in chapter 3. In contrast to chapter 2, chapter 3 deals mainly with riverine bulk TA. New river loads of bulk TA and DIC are introduced into the model that are based on monthly mean concentrations of TA and DIC. An effective river load (Riv_{eff}) is defined in this chapter. This quantity incorporates the effect of dilution by freshwater discharge onto river inputs. Hence, it is possible to compare the impact of river loads and internal turnover of TA on TA concentration changes.

In chapter 4, sources and sinks of TA are implemented into the model that identify the dynamic behavior of the Wadden Sea as an area of effective production and decomposition of organic material. The exchange rates are based on measured pelagic TA and DIC concentrations in the Wadden Sea and modeled tidal water mass exchange. The TA and DIC export rates from the Wadden Sea into North Sea are calculated in this chapter. Simulated scenarios of every chapter are validated with observations and it is assessed whether it is possible to reproduce the observations. Furthermore, seasonal and interannual variabilites of these scenarios are examined here. Finally, a seasonal TA budget for the year 2008 and an interannual budget in the period of 2001 to 2009 are compiled for the scenario closest to observations.

2 Turnover of total alkalinity in the southern North Sea and benthic denitrification

2.1 Introduction

Changes in TA concentrations in coastal environments underlie different biogeochemical processes such as calcification and decalcification as well as the uptake and release of nutrients into the water column (Wolf-Gladrow et al., 2007). Many of these processes are reversible on short to medium spatial and temporal scales and thus do not change the irreversible production of net TA that can get exported to the open ocean (Hu & Cai, 2011). Only the permanent loss of anaerobic remineralisation products could contribute to the production of net TA on larger scales. For that reason, former studies derived biogeochemical TA production on the shelf from denitrification rates (e.g. Chen & Wang, 1999; Chen, 2002; Thomas et al., 2009). This is an appropriate way if approximations of annual TA budgets are intended.

Nevertheless, more precise calculations of TA concentrations during the course of a year can not be based on denitrification rates alone. For instance, a depletion of nutrients during phytoplankton blooms causes a rapid increase of TA production rates on relatively short time scales (Wolf-Gladrow, 2007). The organically bound nitrogen can be remineralised and nitrified either in the water column or in the benthos. In the North Sea, benthic denitrification is mainly fuelled by nitrate produced during nitrification in the upper layer of the sediment (Raaphorst et al., 1990; Seitzinger & Giblin, 1996; Pätsch & Kühn, 2008). This coupling of benthic nitrification and denitrification does not change TA in total because the ammonification of 1 mol nitrogen increases TA by 1 mol, nitrification of 1 mol ammonium decreases TA by 2 mol and finally denitrification of 1 mol nitrate increases TA by 1 mol (Hu & Cai, 2011). Consequently, estimations of nitrogen-related North Sea TA budgets that only consider denitrification for TA changes reveal inconsistencies due to two main reasons:

1. Only the denitrification of allochthonous nitrate (in small quantities also ammonium) can produce (consume) net TA irreversibly (Hu & Cai, 2011). The denitrification of organically bound nitrogen does not change TA if it enters the North Sea e.g. by river

input. Thus, annual TA budgets based on denitrification rates overestimate the net TA production.

2. Benthic denitrification is mainly fuelled by nitrification in upper sediment layers. Most of the allochthonous nitrate was taken up by phytoplankton prior to denitrification. In fact, this means that most of net TA is already produced prior to denitrification. If only denitrification rates of small areas were examined it is likely that their contribution to the North Sea TA budget will be miscalculated because denitrification and TA production itself can take place separately.

The first aim of this chapter is to have a closer look on TA production rates, the underlying processes and the resulting TA concentrations in the southern North Sea during the course of the year. Therefore, a prognostic treatment of TA was implemented into the biogeochemical model ECOHAM that enables calculations of TA concentrations due to calcification and decalcification as well as uptake and release of nutrients into the water column. The calculated turnover rates of TA were compared to denitrification rates in order to estimate their spatiotemporal deviations. It should be assessed at which spatial and temporal scales it is adequate to use denitrification rates as a shortcut for TA budgets in the southern North Sea. For this purpose, the year 2008 was examined exemplarily. Furthermore, annual budgets of internal TA turnover and denitrification rates were compared for the years 1977 to 2009.

The second aim of this chapter is to examine the impact of different river loads of nitrate and ammonium on the TA turnover rate. Thomas et al. (2009) observed high TA concentrations in the German Bight in summer 2001 that could also be observed in summer 2008 (Salt et al., subm.). These findings could not be reproduced by this model setup in the respective years but it should be estimated if high river loads could induce high TA turnover rates that increase TA concentrations in the German Bight significantly. Therefore, three years simulated in the period of 1977 to 2009 with high river loads were examined as well as one year with low river loads.

2.2 Methods

2.2.1 Model description

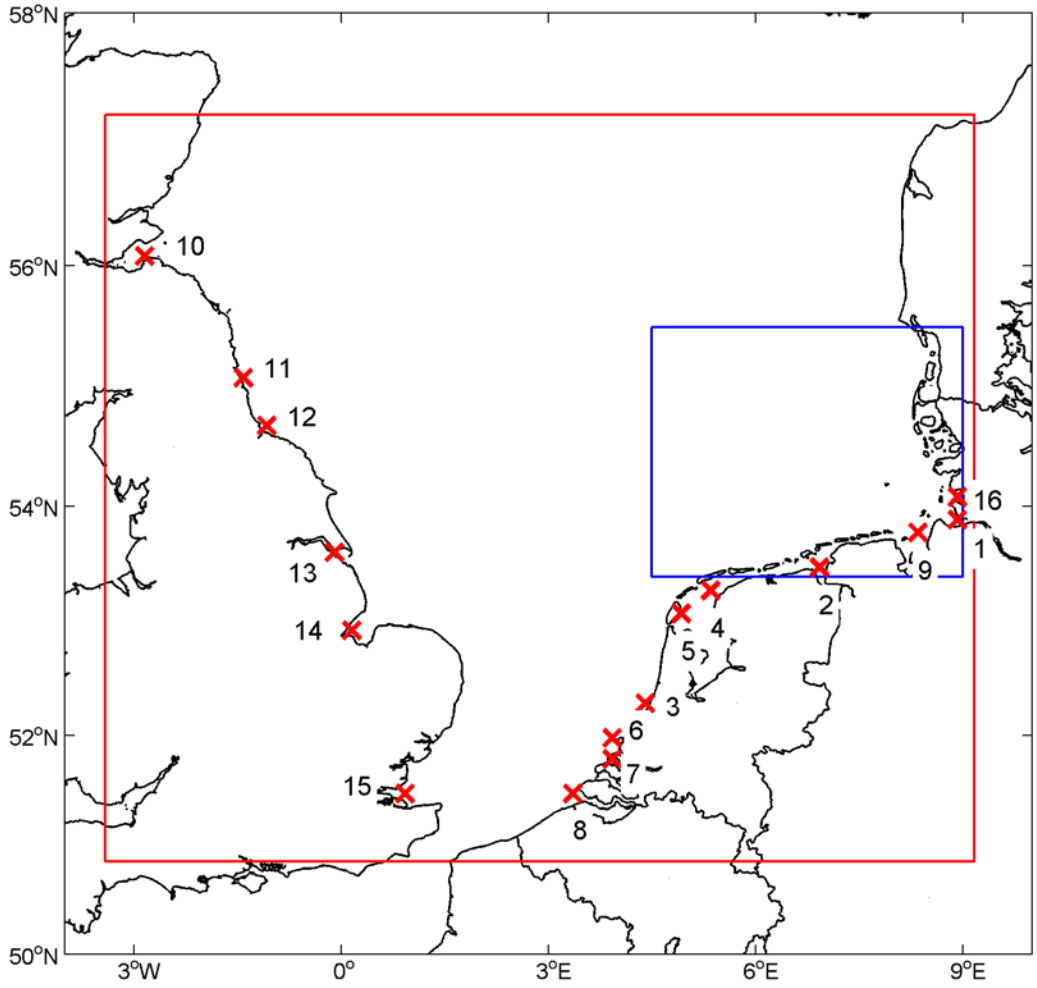

Figure 2.1: Model domain of ECOHAM (red, 3.4°W 50.9°N – 9.2°E 57.2°N), the validation area (blue, 4.5°E 53.5°N – 9.2°E 55.5°N) and the positions of rivers 1 – 16 (see table 2.1).

The original model domain was first applied in the study of Pätsch et al. (2010) and adapted to the scientific questions in the work at hand. The model domain (ECOHAM) was scaled into a 39 x 33 grid field with 21 layers at maximum depth and included the southern and central North Sea (Fig. 2.1). The surface layer had a time varying thickness (5 m on average) due to surface elevation. The longitudinal / latitudinal resolution of the model was 0.33° / 0.2°. The eastern edge of the English Channel was defined as the southern boundary. The northern boundary ranged from the British coast to the most northern tip of Denmark. As our investigations mainly focused on the area of the German Bight the corresponding relevant dynamics as the wind, tidal-induced alongshore anti-clockwise current and the tidal dynamics itself were captured with this

choice of the simulation area. An area was chosen for model validations (validation area, Fig. 2.1) that included the German Bight as well as parts of the Danish and the Dutch coast. It was located east of 4.5°E, north of 53.5°N and south of 55.5°N. Simulations were conducted in the period 1977 – 2009. High TA and DIC concentrations were observed in the eastern part of this area (east of 7°E), whereas lower values occurred in the western part (Thomas et al., 2009, Salt et al., subm.).

2.2.2 The hydrodynamic module

The physical parameters temperature, salinity, horizontal and vertical advection as well as turbulent mixing were calculated by the submodule HAMSOM (Backhaus, 1985), which was integrated in the ECOHAM model. Details were described by Backhaus & Hainbucher (1987) and Pohlmann (1996). The shallow water equations were applied for calculations of advection, the Boussinesq approximation was applied (Pohlmann, 1991) and vertical mixing was calculated after Kochergin (1987). The hydrodynamic model ran prior to the biogeochemical part. Daily result fields were stored for driving the biogeochemical model in offline mode. Surface elevation, temperature and salinity resulting from the Northwest European Shelf model application (Lorkowski et al., 2012) were used as boundary conditions at the southern and northern boundaries.

Two main changes had to be done in order to enable the application of HAMSOM on the ECOHAM grid field in this study:

1. Tides had to be considered for the lateral exchange at the southern boundary of the model domain. HAMSOM was used for larger model domains so far and exchange at model boundaries was applied with a three day relaxation to enable a smooth and realistic input if the flow direction turns towards the model domain. The southern model boundary in the study at hand was at the eastern edge of the English Channel, where strong tides occur. The flow direction changed with the frequency of tides, so a three day relaxation of boundary input would result in almost no boundary input. Therefore, the respective relaxation was reduced to 2.4 hours.

2. River-induced horizontal transport had to be adapted on freshwater input. In former model setups the hydraulic gradient that was induced by freshwater discharge was too low or even neglected (Kühn et al., 2010). As a consequence, the horizontal advection at river mouths was underestimated. The hydrodynamic induced horizontal transport now corresponds to the amount of freshwater discharge.

2.2.3 Freshwater fluxes

The freshwater discharges of 16 rivers were used to calculate salinity and the river induced horizontal transport. The data used for continental river discharges (Pätsch & Lenhart, 2008) based on daily observations. Climatological monthly mean data of runoff were used for the British rivers (pers. comm. Kieran O'Driscoll). These freshwater fluxes govern the salinity gradient from the coast toward the North Sea and enhance the advection from the river mouths into the sea. Fig. 2.2 illustrates the sea surface salinity (SSS) in February (left) and August (right) of 2008. It can be seen that the strong freshwater fluxes in winter (mean river Elbe discharge in February: 1420 $m^3 s^{-1}$) led to lower salinities in the German Bight than in summer (mean river Elbe discharge in August: 300 $m^3 s^{-1}$).

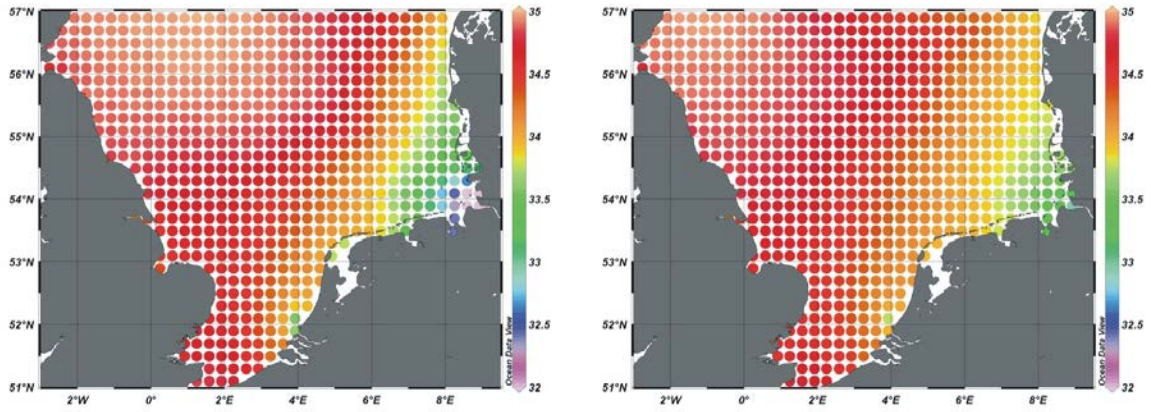

Figure 2.2: Simulated salinity [PSU] in February (left) and August (right) 2008.

2.2.4 Meteorological forcing

The meteorological forcing was provided by NCEP Reanalysis (Kalnay et al., 1996) and interpolated on the model grid field. It consisted of six-hourly fields of air temperature, relative humidity, cloud coverage, wind speed, atmospheric pressure, and wind stress for every year. 2-hourly and daily mean short wave radiation were calculated from astronomic insolation and cloudiness as already described by Lorkowski et al. (2012).

2.2.5 The biogeochemical module

2.2.5.1 General remarks

The respective biogeochemical processes and their parameterisations were described in Lorkowski et al. (2012) in detail. In general, the biogeochemical part of the model was kept as in that study and is briefly described here: The version of the model (ECOHAM4) used for the study at hand included four nutrients (nitrate, ammonium, phosphate and silicate), two phytoplankton groups (diatoms and flagellates), micro- and mesozooplankton, fast (10 m d^{-1}) and slowly (0.4 m d^{-1}) sinking detritus, bacteria, labile dissolved organic matter, semi-labile organic carbon, oxygen, calcite (pelagic and benthic), dissolved inorganic carbon (DIC) and benthic particulate organic matter (carbon, nitrogen, phosphorous and silicate). Mortality of both planktonic groups and fecal pellet production were the sources for the detritus. 85% of the produced detritus was assumed as slowly sinking, 15% was assumed as fast sinking. The sinking velocities and decay rates (to labile organic matter) mainly determined the ratio between pelagic and benthic remineralisation. Pelagic remineralisation of labile organic matter was induced by bacteria. Oxygen dynamics were formulated according to Neumann (2000) and Fennel et al. (2006). They were involved in the primary production, in the remineralisation process, in nitrification and denitrification. Fixed C:N:P ratios were used for the phytoplankton groups (C:N = 6.625 mol C mol^{-1} N, N:P = 20 mol N mol^{-1} P) (Quigg et al., 2003), both zooplankton groups (C:N = 5.5 mol C mol^{-1} N, N:P = 20 mol N mol^{-1} P) and bacteria (C:N = 4.0 mol C mol^{-1} N, N:P = 10 mol N mol^{-1} P). Ratios of the two detritus fractions and DOM were freely varying.

Dry and wet depositions of oxidized and reduced nitrogen onto the North Sea were also included into the model (see also Pätsch & Kühn, 2008; Lorkowski et al. 2012). Data were adapted given by EMEP (Cooperative program for monitoring and evaluation of the long-range transmissions of air pollutants in Europe) and interpolated on the model domain.

The production of calcium carbonate was simulated in a simplified way (Kühn et al., 2010; Lorkowski et al. 2012). Flagellates produced calcite in proportion to organic matter, so a fixed POC:PIC ratio of 40:1 mol C mol^{-1} C was assumed for this group in the present study, according to lower estimates by Chung et al. (2003) and Langer (2008). The carbonate shells had a sinking velocity of 10 m d^{-1} and can be dissolved in the water column or in the sediment as a function of the calcium carbonate saturation state (Ω).

So far, in former model setups TA was restored to prescribed values derived from observations (Thomas et al., 2009) with a relaxation time of two weeks (Kühn et al., 2010; Lorkowski et al., 2012). The changes in TA treatment for the study at hand will be described below. Results from the Northwest European Shelf model application (Lorkowski et al., 2012) were used as

boundary conditions for the recent biogeochemical simulations at the southern and northern boundaries (Fig. 2.1). To continue the time interval to 2009 the same model setup was used as in Lorkowski et al. (2012). Model results were calculated daily.

2.2.5.2 Benthic remineralisation and denitrification

Van Beusekom et al. (1999) estimated that 10 – 20% of the carbon produced in the German Bight is remineralised in the sediment, which is a considerable fraction. Therefore, a simplified approach to simulate sedimentary remineralisation processes was introduced into ECOHAM with the model development by Pätsch & Kühn (2008): The sinking material was collected below the deepest pelagic layer by a layer without vertical extension (Moll, 1998). A similar approach for benthic remineralisation was applied as used by Fennel et al. (2006). The benthic oxygen consumption reduced the oxygen concentration in the lowest pelagic layer and also the remineralisation products were released there. Benthic denitrification was calculated following the suggestion by Seitzinger and Giblin (1996) of a tight coupling between benthic nitrification and denitrification. The latter depended on the benthic oxygen consumption. Therefore, a ratio of 0.116 mol N mol^{-1} O (Seitzinger and Giblin, 1996) was applied. Additionally, pelagic denitrification was also included but it did not occur in the model area.

2.2.6 River input

River load data for the main continental rivers were taken from a report by Pätsch & Lenhart (2008) that was kept up to date continuously so that data for the years 2007 – 2009 were also available. They calculated daily loads of nutrients and organic matter based on data provided by the different river authorities. They also calculated data of TA and DIC loads for the rivers Elbe, Ems, Rhine (both river mouths: Nieuwe Waterweg and Haringvliet) and Scheldt. According to the study of Lorkowski et al. (2012) the TA and DIC concentrations of the river Rhine were used to calculate loads of the remaining Dutch river outlets Noordzeekanaal and Ijsselmeer (east and west) in the study at hand. Mean values for TA and DIC concentrations of the rivers Elbe and Ems were used to calculate loads of the river Weser. Loads of the river Eider were calculated according to Johannsen et al. (2008). Nutrient loads of the British rivers were calculated after Heath et al. (2002) together with climatological data of river runoff developed by Kieran O'Driscoll (personal communication) that represented the year 1990. TA and DIC river concentrations used for river load calculations were obtained by measurements carried out by Neal (2002) in either the same rivers or in rivers with similar catchment areas.

Table 2.1: River numbers in Fig. 1, their positions and source of data for simulations.

Number in Fig. 1	Name	River mouth position	Data source
1	Elbe	53° 53' 20" N 08° 55' 00" E	Pätsch & Lenhart, 2008
2	Ems	53° 29' 20" N 06° 55' 00" E	As above
3	Noordzeekanaal	52° 17' 20" N 04° 15' 00" E	As above
4	Ijsselmeer (east)	53° 17' 20" N 05° 15' 00" E	As above
5	Ijsselmeer (west)	53° 05' 20" N 04° 55' 00" E	As above
6	Nieuwe Waterweg	52° 05' 20" N 03° 55' 00" E	As above
7	Haringvliet	51° 53' 20" N 03° 55' 00" E	As above
8	Scheldt	51° 29' 20" N 03° 15' 00" E	As above
9	Weser	53° 53' 20" N 08° 15' 00" E	As above
10	Firth of Forth	56° 05' 20" N 02° 45' 00" W	Based on Neal, 2002
11	Tyne	55° 05' 20" N 01° 25' 00" W	As above
12	Tees	54° 41' 20" N 01° 05' 00" W	As above
13	Humber	53° 41' 20" N 00° 25' 00" W	As above
14	Wash	52° 53' 20" N 00° 15' 00" E	As above
15	Thames	51° 29' 20" N 00° 55' 00" E	As above
16	Eider	54° 05' 20" N 08° 55' 00" E	Johannsen et al, 2008

2.2.7 Concept of Alkalinity and the carbonate system

The carbonate system is defined by six variables: CO_2, HCO_3^-, CO_3^{2-}, H^+, DIC and TA. If there are any two variables given, one may calculate the others (Deffeyes, 1965, Park, 1969). In this model changes of DIC and TA were calculated from physical and biogeochemical processes. These parameters are conservative quantities with respect to mixing and changes in temperature and pressure and are thus most qualified to calculate the remaining variables of the carbonate system diagnostically (Wolf-Gladrow, 2007). For this purpose the equilibrium constants of Mehrbach et al. (1973) as refitted by Dickson & Millero (1987) were used and adapted to the seawater scale.

Apart from the previously mentioned changes in river loads the same treatment for DIC was used as already explained in the work of Lorkowski et al. (2012). The main extension in the study at hand considering the carbonate system was the introduction of a prognostic treatment of TA in order to study the impact of biogeochemical and physical changes of TA onto the carbonate system and especially on acidification. The physical part contained advective and mixing processes as well as dilution by riverine freshwater input. The biogeochemical part was driven by uptake and release of calcium and nutrients in the water column and also by atmospheric deposition of reduced and oxidised nitrogen. The modelled internal processes that altered TA were changes of calcium, nitrate, ammonium and phosphate. The gain of calcium

and ammonium in the water column increased TA as well as the decline of nitrate and phosphate. Vice versa the decline of calcium and ammonium as well as the gain of nitrate and phopshate decreased TA. Denitrification was no part of the prognostic treatment of TA because only benthic denitrification occurred in the model and this was driven by coupled ammonification / nitrification (Seitzinger & Giblin, 1996), which does not result in changes of TA in total. This effect will be discussed later. The respective fluxes included in the prognostic treatment of TA were identified as internal fluxes ($F_{1\text{-}17}$) and are as follows:

1) Pelagic calcite dissolution
2) Calcite formation
3) Benthic calcite dissolution
4) Nitrification
5) Uptake of nitrate
6) Excretion of ammonium by zooplankton
7) Excretion of ammonium by bacteria
8) Uptake of ammonium by phytoplankton
9) Uptake of ammonium by bacteria
10) Benthic remineralisation of ammonium
11) Atmospheric deposition of ammonium
12) Atmospheric deposition of nitrate
13) Benthic remineralisation of phosphate
14) Uptake of phosphate by phytoplankton
15) Uptake of phosphate by bacteria
16) Excretion of phosphate by zooplankton
17) Excretion of phosphate by bacteria

The biogeochemical fluxes changed the simulated TA concentration in the following way:

$$\frac{\partial TA}{\partial t} = 2\left(F_1 - F_2 + F_3 - F_4\right) + F_5 + F_6 + F_7 - F_8 - F_9 + F_{10} + F_{11} - F_{12} - F_{13} + F_{14} + F_{15} - F_{16} - F_{17} \quad (2.1)$$

All calcium-related fluxes (1 – 3) were included twice into the TA budget because TA keeps track of the level of protons of the respective ions (Dickson, 1981). Hence one mol of calcium released into the water column by calcite dissolution caused an increase of TA by two mol.

Furthermore, nitrification caused a twofold decrease because two ions were involved: the consumption of ammonium decreased TA as well as the subsequent production of nitrate.

It should be pointed out that riverine TA entered the model as bulk TA. TA was not changed directly due to riverine nutrient loads because they were already included in riverine TA loads. However, they had an indirect effect on TA because the nutrient loads drove the internal TA variability that was related to nutrients.

2.2.7.1 Theoretical background:

Regarding the biogeochemical part of the model that calculated the carbonate system, the theoretical background was best explained in the work of Wolf-Gladrow et al. (2007). All following short explanations in this chapter refer to that study and give an overview how $F_{1\text{-}17}$ can change TA.

TA is defined by the excess of proton acceptors over proton donors with respect to a certain zero level of protons for each acid-base system. It could be written for seawater as follows (Dickson, 1981):

$$\begin{aligned} TA = {} & \left[HCO_3^-\right] + 2\left[CO_3^{2-}\right] + \left[B(OH)_4^-\right] + \left[OH^-\right] + \left[HPO_4^{2-}\right] \\ & + 2\left[PO_4^{3-}\right] + \left[H_3SiO_4^-\right] + \left[NH_3\right] + \left[HS^-\right] \\ & - \left[H^+\right] - \left[HSO_4^-\right] - \left[HF\right] - \left[H_3PO_4\right] \end{aligned} \tag{2.2}$$

To distinguish between the species of each acid-base system a single pK value is defined at $pK_{zlp} = 4.5$ that applies for all systems. All bases formed from weak acids with $pK > pK_{zlp}$ are to be considered proton acceptors and acids with $pK \leq pK_{zlp}$ are to be considered proton donors (Dickson, 1981). The chemical species with the largest concentration at $pH = pK_{zlp}$ defines the zero level of protons for the respective acid-base system. The coefficients in (2.2) indicate how many protons the chemical species could donate or accept when they are converted to their respective zero level of protons.

Simulated biogeochemical changes of TA ($F_{1\text{-}17}$) were related to calcite, nitrate, ammonium and phosphate. The impact of calcite-related processes (calcium carbonate precipitation and dissolution (2.3), (2.4))

$$Ca^{2+} + 2HCO_3^- \Leftrightarrow CaCO_3 + CO_2 + H_2O \tag{2.3}$$

$$Ca^{2+} + CO_3^{2-} \Leftrightarrow CaCO_3 \tag{2.4}$$

on alkalinity can be directly explained by Dickson's definition due to changes in carbonate and bicarbonate ions. In contrast, the impact of changes in nutrient concentrations on TA has to be explained by the 'nutrient-H^+-compensation principle' that was also introduced by Wolf-Gladrow et al. (2007). Although nitrate and ammonium are no part of Dickson's TA-definition (Dickson, 1981) their uptake or release by algae results in changes of TA in the respective environment. The absorbing cell has to maintain electroneutrality, so e.g. an uptake of one molecule of nitrate is accompanied by the uptake of one proton (symport) or a release of one hydroxide ion (antiport), which both are again part of Dickson's definition.

Wolf-Gladrow et al. (2007) introduced an equivalent expression to Dickson's definition of TA that is called 'the explicit conservative form of total alkalinity' (TA_{ec}). It enables to explain changes of TA due to nutrient assimilation and other biogeochemical processes in a simple way. The foundation of this expression is the assumption of electroneutrality of aqueous solutions, so that the sum of all charges is zero (the ellipses stand for ions with minor concentrations):

$$\begin{aligned}&\left[Na^+\right]+2\left[Mg^{2+}\right]+2\left[Ca^{2+}\right]+\left[K^+\right]+2\left[Sr^{2+}\right]+\ldots+\left[NH_4^+\right]+\left[H^+\right]+\ldots\\&-\left[Cl^-\right]-2\left[SO_4^{2-}\right]-\left[Br^-\right]-\left[NO_3^-\right]-\left[NO_2^-\right]-\ldots-\left[HCO_3^-\right]-2\left[CO_3^{2-}\right]\\&-\left[B(OH)_4^-\right]-\left[OH^-\right]-\left[HS^-\right]-\left[H_3SiO_4^-\right]-\left[HSO_4^-\right]-\left[F^-\right]-\left[H_2PO_4^-\right]\\&-2\left[HPO_4^{2-}\right]-3\left[PO_4^{3-}\right]=0\end{aligned} \tag{2.5}$$

If this equation is rearranged so that Dickson's expression appears on the right-hand side, the expression for TA_{ec} appears on the left-hand side:

$$\begin{aligned}&\left[Na^+\right]+2\left[Mg^{2+}\right]+2\left[Ca^{2+}\right]+\left[K^+\right]+2\left[Sr^{2+}\right]+\ldots\\&-\left[Cl^-\right]-\left[Br^-\right]-\left[NO_3^-\right]-\ldots TPO_4\\&+TNH_3-2TSO_4-THF-THNO_2\\&=TA_{ec}\end{aligned} \tag{2.6}$$

where

$$\begin{aligned}TPO_4&=\left[H_3PO_4\right]+\left[H_2PO_4^-\right]+\left[HPO_4^{2-}\right]+\left[PO_4^{3-}\right]\\TNH_3&=\left[NH_3\right]+\left[NH_4^+\right]\\TSO_4&=\left[SO_4^{2-}\right]+\left[HSO_4^-\right]\\THF&=\left[F^-\right]+\left[HF\right]\\THNO_2&=\left[NO_2^-\right]+\left[HNO_2\right]\end{aligned}$$

are total phosphate, ammonium, sulphate, fluoride and nitrite respectively.

Of course, there are many other biogeochemical processes involved in changes of TA in seawater that were not considered in this model. Beside the calcium-related fluxes other internal processes ($F_{4\text{-}12}$) were chosen that were directly affected by the modelled riverine and atmospheric input of nitrogen. These processes were supposed to have the largest biogeochemical impact on TA.

Considering the above mentioned (chapter 2.2.5) planktonic C:N:P ratios the phosphate-related processes ($F_{13\text{-}17}$) had minor impact on TA compared to the other fluxes. It has to be pointed out that the change of TA is independent of the phosphate species. A change of 1 mol of phosphate (H_3PO_4, $H_2PO_4^-$, HPO_4^{2-} or PO_4^{3-}) results in a change of 1 mol TA (Wolf-Gladrow et al., 2007). In accordance with the nutrient-H^+-compensation principle the uptake of 1 mol PO_4^{3-} by algae is associated with the symport of 3 mol H^+ (or antiport of 3 mol OH^-). Analogously, the uptake of 1 mol HPO_4^{2-} would be associated with the symport of 2 mol H^+ (or antiport of 2 mol OH^-). Nevertheless, the difference in the level of protons of each phosphate species and the amount of compensatory H^+ (or OH^-) is always -1, because the zero level of protons in this system is $H_2PO_4^-$.

The advantage of TA_{ec} is that changes in TA that are driven by biogeochemical processes could be easily explained with one formula (2.6) without considering the nutrient H^+-compensation principle.

2.3 Results

2.3.1 TA turnover rate and underlying fluxes in 2008

The prognostic treatment of TA in this model study included 17 different fluxes ($F_1 – F_{17}$) that were referred to calcite, nitrate, ammonium and phosphate. The cumulative impact of these fluxes on TA was examined in the validation area (59,338 km²) and in the whole model domain (332,050 km²) (Fig. 2.3 – 2.7) in order to detect the most important fluxes that govern the modelled TA production during the course of the year 2008. Therefore, the fluxes were divided into four components, one for calcite and one for each nutrient. Note that the impact on TA is shown in Fig. 2.3 – 2.7 including the prefactors of each flux (compare (2.6)). Hence, every calcite-related process ($F_1 – F_3$) is considered twofold because the dissolution / formation of 1 mol calcite results in a production / consumption of 2 mol TA. The twofold impact of nitrification (F_4) was allocated to nitrate and ammonium. Hence, 1 mol nitrogen that got nitrified is included onefold in both components (Fig. 2.4, 2.5).

2.3.1.1 Calcite

The impact of calcite-related processes ($F_1 – F_3$) on modelled TA turnover is shown in Fig. 2.3. All processes showed a similar progress in both areas. Calcite formation and dissolution was almost balanced at the end of 2008 but not during the course of the year. Calcite dissolution exceeded calcite formation slightly in autumn and winter. In spring and summer, calcite formation exceeded calcite dissolution. About 95% of the overall calcite dissolution took place in the sediment in both examined areas.

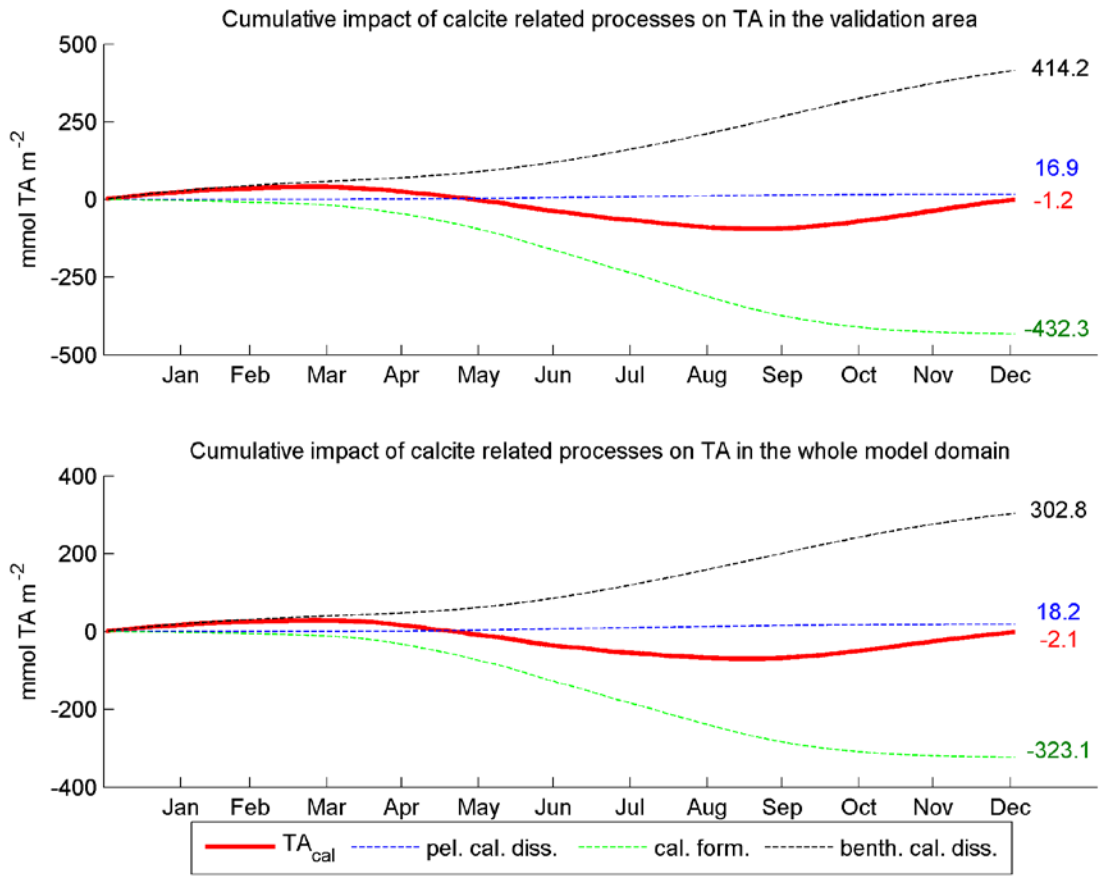

Fig. 2.3: The cumulative impact of calcite-related processes [mmol TA m^{-2}] on TA (TA_{cal}) in the validation area (top) and the whole model domain (bottom) in 2008. F_1: pelagic calcite dissolution, F_2: calcite formation and F_3: benthic calcite dissolution.

2.3.1.2 Nitrate

The impact of nitrate-related processes (F_4, F_5, F_{12}) on modelled TA turnover is shown in Fig. 2.4. All processes showed a similar progress in both areas. Nitrification decreased the TA turnover continuously during the course of the year. The uptake of nitrate by phytoplankton exceeded nitrification from March to September but especially in spring, when the phytoplankton bloom occurred (Lorkowski et al., 2012). This effect governed the nitrate-related impact on TA at that time. The processes that decreased TA exceeded the uptake of nitrate in autumn and winter. In comparison to the other components, the nitrate-related component was significantly unbalanced at the end of the year.

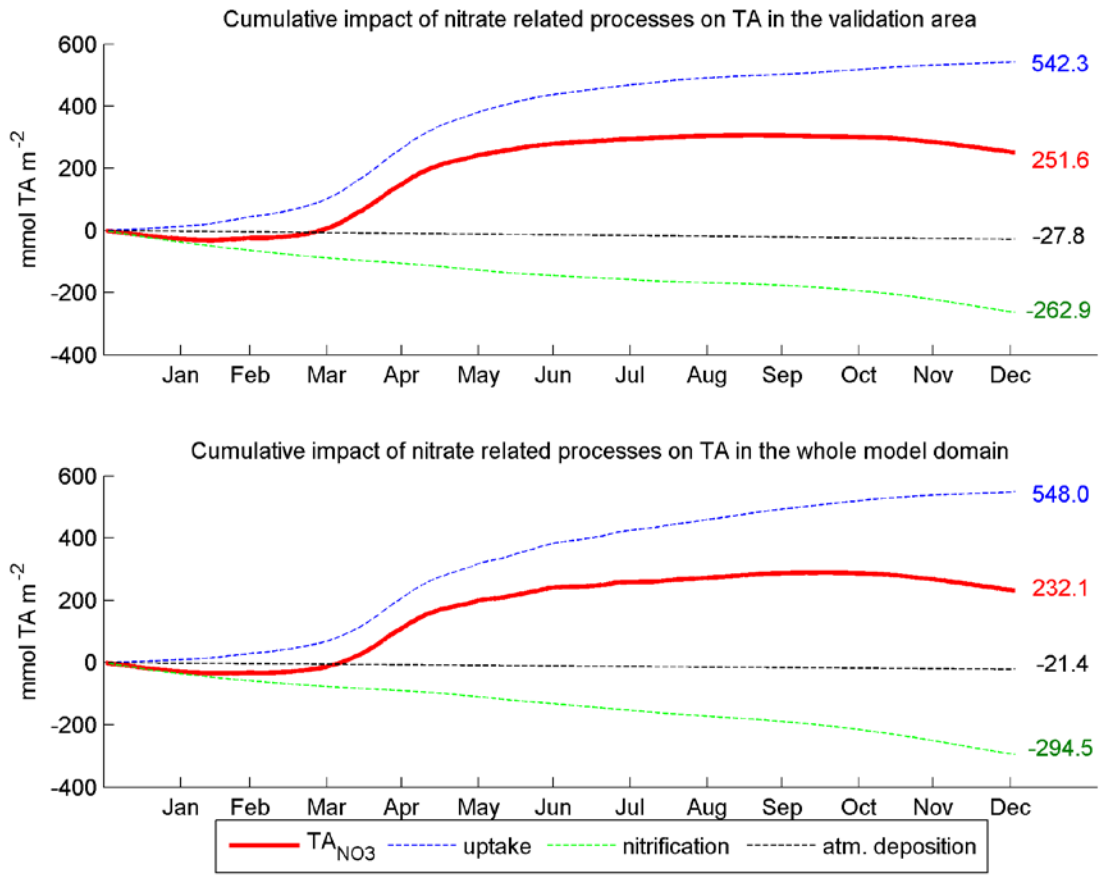

Fig. 2.4: The cumulative impact of nitrate-related processes [mmol TA m^{-2}] on TA (TA_{NO3}) in the validation area (top) and the whole model domain (bottom) in 2008. F_4: nitrification, F_5: uptake and F_{11}: atmospheric deposition.

2.3.1.3 Ammonium

The impact of ammonium-related processes (F_4, $F_6 – F_{11}$) on modelled TA turnover is shown in fig. 2.5. It was decided to sum up the excretion and uptake of ammonium ($F_6 – F_9$) to one net flux ("excr. – uptake") in order to keep the figure clear and legibly scaled. These fluxes were up to 2190 mmol TA m^{-2} yr^{-1} in the validation area and up to 1837 mmol m^{-2} yr^{-1} in the whole model domain. The impact of ammonium-related processes on TA turnover decreased slightly in the validation area until August, whereas it decreased in the whole model domain until March and was almost stagnant until September. Afterwards, it slightly increased in both areas in autumn. Pelagic remineralisation is included in the excretion of ammonium by bacteria (F_7). This process governed the sub-component "excr. – uptake" in autumn, because less ammonium was taken up by phytoplankton (F_8). In short, remineralised or excreted ammonium was almost completely nitrified or taken up immediately. This is why no pronounced imbalances occurred during the course of the year. In contrast to the other components, the impact of ammonium-

related processes on TA turnover revealed a slightly higher imbalance in the validation area than in the whole model domain.

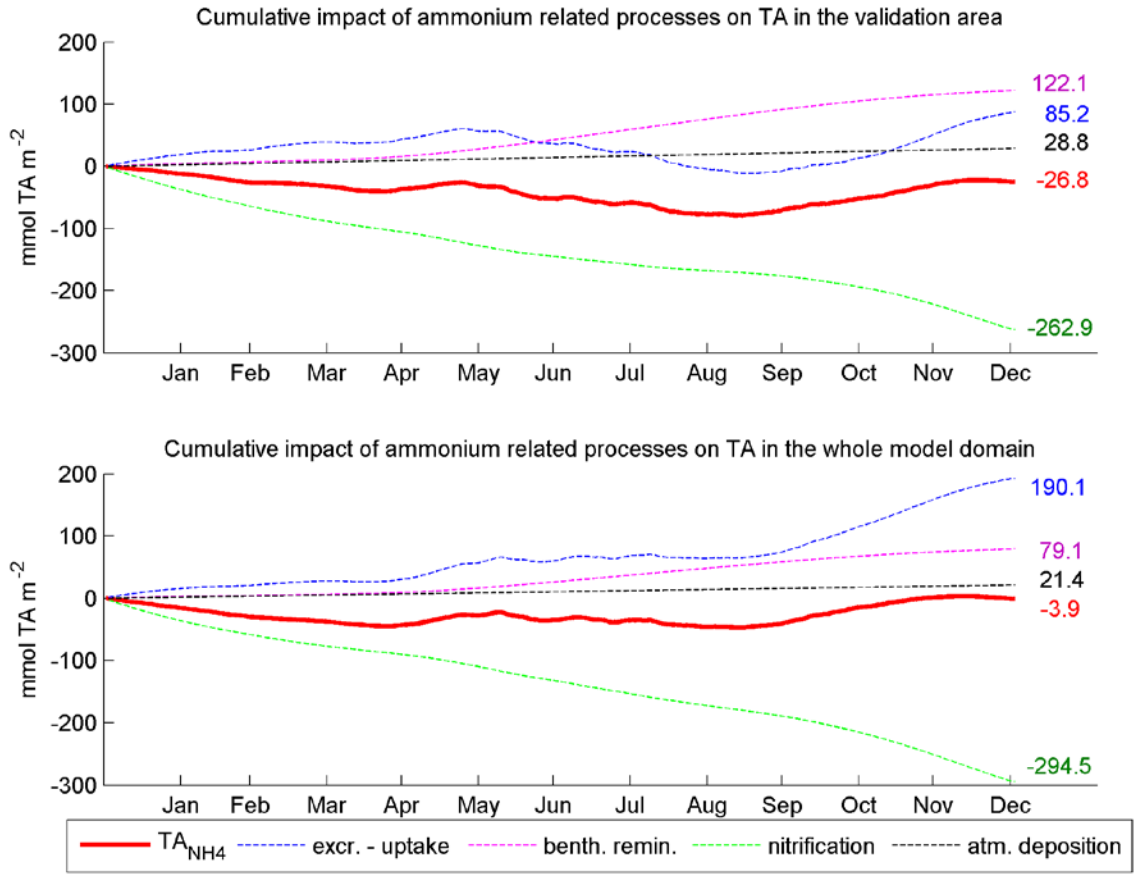

Fig. 2.5: The cumulative impact of ammonium-related processes [mmol TA m^{-2}] on TA (TA_{NH4}) in the validation area (top) and the whole model domain (bottom) in 2008. $F_6+F_7+F_8+F_9$: excretion - uptake, F_{10}: benthic remineralisation, F_4: nitrification and F_{11}: atmospheric deposition.

2.3.1.4 Phosphate

The impact of phosphate-related processes (F_{13} – F_{17}) on modelled TA turnover is shown in Fig. 2.6. It was decided to sum up the uptake of phosphate by phytoplankton (F_{14}) and bacteria (F_{15}) to one flux ("uptake") as well as the excretion of phosphate by zooplankton (F_{16}) and bacteria (F_{17}) ("excretion"). The latter also included pelagic remineralisation. All processes showed a similar progress in both areas. The uptake exceeded the excretion and benthic remineralisation slightly in April and May. Afterwards, it was almost balanced until September. The excretion and benthic remineralisation exceeded the uptake in autumn. At the end of the year the overall impact of phosphate-related processes on TA was almost balanced.

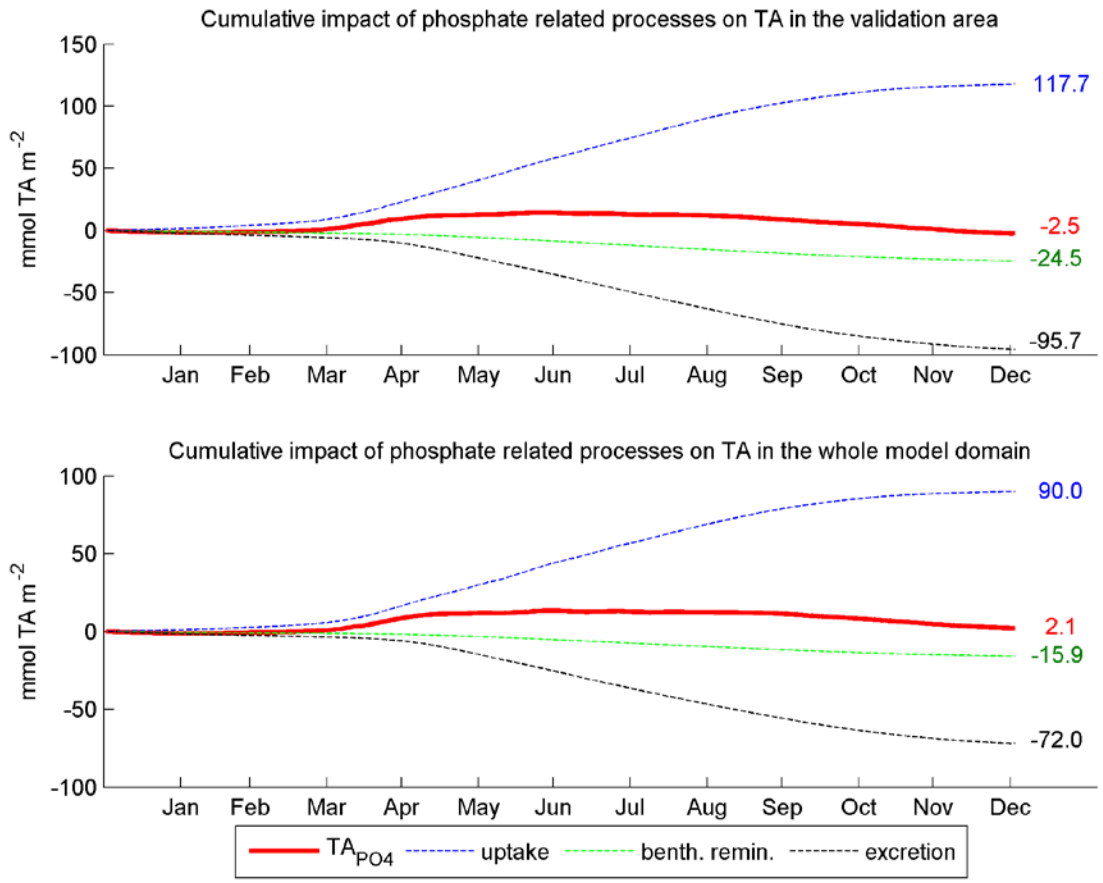

Fig. 2.6: The cumulative impact of phosphate-related processes [mmol TA m^{-2}] on TA (TA_{PO4}) in the validation area (top) and the whole model domain (bottom) in 2008. $F_{14}+F_{15}$: uptake, F_{13}: benthic remineralisation and $F_{16}+F_{17}$: excretion.

2.3.1.5 TA turnover rate and denitrification

The impact of all four components on modelled TA turnover, the resulting TA turnover rate itself and the modelled denitrification rate are shown in Fig. 2.7. Note that denitrification is only shown in order to enable a comparison with the TA turnover rate. It was no part of the prognostic treatment of TA and did not impact the TA turnover itself directly. Until May the TA turnover rate was governed by the impact of nitrate-related processes in both areas. Hence, the rapid increase of TA turnover in April and May was due to enhanced uptake of nitrate during the phytoplankton spring bloom. Afterwards, a slight imbalance in the ammonium-related processes and enhanced calcite formation caused a decrease in the TA turnover in the validation area and stagnancy in the whole model domain until September. The turnover rate increased in October and November caused by enhanced benthic calcite dissolution. Denitrification steadily increased during the course of the year and exceeded the amount of TA that was converted by 149 mmol m^{-2} yr^{-1} in the validation area and by 12.8 mmol m^{-2} yr^{-1} in the whole model domain

at the end of the year. A total amount of 80 / 22 Gmol N yr^{-1} was denitrified in the whole model domain / validation area, whereas an amount of 76 / 13 Gmol TA yr^{-1} was produced.

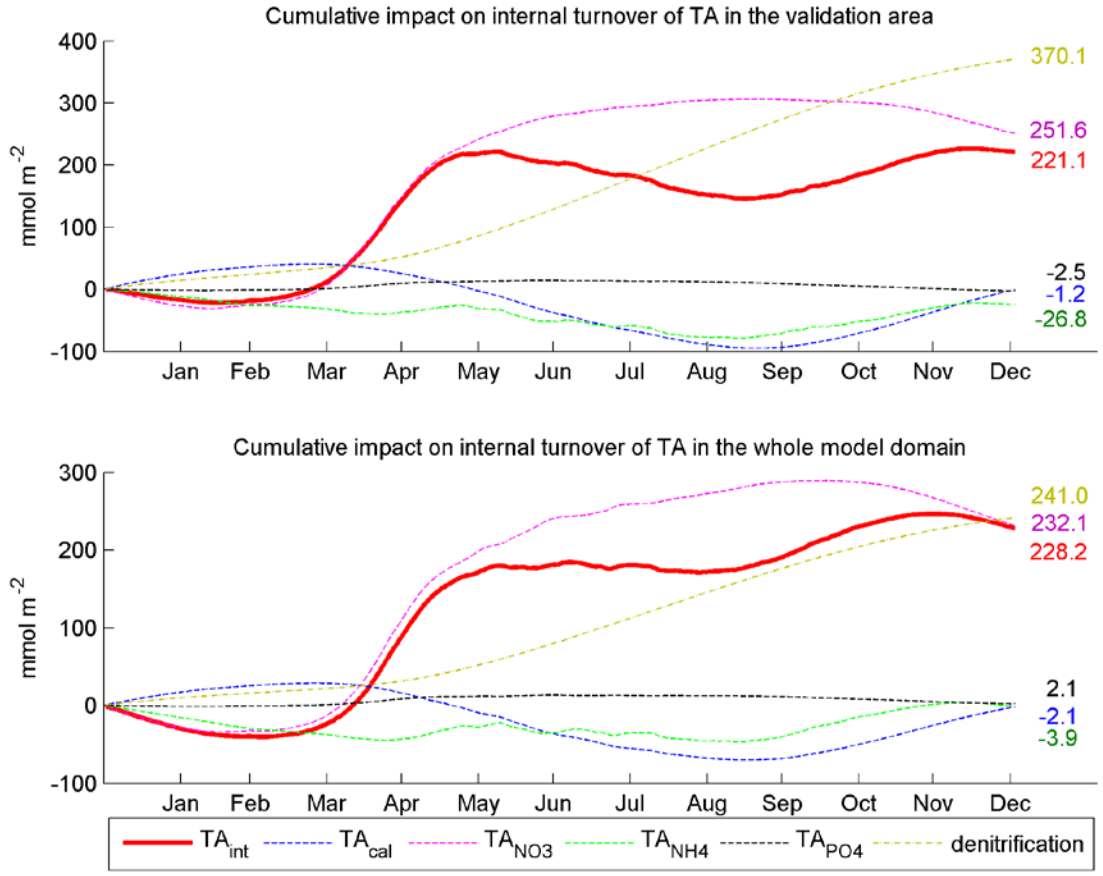

Fig. 2.7: The cumulative impact of all four components [mmol TA m^{-2}] on TA (TA_{int}) and denitrification [mmol N m^{-2}] in the validation area (top) and the whole model domain (bottom) in 2008. TA_{cal}: impact of calcite-related processes, TA_{NO3}: impact of nitrate-related processes, TA_{NH4}: impact of ammonium-related processes and TA_{PO4}: impact of phosphate-related processes.

2.3.2 Impact of internal TA turnover on TA concentrations in 2008

One of the main aims of this study is to reproduce high TA concentrations observed in the German Bight in summer (Thomas et al., 2009; Salt et al., subm.). Monthly mean surface concentrations of TA and the cumulative TA concentration differences [µmol kg^{-1}] caused by the internal turnover are shown in Fig. 2.8 for February, May, August and November. The latter were calculated as the difference of two simulations with and without implemented prognostic treatment of TA. The superposition was acceptable due to the conservative characteristics of TA. The impact of the internal turnover on monthly TA concentration changes is shown in Fig. 2.9. Therefore, monthly values of the internal turnover rates of TA [mmol m^{-2} mon^{-1}] are shown on the right side and the respective TA concentration differences between the last and the first day of the month [µmol kg^{-1}] caused by the internal turnover are shown on the left side of Fig. 2.9. The concentration differences shown in Fig. 2.9 differ from the concentration differences shown in Fig. 2.8 because they show differences that occurred in the course of one month. Thus, they can be related to the TA turnover rates also shown in Fig. 2.9. The concentration differences shown in Fig. 2.8 are cumulative and are related to the TA produced during the year until the shown month. So they show how much TA is converted in total also incorporating the months not shown in Fig. 2.8.

In February, TA concentrations ranged between 2275 µmol kg^{-1} at the Elbe estuary and 2450 µmol kg^{-1} at the Thames estuary (Fig. 2.8, left side). In addition, the concentration pattern was homogeneous in the German Bight and the central North Sea. TA was produced near the estuaries Thames, Wash, Ems and Elbe, the outlet of the Ijsselmeer and east of 8°E significantly (Fig. 2.9, right side), whereas it was slightly consumed (about 40 mmol m^{-2} mon^{-1}) in large parts of the model domain, especially in the northwest. The resulting concentration differences in February (Fig. 2.9, left side) were marginally negative (about 1 µmol kg^{-1}) in the model domain. The cumulative concentration differences caused by the internal turnover of TA occurred especially east of 7°E and increased the concentration up to 20 µmol kg^{-1} (Fig. 2.8, right side). This was mainly due to consumed TA in January (Fig. 2.7).

In May, TA concentrations ranged between 2275 µmol kg^{-1} at the Elbe and 2435 µmol kg^{-1} at the Thames estuary (Fig. 2.8, left side). The concentration pattern was more heterogeneous than in February, because concentrations increased near the river Rhine (2380 µmol kg^{-1}), in the Jade Bay (2350 µmol kg^{-1}, located around 8.3°E and 53.5°N) and near the island of Sylt (2340 µmol kg^{-1}). TA was produced in large parts of the model domain especially in the western part, near the outlet of the river Rhine and in the German Bight, whereas it was slightly consumed especially near the Danish coast (Fig. 2.9, right side). The resulting concentration differences in May (Fig. 2.9, left side) occurred at the same places and were also more distributed. The resulting cumulative concentration differences were highest in the eastern part of the model

domain, near the Dutch coast and especially in the German Bight, where concentrations increased up to 40 µmol kg^{-1} due to the TA turnover.

In August, TA concentrations ranged between 2290 µmol kg^{-1} in the northwestern part of the model domain, 2360 µmol kg^{-1} at the western part of the Dutch coast and 2380 µmol kg^{-1} at the Thames estuary (Fig. 2.8, left side). Concentrations in the German Bight were lower than in May and less heterogeneous. TA was produced at some river outlets of the British coast, the outlet of the rivers Rhine, Weser and Elbe as well as in some small areas in the north western part of the model domain, whereas it was slightly consumed in large parts of the model domain (Fig. 2.9, right side). The concentrations in August only decreased near the river Rhine and south of the island of Sylt significantly (Fig. 2.9, left side). The cumulative differences in concentrations that were caused by the TA turnover were pronounced east of 7°E and in the German Bight and increased up to 40 µmol kg^{-1} (Fig. 2.8, right side).

In November, TA concentrations ranged between 2280 µmol kg^{-1} in the northwestern part of the model domain and 2395 µmol kg^{-1} at the Thames estuary (Fig. 2.8, left side). The concentration pattern was more homogeneous in the German Bight and in the central part of the North Sea compared to concentrations in May and August. Analogously to August, TA was produced at some river outlets but it was also slightly produced (20 – 40 mmol m^{-2} mon^{-1}) in large areas in the central and eastern part of the model domain. The TA production in these areas could be related to calcite dissolution in the sediment (Fig. 2.3, 2.7). The cumulative differences in concentrations that were caused by the TA turnover were still pronounced east of 7°E and increased up to 25 µmol kg^{-1} (Fig. 2.8, right side).

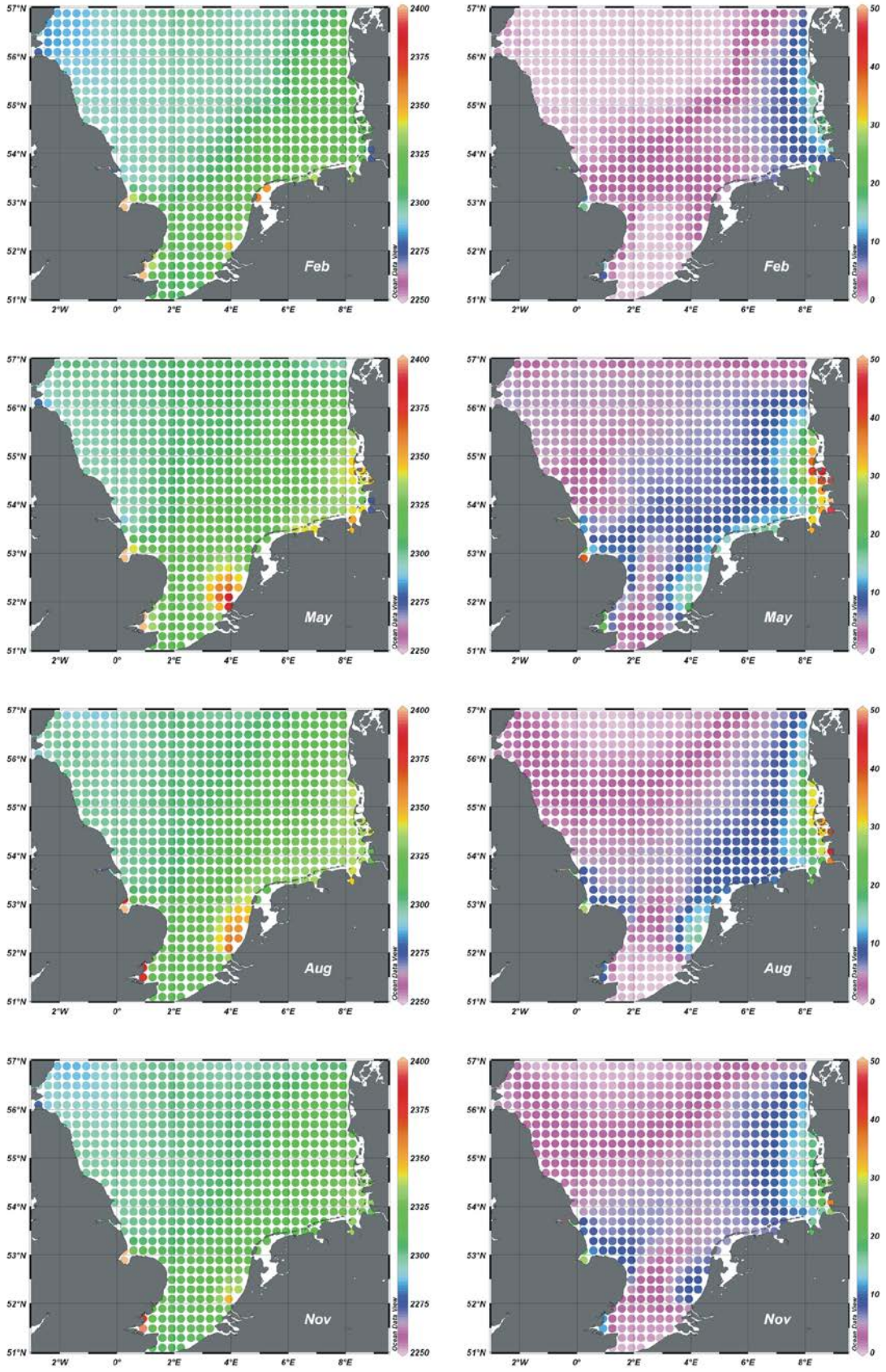

Fig. 2.8: Left side: simulated monthly mean surface TA concentrations [µmol kg^{-1}]. Right side: cumulative concentration differences [µmol kg^{-1}] caused by internal turnover of TA in 2008.

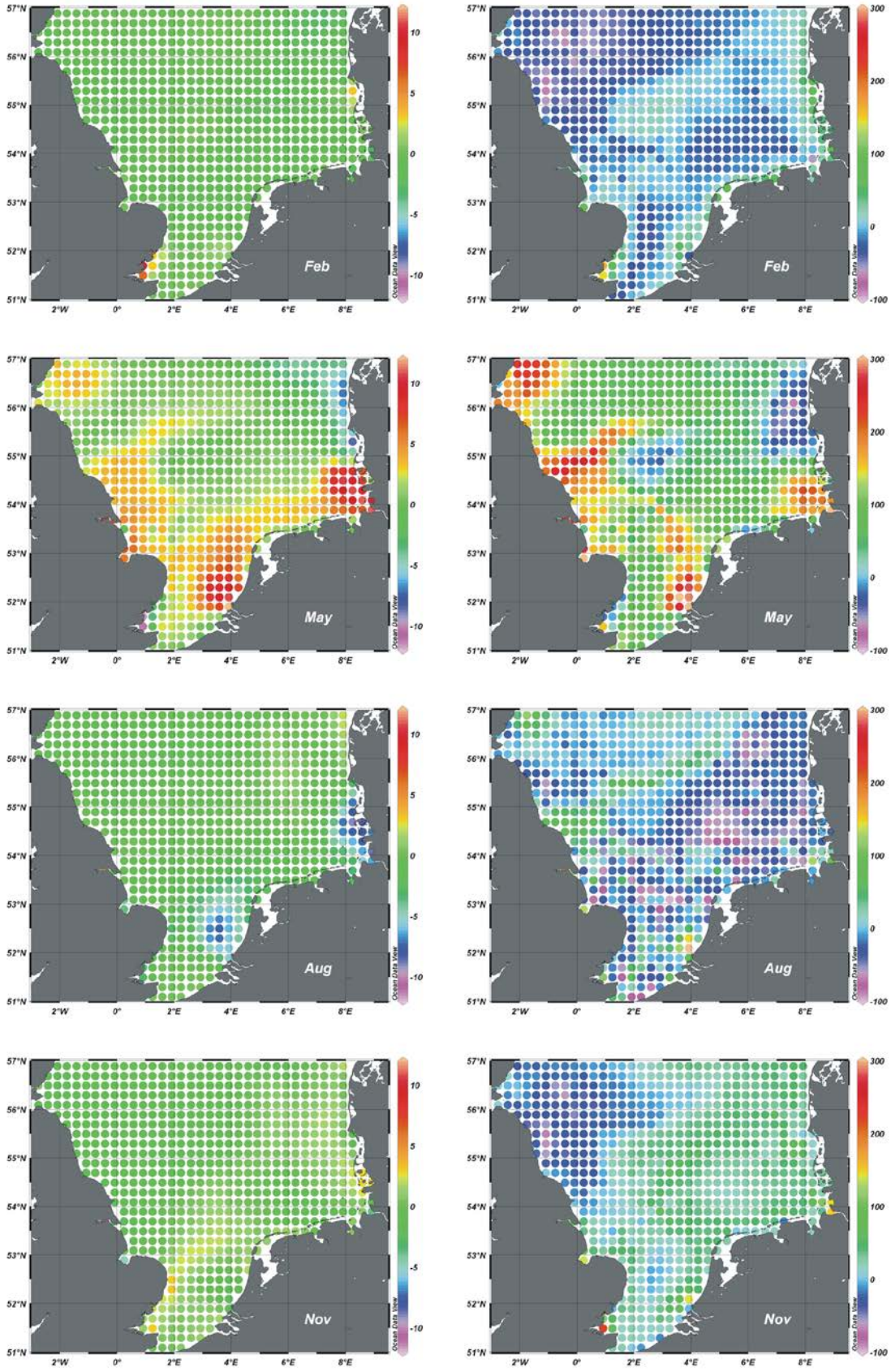

Fig. 2.9: Left side: concentration differences of the last and first day of the month caused by TA turnover [µmol kg^{-1}]. Right side: monthly turnover rate of TA [mmol m^{-2} mon^{-1}].

2.3.3 Impact of nutrient river loads on TA turnover in 1977 - 2009

Previous results in this chapter show that TA turnover rate is mainly driven by nitrate-related processes (Fig. 2.4, 2.7). During the simulated period, river loads of nutrients, especially loads of nitrate, fluctuated significantly (Fig. 2.10). TA turnover and nitrogen loads of the three main rivers discharging into the German Bight correlated well ($R^2 = 0.82$) if loads of ammonium were considered negatively because the uptake of ammonium reduces TA. Thus far, the year 2008 was examined in detail but river loads of nitrate were low (8.1 Gmol N yr^{-1}) compared to the years 1987 (20.0 Gmol N yr^{-1}), 1994 (16.9 Gmol N yr^{-1}) or 2002 (14.7 Gmol N yr^{-1}).

Observed surface TA concentrations and simulated monthly mean surface concentrations in August 2008 are shown in Fig. 2.11 as well as TA concentrations in May and August in the years 1987, 1994 and 2002. This was done in order to compare years with high river loads and thus high turnover rates of TA (Fig. 2.10) with observations. So far, the observed high TA concentrations in the German Bight could not be adequately reproduced with this model setup in 2008. The overarching question in this paragraph is whether river loads of nutrients could be the origin of high TA concentrations in summer.

The results were also compared in a Taylor diagram (Taylor, 2001) in Fig. 2.12 in order to give a statistical overview. Observations of 10 different stations were available in the validation area (Fig. 2.1), each with four to six measurements at different depths (52 measured points). Measured TA concentrations of each point were compared with the modeled TA concentrations in the respective grid cells. The correlation coefficients, the standard deviations (STD) and the root mean square errors (RMSE) were calculated for each simulation.

With focus on the German Bight, the highest TA concentrations were simulated in May and August 1994 (Fig. 2.11), when the annual amount of produced TA was highest (21.0 Gmol yr^{-1}) in the simulated period (Fig. 2.10). Nevertheless, observations could not be reproduced adequately in May or in August of any of the examined years (Fig. 2.12). The deviations from observation were represented by RMSE values of 28 µmol kg^{-1} for the years 1987, 2002 and 2008 and 25 µmol kg^{-1} for the year 1994 and thus did not differ significantly.

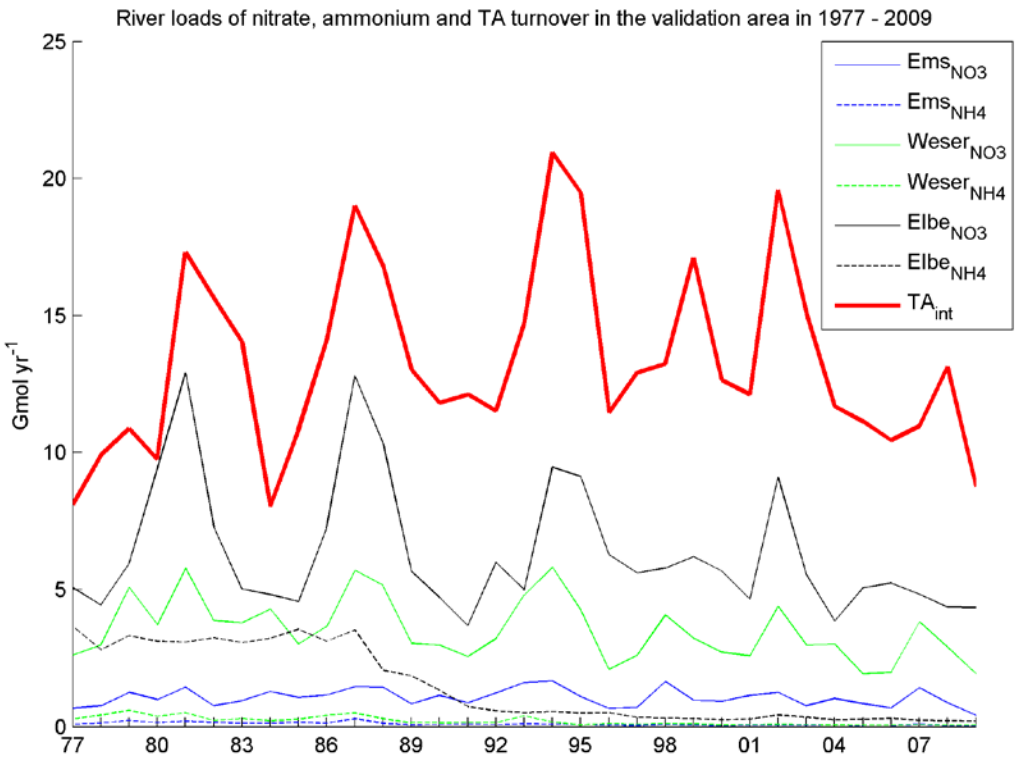

Fig. 2.10: River loads of nitrate and ammonium of the main rivers in the German Bight as well as TA turnover in the validation area [Gmol yr^{-1}].

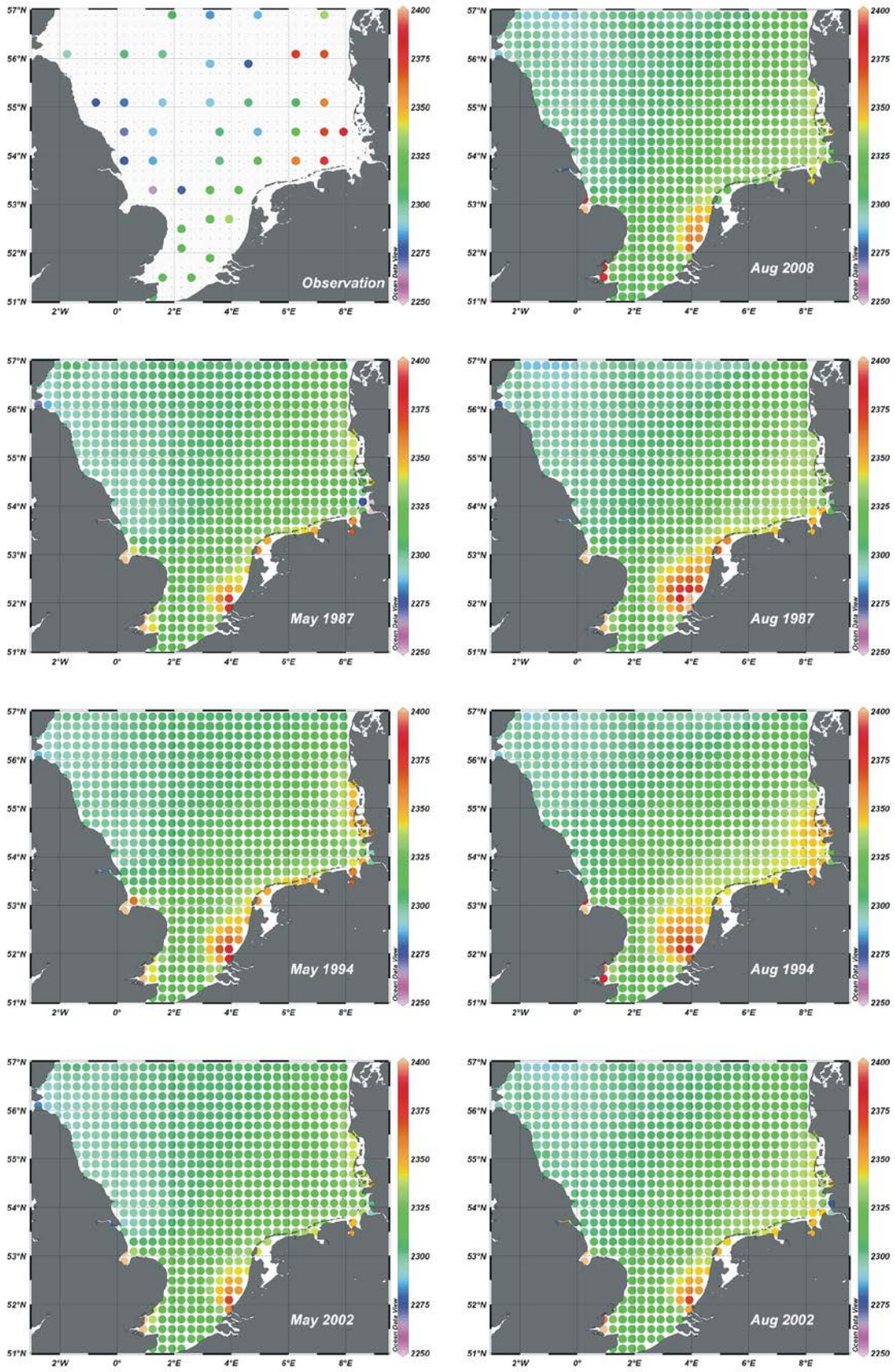

Fig. 2.11: Observed surface TA concentrations (August 2008) and simulated monthly mean surface TA concentrations [µmol kg^{-1}].

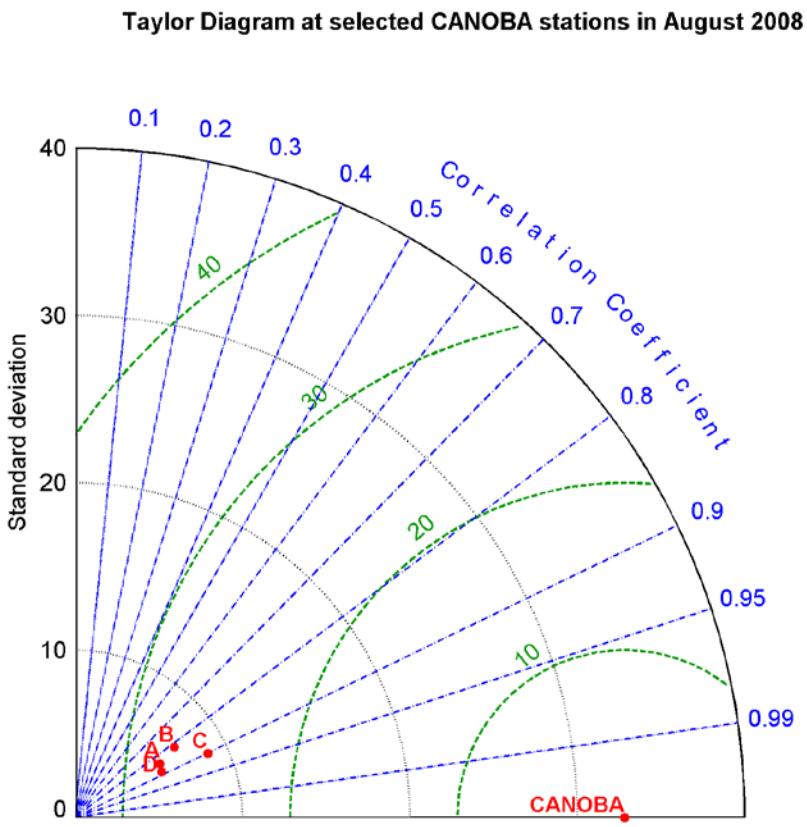

Fig. 2.12: Taylor diagram of simulated TA concentrations in 2008 (A), 1987 (B), 1994 (C) and 2002 (D) compared to observed TA concentrations (52 measurements) in the validation area.

2.4 Discussion

2.4.1 The impact of internal processes on TA

Modelled TA in this study was calculated prognostically. Changes of nitrate, ammonium and phosphate concentrations changed the TA concentration as well as calcification and decalcification. Phosphate-related processes (F_{13-17}) have only minor impact on TA compared to nitrogen-related processes because fixed N:P ratios were assumed (see 2.2.5). Ammonium-related processes (F_4, F_{6-11}) did not lead to changes in net TA because ammonium is an intermediate product produced through incomplete oxidation of organic matter (Hu and Cai, 2011). Nevertheless, it was important to include these processes into the model in order to obtain a closed TA budget even on smaller temporal and spatial scales, because these processes could potentially occur in different areas. During the course of the year calcification and decalcification affected the TA turnover noticeably, but they were balanced at the end of the year (Fig. 2.3). The amplitudes of their influences were determined by an assumed ratio of POC / PIC = 40 mol C mol^{-1} C for flagellates, which was a rather low estimate compared to other model studies that applied ECOHAM (Kühn et al., 2010; Lorkowski et al., 2012). However, higher values would increase the overall TA turnover only marginally in summer.

The main internal processes that changed TA in this model were nitrogen-related. In this context Hu and Cai (2011) discussed the amount of irreversibly produced net TA of ocean margins that is exported to the open oceans. Only the permanent loss of anaerobic remineralisation products could contribute to the production of TA on larger spatial and temporal scales, e.g. due to denitrification and pyrite burial. Hu and Cai (2011) also stated that a complete coupling of ammonification (+1), nitrification (-2) and denitrification (+1) would not lead to a net TA gain (numbers in brackets show the changes in TA due to the amount of nitrogen that gets converted). The coupling of these processes occurs widely in continental shelves (Seitzinger et al., 2006) and dominates also in the North Sea (except for the Wadden Sea) (Raaphorst et al., 1990; Seitzinger & Giblin, 1996). Only the denitrification of allochthonous nitrate leads to a net increase of TA. This does not apply to the atmospheric deposition of nitrogen because if atmospheric nitrate / ammonium enters the water column it decreases / increases the TA concentration at first, which counteracts the impact on TA when the respective species is taken up.

The corresponding process in this model that removes anaerobic remineralisation products was benthic denitrification fuelled by benthic nitrification. Benthic denitrification fuelled by pelagic nitrate invading the sediment from overlaying layers was neglected due to the lack of a vertical resolution of the sediment module (Pätsch & Kühn, 2008). In this case, denitrification would directly affect the TA turnover because it consumes pelagic nitrate, which is in contrast to

denitrification coupled with nitrification. Nevertheless, former studies revealed that denitrification is mainly coupled with nitrification in North Sea sediments (except for the Wadden Sea), so that the relating uncertainty should be small (Raaphorst et al., 1990; Seitzinger & Giblin, 1996; Pätsch & Kühn, 2008). According to the model developments by Pätsch & Kühn (2008), pelagic denitrification under anoxic conditions was also included in the model but did not occur.

During benthic remineralisation the nitrogen was released from the sediment as ammonium (F_{10}) that could be nitrified afterwards (F_4) and released as molecular nitrogen (N_2). The coupling of sedimentary ammonification, nitrification and denitrification of remineralised nitrogen was parameterised as in Pätsch & Kühn (2008) and depends on oxygen consumption (Seitzinger and Giblin, 1996). Hence, it was calculated without simulating the intermediate products of denitrification. Benthic denitrification itself was not included in the prognostic treatment of TA (compare (2.1)) because it was driven directly by organic nitrogen that was remineralised in the sediment. This is in accordance with the statement of Hu & Cai (2011) that the complete coupling of ammonification, nitrification and denitrification has no effect on net TA. They also stated that only the denitrification of allochthonous nitrate produces TA irreversibly, but this is not restricted to denitrification fuelled by pelagic nitrate. Changes in TA concentrations caused by denitrification of allochthonous nitrate were already included in the internal fluxes that consider the uptake of nitrogen (F_5, F_8). As a consequence, this means that most of net TA was already produced prior to denitrification, when nitrate was taken up by phytoplankton.

The produced TA in the validation area was 13.12 Gmol yr^{-1} in 2008, which could be mostly attributed to 14.93 Gmol yr^{-1} of incorporated allochthonous nitrate that entered the validation area either by river loads or by exchange with the adjacent North Sea (Fig. 2.7). The remaining -1.81 Gmol yr^{-1} could be attributed to short-time scale processes of the nitrogen cycle (-1.59 Gmol yr^{-1}), phosphate (-0.15 Gmol yr^{-1}) and calcite (-0.07 Gmol yr^{-1}).

The impact of evaporation and precipitation on TA concentration was also evaluated. The evaporation was calculated during the hydrodynamical part of the simulations and compared with climatological data of precipitation. Both effects were almost balanced out and ranged between 700 and 800 mm yr^{-1} in the German Bight. It was decided not to include evaporation and precipitation because the available data of precipitation (NCEP Reanalysis, Kalnay et al., 1996) were erroneous. They showed high deviations from the climatological data in the German Bight that decreased with distance to the coast.

2.4.2 Denitrification rate as an estimate of TA production

The prognostic treatment of TA implemented in this model study considered 17 different fluxes. It was shown that TA turnover and denitrification rates proceeded differently during the course of the year (Fig. 2.7). Nevertheless, they converged at the end of the year 2008, so it is worth estimating whether denitrification could be used as an estimate for nitrogen based TA turnover rates on annual scales.

The spatial distributions of annual mean denitrification and TA turnover rates are shown in Fig. 2.13 as well as the differences between them. Denitrification was steadily decreasing from the southeastern part to the northwestern part of the model. TA turnover rates showed a more complicated pattern in the whole model domain: the highest values were simulated near the outlet of the river Rhine, in the German Bight and near the outlets of the Thames and Wash estuaries. The pattern of TA turnover rates in the validation area was more heterogeneous than denitrification with high values in the eastern part and low values in the western part. The most differences occurred in an area that extended from the northern Dutch coast to the Danish coast. Denitrification rates were up to 1.2 mmol N m^{-2} d^{-1} higher than TA turnover rates in that area. Against this, TA turnover rates were up to 3.5 mmol TA m^{-2} d^{-1} higher than denitrification rates near the outlets of the rivers Rhine, Thames and Wash and about 0.3 mmol TA m^{-2} d^{-1} higher in some minor parts of the central North Sea.

The spatial deviation of denitrification and TA turnover can be due to three main reasons:

1. Denitrification does not change TA if the respective nitrogen source enters the model domain as total organic nitrogen (TON) e.g. via rivers or the southern and northern lateral boundaries of the model domain. In this case, denitrification exceeds TA turnover.

2. Atmospheric deposition of nitrogen does not change net TA after denitrification, although it is allochthonous. If 1 mol atmospheric nitrate / ammonium enters the water column, TA decreases / increases by 1 mol (compare F_{12} and F_{11} in (2.1)). The uptake of 1 mol nitrate / ammonium increases / decreases TA by 1 mol and thus counteracts the previous TA change. If this organic nitrogen gets denitrified, denitrification exceeds TA turnover.

3. Allochthonous nitrate is taken up by phytoplankton prior to denitrification in the model, which means that net TA is already produced prior to denitrification. In this case either TA turnover or denitrification exceeds the other process.

The spatial deviation of denitrification and TA turnover can lead to misinterpretations of pelagic TA concentrations, the respective sources of TA and measured denitrification rates of the underlying sediment if the source of nitrate for denitrification is unclear. In this case, the correct sources of TA can be missed unintentionally. Denitrification does only change TA on site if it is fuelled by pelagic nitrate invading the sediment. As it was already discussed above, benthic denitrification is supposed to be fuelled by benthic nitrification in the North Sea (except for the Wadden Sea), but pelagic nitrate as source for denitrification should not be excluded completely. In short, local pelagic TA concentrations can hardly be attributed to denitrification rates in the North Sea.

Nevertheless, the annual biogeochemical TA production can be estimated from denitrification on larger spatial scales (e.g. Chen & Wang, 1999; Chen, 2002; Thomas et al., 2009). The annual amounts of produced TA and denitrified nitrogen are shown in Fig. 2.14 for the validation area and the whole model domain in the period 1977 - 2009. Denitrification was about 11.3 ± 3.4 Gmol yr^{-1} higher than TA turnover in the validation area in every year. The differences ranged from 4.8 Gmol yr^{-1} in 2002 to 29.6 Gmol yr^{-1} in 1979. Denitrification was about 12.6 ± 8.7 Gmol yr^{-1} higher than TA turnover in the whole model domain. TA turnover slightly exceeded denitrification only in 2002. The differences in the whole model domain ranged from -0.5 Gmol yr^{-1} in 2002 to 24.3 Gmol yr^{-1} in 1996 and were more variable than in the validation area. The differences between denitrification and TA turnover were higher in the first half of the simulation period than in the second half. Until / after 1992 the mean deviation was 13.9 Gmol yr^{-1} / 9.1 Gmol yr^{-1} in the validation area and 18.1 Gmol yr^{-1} / 7.7 Gmol yr^{-1} in the whole model domain.

The differences between denitrification and TA turnover in the whole model domain showed a higher variability than in the validation area. This is due to the amount of allochthonous TON that was denitrified in the respective areas. The validation area receives a permanent supply of TON mainly by rivers, whereas the whole model domain receives TON by rivers and via the lateral boundaries in the south and north. The latter underlie hydrodynamic variations that could exhibit unusual stream patterns in some years (compare Pätsch & Kühn, 2008), which in turn affected the TON supply in the model. This effect will also be discussed in a following chapter of this study.

The greatest deviation in the first half of the period was caused by elevated river loads of ammonium (Fig. 2.10) that were up to 4 Gmol yr^{-1} for all rivers in the German Bight in that time. The consumption of ammonium, either by uptake or by nitrification, consumes TA irreversibly. The uptake of 1 mol ammonium decreases TA by 1 mol, which becomes irreversibly if the produced TON is denitrified. Nitrification of 1 mol ammonium decreases TA

by 2 mol and the subsequent uptake of 1 mol nitrate increases TA by 1 mol, which also results in a decrease of TA by 1 mol.

The mean amount of nitrogen that was denitrified exceeded the mean amount of TA that was produced by about 85% in the validation area and by about 17% in the whole model domain. If only the second half of the simulated period is considered, denitrification exceeded TA turnover by about 65% in the validation area and by about 10% in the whole model domain. If the amount of TA that is produced by nitrogen-related processes should be assessed, the spatial and temporal extent of the entire redox cycle has to be considered. As a consequence, the contribution of TA that is produced in the German Bight to an overall North Sea TA budget can not be derived from denitrification solely. In contrast to this, annual TA production in the whole model domain can be approximated from denitrification, if a certain inaccuracy is accepted. This inaccuracy may further decrease if the entire northwest European Shelf is considered.

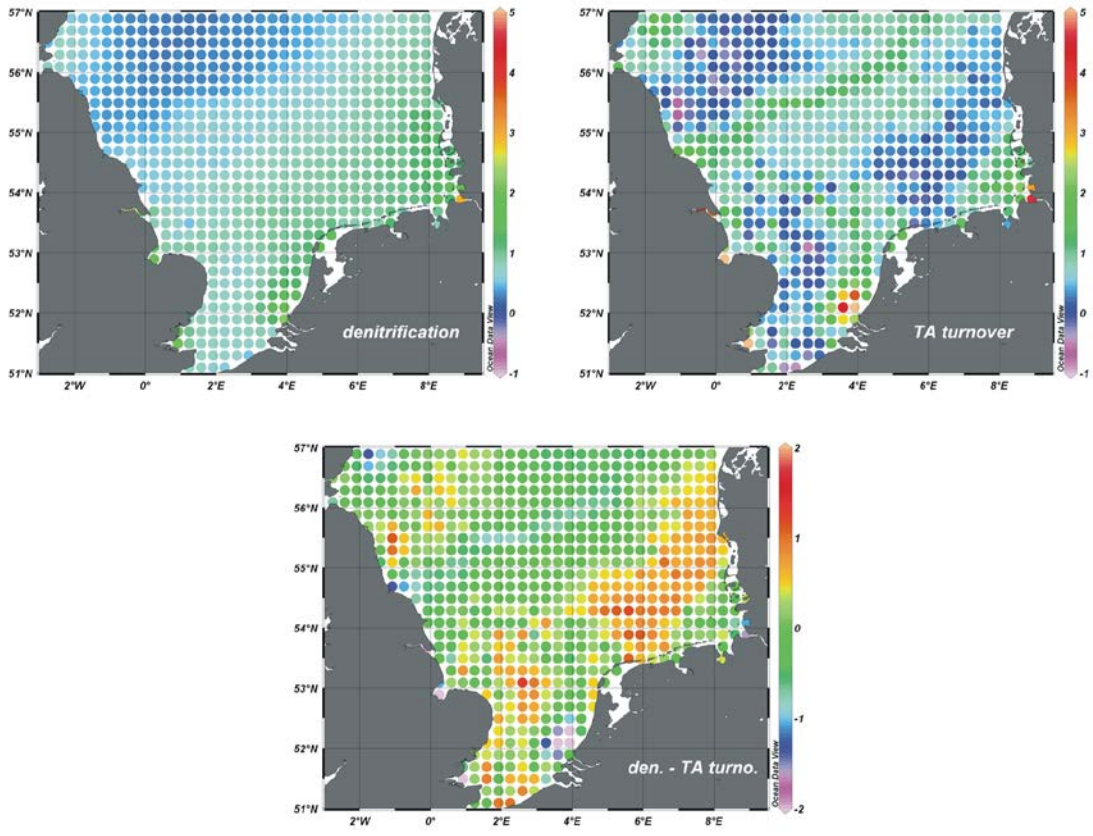

Fig. 2.13: Annual mean denitrification and TA turnover rates (top) and the differences (bottom) [mmol m^{-2} d^{-1}] in 2008.

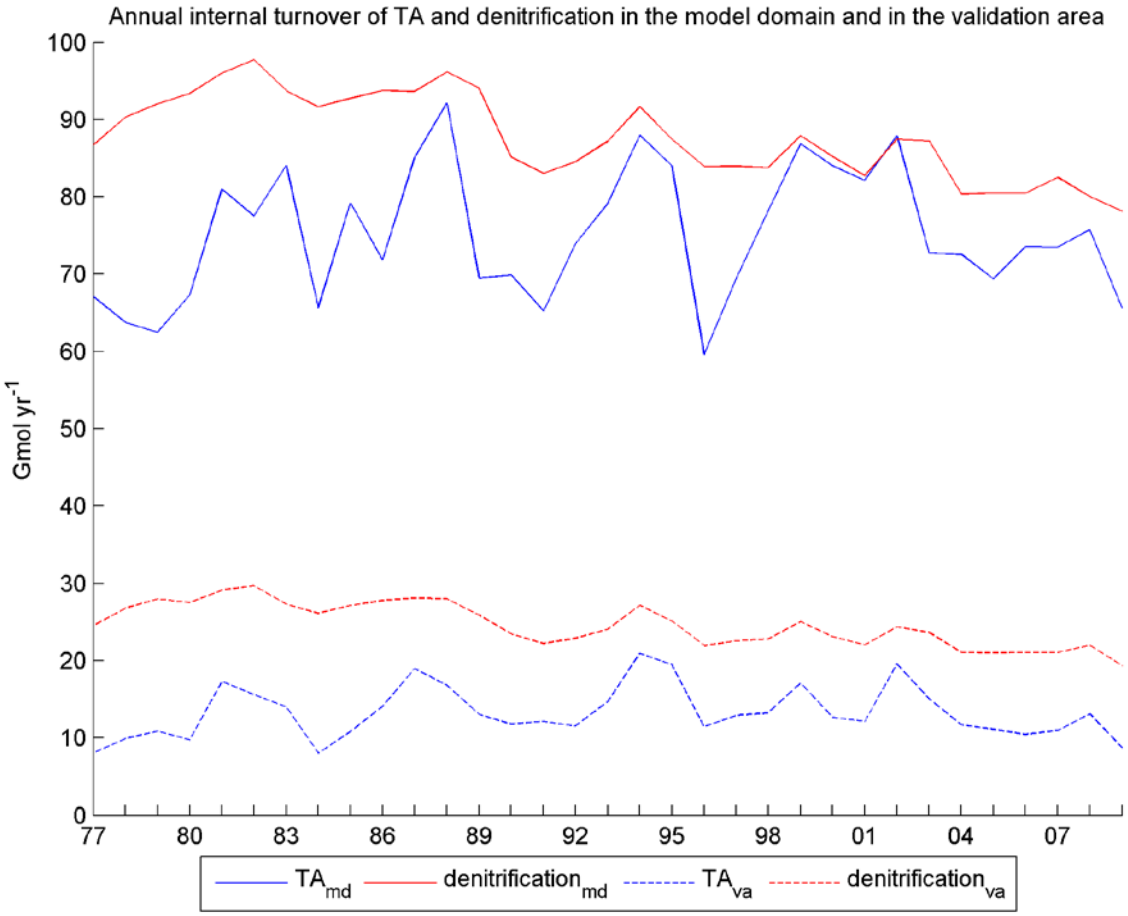

Fig. 2.14: Annual amounts of produced TA [Gmol yr^{-1}] and denitrification [Gmol N yr^{-1}] in the whole model domain (md) and in the validation area (va).

2.4.3 Model validation

Recent observations in the North Sea revealed high TA concentrations in the German Bight in summer. These values could not be reproduced with this model setup so far, neither in the respective year of observation (2008) nor in years with high river loads of nutrients (Fig. 2.11, 2.12). In 2008, most of TA was produced in April and May (Fig. 2.7) and caused the highest TA concentrations in these months (Fig. 2.8). In the simulated period, the highest TA concentrations in the German Bight were calculated in August 1994 (Fig. 2.11), which could not reproduce the observations either (Fig. 2.12). As a consequence, high TA concentrations in summer can not only be related to the turnover of allochthonous nitrogen, even if the highest differences in TA concentrations caused by TA turnover occur in the German Bight (Fig. 2.9).

2.5 Conclusion

Denitrification is only partly applicable as a proxy for annual TA production. It depends on the spatial extend of the investigated area. Thomas et al. (2009) considered modelled denitrification rates for their calculation of TA production in the North Sea, which was applicable as a first-order estimate of an overall annual budget. They also compared their calculation of TA exported from the Wadden Sea with denitrification rates measured in the Wadden Sea and assessed their own estimate as rather too low. Nevertheless, the findings in this chapter about the deviation of denitrification from TA turnover are also applicable for the Wadden Sea. Studies revealed a minor significance of coupled nitrification and denitrification there (Jensen et al., 1996; Deek et al., 2012) but in terms of TA production the coupling can be considered for a whole tidal basin. It does not matter for the TA exchange budget of a tidal basin whether denitrification is fuelled directly by nitrification in the respective upper sediment layer or by nitrification elsewhere in the tidal basin, but this will be discussed in more detail in a following chapter.

Furthermore, more sources of TA have to be identified in order to reproduce high TA concentrations in summer. The indirect impact of riverine nutrient loads was investigated in this chapter, but river loads of bulk TA can cause high variabilities during the course of the year that have not been considered in the model setup so far. In the next chapters, the impact of riverine TA loads and Wadden Sea exchange rates will be estimated.

3 Impact of river input on alkalinity concentrations in the southern North Sea

3.1 Introduction

Rivers are important sources of nutrients, TA, DIC and other components in coastal areas. The impact of riverine nutrient loads on TA concentrations in the German Bight is discussed in chapter 2. River loads of the British rivers were based on the report of Heath et al. (2002). The river loads of the more important continental rivers were based on the report of Pätsch & Lenhart (2008). This data set was also used in former model studies of the carbonate system of the North Sea and the northwest European Shelf (Artioli et al., 2012, Lorkowski et al., 2012). The data provide daily river loads for nutrients that were based on measured freshwater discharges and concentrations for each river. The data sets for TA and DIC were also based on measured daily freshwater discharges, whereas the concentrations for TA and DIC were based on one single concentration value in each case for each river. These concentrations were defined by the application of the end member approach as in Hjalmarsson et al. (2008).

River loads of bulk TA and bulk DIC are in focus of this chapter, because their variations could potentially lead to the observed high TA concentrations in the German Bight in summer. The direct effect of river loads on TA is in focus here, whereas the indirect effect of riverine nutrients is in focus of chapter 2. Especially variations in TA concentrations in the Elbe estuary can significantly affect TA concentrations in the German Bight (Brasse et al., 2002). Riverine TA and DIC concentrations can increase, e.g., due to increasing freshwater discharge in the Elbe estuary (Amann, 2013). Certainly, this correlation depends on the composition of the river catchment area and it can also be inverse in other estuaries as it was stated by Gypens et al. (2009) for the river Scheldt. Furthermore, also the plume of the river Rhine can affect TA concentrations in the German Bight (Hoppema, 1990; van den Berg et al., 1996) either directly due to its relatively high loads of TA (170 Gmol yr^{-1} in 2008) or indirectly due to high loads of nitrate (12.5 Gmol yr^{-1} in 2008). However, the respective data sets of TA and DIC loads provided by Pätsch & Lenhart (2008) are an adequate basis for calculations of the carbonate system in the open North Sea even if they lack seasonal accuracy, because seasonality is only

given by freshwater discharge. Nevertheless, variations in riverine TA concentrations have to be considered in order to get a more precise budget of TA sources and sinks in the German Bight.

The aim of this chapter is to improve the data basis for river loads in order to study the riverine impact on TA concentrations and thus the carbonate system in the German Bight. The overarching question is: Can seasonal variations in river loads of TA explain the observed high TA concentrations in the German Bight in summer 2008?

The first step is to take into account additional drainage of German rivers that originated from the areas downstream of the respective points of observation. Therefore, the freshwater discharges as well as the river loads of the rivers Elbe, Weser and Ems were increased by 21%, 19% and 30%. These corrective factors were already mentioned in the report of Pätsch & Lenhart (2008) but not adapted to the datasets. The increase of TA and nutrient river loads affected the TA concentrations in the German Bight directly and indirectly (e.g. by the uptake of nitrate). As a second step monthly variations in riverine TA and DIC concentrations of the most important continental rivers were implemented into the model. These improvements were based on different measurements of the carbonate system in the respective rivers (www.waterbase.nl, Amann, 2013). As a third step the impact of the river Rhine on TA concentrations in the German Bight was investigated. For this purpose, simulations without loads of the river Rhine were carried out.

The implemented changes in river loads also affected nutrient loads, especially loads from the German rivers. Therefore it was also investigated how much TA was additionally converted internally and where it was converted. These investigations can help to understand the spatial extent of a river plume of (indirect) potential TA that can differ from (direct) bulk TA. In order to compare the amounts of TA that were produced internally with TA river loads the “effective riverine TA” (Riv_{eff}) was defined. It was necessary because changes of TA concentrations came along with changes in (water) volume due to freshwater discharge, which also dilutes TA in the respective grid cell of the model.

The results of the simulations were compared with observations from August 2008 (Salt et al., subm.) when the high TA concentrations were observed in the German Bight.

3.2 Methods

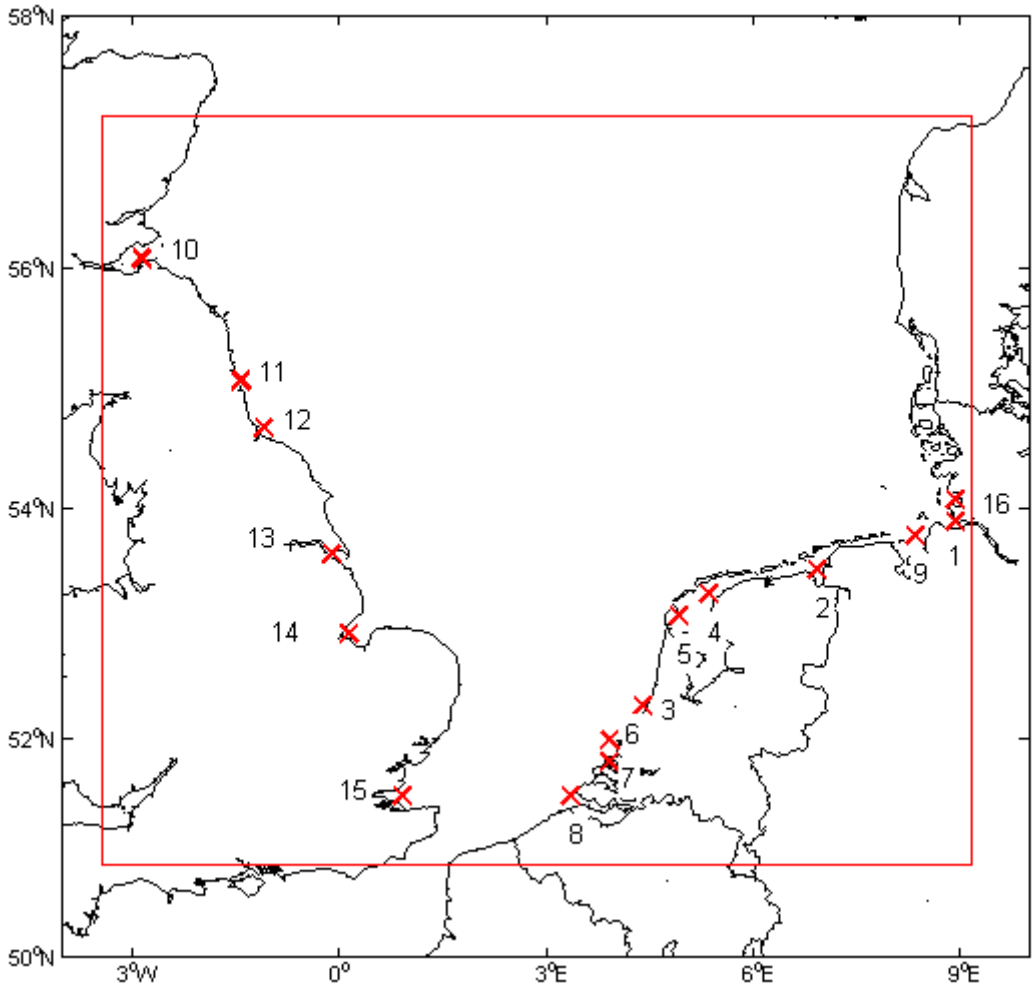

Figure 3.1: Model domain and the positions of rivers 1 – 16 (Tab. 3.1).

3.2.1 Freshwater discharge

The aim of this chapter is to improve the data basis for river loads. The implemented improvements also included the discharges of some rivers in the model, because climatological data sets (British rivers) were used or the respective point of observation was located far off the river mouth so that the data sets did not represent the whole catchment area of the river (German rivers).

Basically, the same model setup was used as in chapter 2: Daily fluxes of freshwater from 16 rivers were used (Fig. 3.1). For the German Bight and the other continental rivers daily observations of runoff were used (Pätsch & Lenhart, 2008). Additionally to the first simulations, the discharges of the rivers Elbe, Weser and Ems were increased by 21%, 19% and 30% in order to take additional drainage into account that originated from the area downstream of the

respective points of observation. These corrective factors were also mentioned in Pätsch & Lenhart (2008) but have not been considered for the calculation of the datasets. The data of HASEC (2012) were implemented for the British rivers with daily values for freshwater. The annual amounts of freshwater of the different rivers are shown in Tab. 1. These freshwater fluxes govern the salinity gradient from the coast into the North Sea and enhance the advection from the river mouths into the sea. Fig. 3.2 illustrates the sea surface salinity (SSS) in February (left) and August (right) of 2008. Riverine freshwater discharge was also considered for the calculation of the concentrations of all biogeochemical tracers in the model. As a consequence, it was possible to simulate dilution effects if the riverine concentration of a tracer was smaller than the concentration in the respective model area where the river discharged.

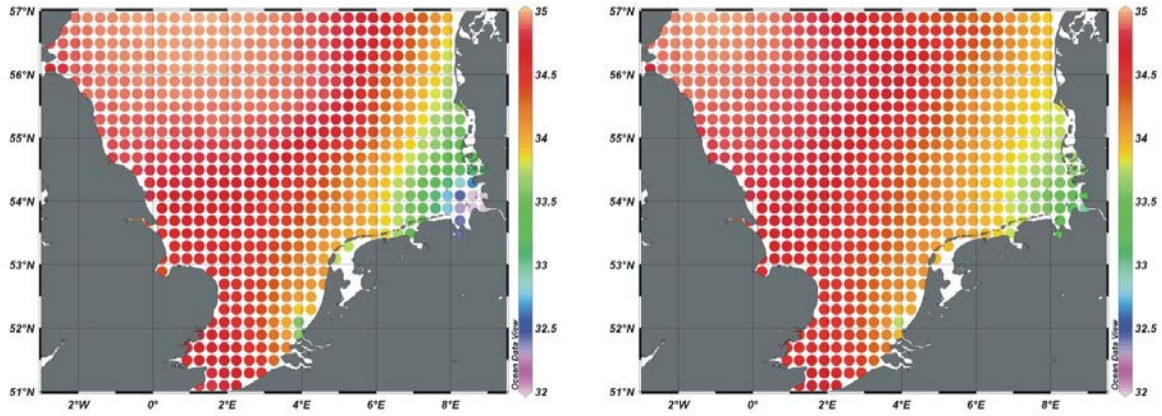

Figure 3.2: Simulated salinity [PSU] in February (left) and August (right) 2008.

It can be seen that the strong freshwater fluxes in winter (mean river Elbe discharge in February: 1420 m^3 s^{-1}) led to lower salinities in the German Bight than in summer (mean river Elbe discharge in August: 300 m^3 s^{-1}).

Table 3.1: Annual riverine freshwater discharge [km³ yr⁻¹].

	2001	2002	2003	2004	2005	2006	2007	2008	2009
Elbe	23.05	43.38	23.95	19.56	25.56	26.98	26.61	24.62	24.28
Ems	3.47	4.48	3.15	3.52	2.99	2.54	4.32	3.32	2.58
Noordzeekanaal	3.21	2.98	2.49	3.05	3.03	2.96	1.55	3.05	2.46
Ijsselmeer (east)	9.55	9.94	6.27	7.97	7.35	7.30	9.10	8.23	6.59
Ijsselmeer (west)	9.55	9.94	6.27	7.97	7.35	7.30	9.10	8.23	6.59
Nieuwe Waterweg	50.37	51.33	34.72	42.91	41.61	44.21	49.59	49.76	44.69
Haringvliet	33.10	35.18	17.92	10.77	12.36	16.02	24.00	15.70	11.06
Scheldt	7.28	2.74	4.31	3.64	3.59	3.74	4.63	4.57	3.63
Weser	11.43	18.97	11.80	10.52	10.37	9.72	16.21	12.59	9.58
Firth of Forth	2.72	3.76	2.06	3.01	3.00	2.84	2.85	3.59	3.66
Tyne	1.81	2.25	1.18	2.04	1.92	1.78	2.09	2.70	2.05
Tees	1.33	1.78	0.94	1.59	1.27	1.45	1.49	1.99	1.55
Humber	10.76	12.10	7.16	10.51	7.68	11.11	12.03	13.87	9.60
Wash	5.46	4.39	3.08	3.91	1.96	2.72	5.24	4.77	3.21
Thames	4.47	3.23	2.41	2.13	0.96	1.57	3.52	3.20	2.38
Eider	0.67	0.97	0.47	0.70	0.68	0.67	0.63	0.58	0.57
Sum	178.20	207.40	128.16	133.78	131.66	142.91	172.94	160.76	134.46

3.2.2 River loads of TA, DIC and nutrients

Up to now, no model setup took variations in riverine TA and DIC concentrations into account. Hence, the contribution of rivers to TA variations in the German Bight might be underestimated. Therefore, the dataset of riverine input was changed compared to the simulations in chapter 2. New data of freshwater discharge were introduced as well as TA and DIC loads for the British rivers (HASEC, 2012). Monthly mean concentrations of TA and DIC were added for the Dutch rivers and for the German river Elbe. The river loads were recalculated together with the respective freshwater discharges. For the Dutch rivers data of bicarbonate and pH of the years 2007 – 2009 (www.waterbase.nl) were used to calculate monthly mean concentrations of TA and DIC by applying CO2sys (Lewis & Wallace, 1998) with the set of constants from Millero (2006). Monthly mean concentrations of nitrate were also calculated for this period, in order to take into account that the riverine TA concentrations also depend on nitrate concentrations.

Additionally, new measurements of TA, DIC, nitrate and ammonium concentrations by Amann (2013) were used to recalculate river loads of the Elbe estuary. Concentrations at 5 km downstream of Glückstadt (km 679, see Tab. 3.2) were used from this data set for the river load

calculations of TA, DIC and nitrate in the model. As no measurements were available in January and June, interpolated concentrations from measurements in December and February or May and July were used. Concentrations of TA and DIC that were used for river load calculations in the study of Lorkowski et al. (2012) were 2231 and 2195 µmol kg^{-1} in every month. In comparison, TA concentrations in the study at hand were higher from November to March (2355 µmol kg^{-1} on average) and lower from April to October (1985 µmol kg^{-1} on average), whereas DIC concentrations were higher from October to March (2373 µmol kg^{-1} on average) and lower from April to September (2021 µmol kg^{-1} on average). The mean concentration of nitrate in the river Elbe used by Lorkowski et al. (2012) was 201 µmol kg^{-1} and was thus only slightly higher than the mean value in this study (197 µmol kg^{-1}). The concentrations used there were measured 51 km upstream (at Seemannshöft, km 628) from the sampling site of the study at hand.

Tab. 3.2: River Elbe concentrations at km 679 for TA, DIC, nitrate and ammonium [µmol kg^{-1}]. N is the number of available measurements. Concentrations in January and June (N=0) were calculated from December and February or from May and July, respectively.

month	N	TA	DIC	NO_3^-	NH_4^+
January	0	2380	2415	247.17	3.55
February	1	2272	2319	330.05	4.93
March	1	2293	2362	277.35	2.76
April	2	2083	2179	224.65	0.58
May	1	2017	2093	192.73	0.83
June	0	1967	2025	160.8	1.07
July	2	1916	1956	128.88	1.31
August	1	1768	1853	103.36	1.32
September	3	1988	2018	111.61	0.15
October	3	2156	2200	157.16	0.75
November	1	2342	2428	266.94	2.80
December	1	2488	2512	164.29	2.17

The data sources and positions of the river mouths of all 16 rivers are shown in Tab. 3.3 and in Fig. 3.1. The respective riverine concentrations of TA, DIC and nitrate are shown in the appendix (A6). Monthly TA- and DIC-concentrations of the river Elbe and the two river mouths of the river Rhine (Nieuwe Waterweg and Haringvliet) are shown in Fig. 3.3. The resulting river loads are shown in Fig. 3.4 – 3.6 and are compared with the previously used river loads in chapter 2. Certainly, river loads of other nutrients also change TA in the German Bight. However, they had only minor impact on TA in the simulated period (2001 – 2009) so it was decided to neglect them in this study in order to keep the changes as simple as possible.

Table 3.3: River numbers in Fig. 3.1, their positions and source of data for simulation C.

Number in Fig. 3.1	Name	River mouth position		Data source
1	Elbe	53°53'20"N	08°55'00" E	Pätsch & Lenhart (2008); TA-, DIC- and nitrate-concentrations by Amann (2013)
2	Ems	53°29'20"N	06°55'00"E	Pätsch & Lenhart (2008)
3	Noordzeekanaal	52°17'20"N	04°15'00"E	Pätsch & Lenhart (2008); TA-, DIC- and nitrate-concentrations from waterbase.nl
4	Ijsselmeer (east)	53°17'20"N	05°15'00"E	As above
5	Ijsselmeer (west)	53°05'20"N	04°55'00"E	As above
6	Nieuwe Waterweg	52°05'20"N	03°55'00"E	As above
7	Haringvliet	51°53'20"N	03°55'00"E	As above
8	Scheldt	51°29'20"N	03°15'00"E	As above
9	Weser	53°53'20"N	08°15'00"E	Pätsch & Lenhart (2008)
10	Firth of Forth	56°05'20"N	02°45'00"W	HASEC (2012)
11	Tyne	55°05'20"N	01°25'00"W	HASEC (2012)
12	Tees	54°41'20"N	01°05'00"W	HASEC (2012)
13	Humber	53°41'20"N	00°25'00"W	HASEC (2012)
14	Wash	52°53'20"N	00°15'00"E	HASEC (2012): sum of 4 rivers: Nene, Ouse, Welland and Witham
15	Thames	51°29'20"N	00°55'00"E	HASEC (2012)
16	Eider	54°05'20"N	08°55'00"E	Johannsen et al, 2008

A statistical analysis of uncertainties of the concentrations used for calculations of the new river loads was not possible, because only 3 values were available for each Dutch river and month. The respective concentrations are shown in the appendix. For the river Elbe only 1 – 3 (0 in January and June) measurements were available (Tab. 3.2).

3.2.3 Simulated scenarios

The years 2001 to 2009 were simulated with three spin-up years in 2000. Six different scenarios (A – F) were conducted as described below. The main differences between the scenarios are summarized in Tab. 3.4. The respective TA and DIC concentrations in the Elbe estuary and the river Rhine are shown in Fig. 3.3, the river loads are shown in Fig. 3.4 – 3.6.

A:

This was the simulation that was already introduced in the previous chapter and is the reference scenario: The prognostic treatment of TA was implemented and constant river concentrations for TA and DIC were used (Pätsch & Lenhart, 2008; Lorkowski et al., 2012). Interannual and seasonal variations of TA and DIC are proportional to freshwater discharges.

B:

This scenario was like A but with increased discharges of the German rivers Elbe, Weser and Ems by 21%, 19% and 30%. These corrective factors were applied to freshwater discharge and river loads. They were already mentioned in the report of Pätsch & Lenhart (2008) but not considered for the calculation of the dataset. This scenario was conducted in order to study the impact of the additional drainage that originated from the area downstream of the respective points of observation.

C:

This simulation was a further development of A because loads of TA and DIC were calculated more precisely for the main continental rivers. For that reason monthly variations of riverine TA and DIC concentrations were integrated (Tab. 3.3) as well as nitrate concentrations that were measured at the same place and time, respectively. All changes of riverine input that have been described in this chapter have been applied for this scenario.

D, E:

Further scenarios were conducted to examine the impact of the river Rhine on TA concentrations in the German Bight. This was an important step in order to localise the main drivers of TA there. River loads and freshwater dilution of the river Rhine were set to 0 in both scenarios. In this context, D and E represented the scenarios C and A with disabled input of the river Rhine.

F:

The impact of internal fluxes ($F_1 – F_{17}$, see chapter 2.2.7) was compared with riverine input of TA. Therefore, the setup of simulation C was used but without the impact of internal fluxes on TA. Note that only the impact on TA was switched off and not the respective fluxes itself.

Tab. 3.4: Summary of the main features of simulations A – F: "Prognostic TA" is the concentration change of TA due to internal processes (see previous chapter). "German river discharge" keeps track of the corrected discharge of the rivers Ems, Weser and Elbe. "River configuration" means the implementation of all described changes in this chapter concerning riverine concentrations and loads of TA, DIC and nitrate. "River Rhine loads" means if the river Rhine is implemented into the model or not.

Simulation	prognostic TA	German river discharge	River configuration	River Rhine loads
A	enabled	uncorrected	unchanged	enabled
B	enabled	**corrected**	unchanged	enabled
C	enabled	**corrected**	**changed**	enabled
D	enabled	**corrected**	**changed**	**disabled**
E	enabled	uncorrected	unchanged	**disabled**
F	**disabled**	**corrected**	**changed**	enabled

3.2.4 Changed river input

As it is shown in Fig. 3.3 (compare "A" and "C"), river Rhine concentrations of TA and DIC were about 100 to 200 µmol kg^{-1} lower in scenario A compared to the annual mean of the concentrations used in scenario C. The TA concentration of the Elbe estuary was about 50 µmol kg^{-1} higher in A compared to the annual mean of the concentrations used in C whereas the DIC concentration did not differ much. In fact the seasonal variability in the Elbe estuary is higher than in the river Rhine, which was represented by low TA and DIC concentrations in summer and high concentrations in winter (compare Tab. 3.2). Concentrations that were used in scenario A were the same as in Lorkowski et al. (2012) or in the report of Pätsch & Lenhart (2008). Especially the low concentrations in the Elbe estuary in August indicated an increased dilution effect in the German Bight near the river mouth that could not be resolved without variations in riverine TA and DIC concentrations.

Compared to scenario A and the report of Pätsch & Lenhart (2008) the implemented changes in riverine concentrations of TA and DIC increased the annual river loads of TA and DIC of the Elbe estuary by 8 to 10 Gmol yr^{-1} and the loads of the river Rhine by 10 to 20 Gmol yr^{-1} (compare figure 3.4). The loads of the remaining continental rivers increased by 5 to 10 Gmol yr^{-1}. There were no current data of TA and DIC measurements available for the rivers Weser and Ems, so the same concentrations (2356 µmol kg^{-1} for both) were used as in the study of Lorkowski et al. (2012). The differences between TA and DIC loads of the British rivers were more diverse because they were already treated more precisely (HASEC, 2012).

River loads of nitrate of the Elbe estuary increased by almost 0 to 1 Gmol yr^{-1} and the loads of the remaining continental rivers increased by 0.2 to 1 Gmol yr^{-1} (figure 3.5). Nitrate loads of the river Rhine were up to 1.5 Gmol yr^{-1} lower in most of the years except for the years 2003 and 2009. Nitrate loads of the British rivers were constantly about 10 Gmol yr^{-1} in scenario A, whereas loads in scenario C ranged between 5.5 and 11.5 Gmol yr^{-1}. This revealed a certain inconsistency because loads of TA and DIC slightly varied. This was mainly because loads of the British rivers were developed step by step for scenario A and thus for river loads that were used in the study of Lorkowski et al. (2012). River loads of nutrients are based on climatological data (Heath et al., 2002) and loads of TA and DIC are partly derived from the study of Neal (2002). The newly implemented data of HASEC (2012) provide a dataset from a single source and allows replacing of the climatological data by daily values.

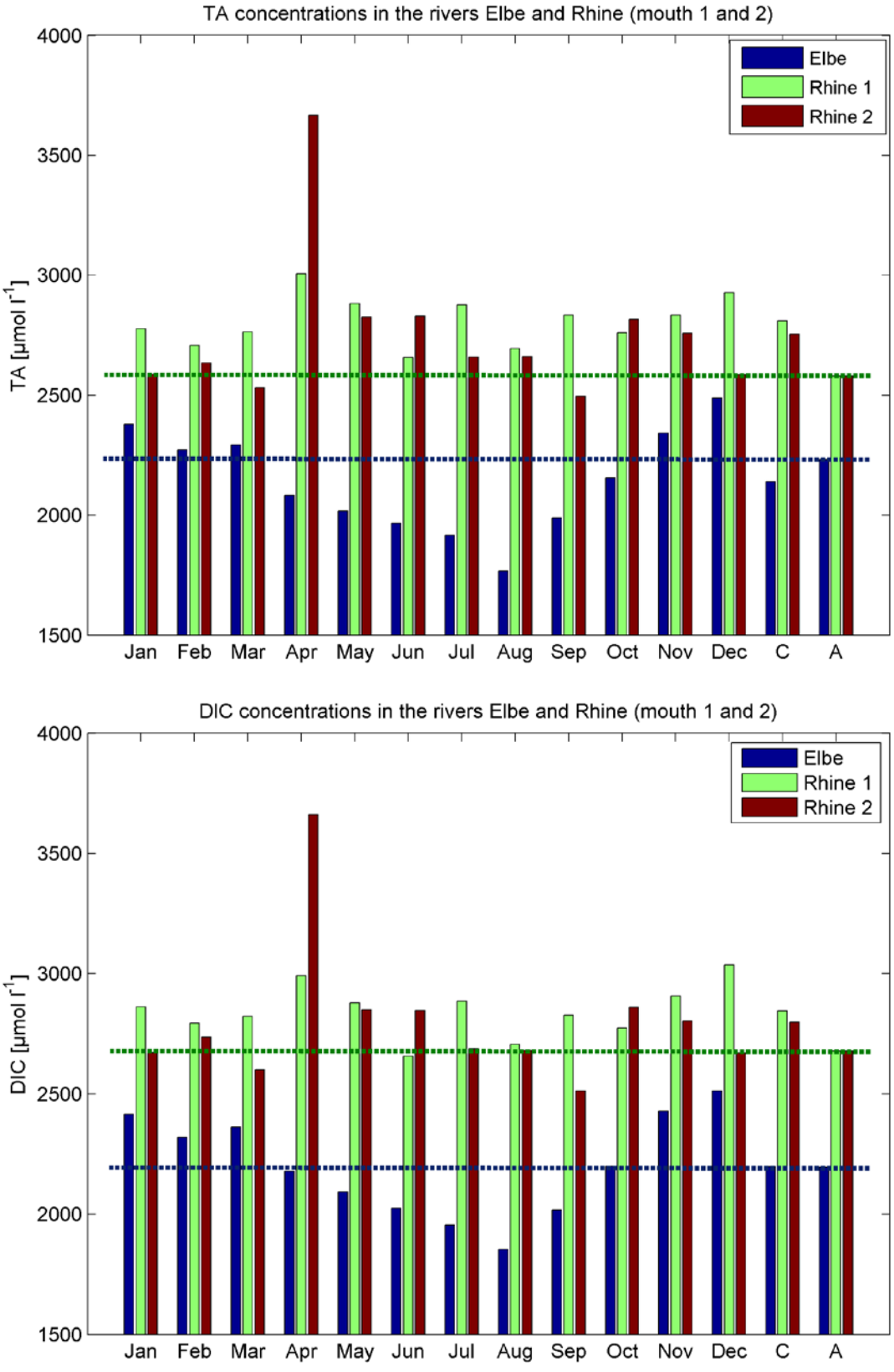

Figure 3.3: Monthly TA and DIC-concentrations [µmol kg^{-1}] in the rivers Elbe and Rhine. Rhine 1 and Rhine 2 are river number 6 and 7 in Fig. 3.1 and Tab. 3.3. The dashed lines are the concentrations that were used in simulation A and in the previous chapter. The annual mean concentration of the new river loads in the recent chapter is defined as "C".

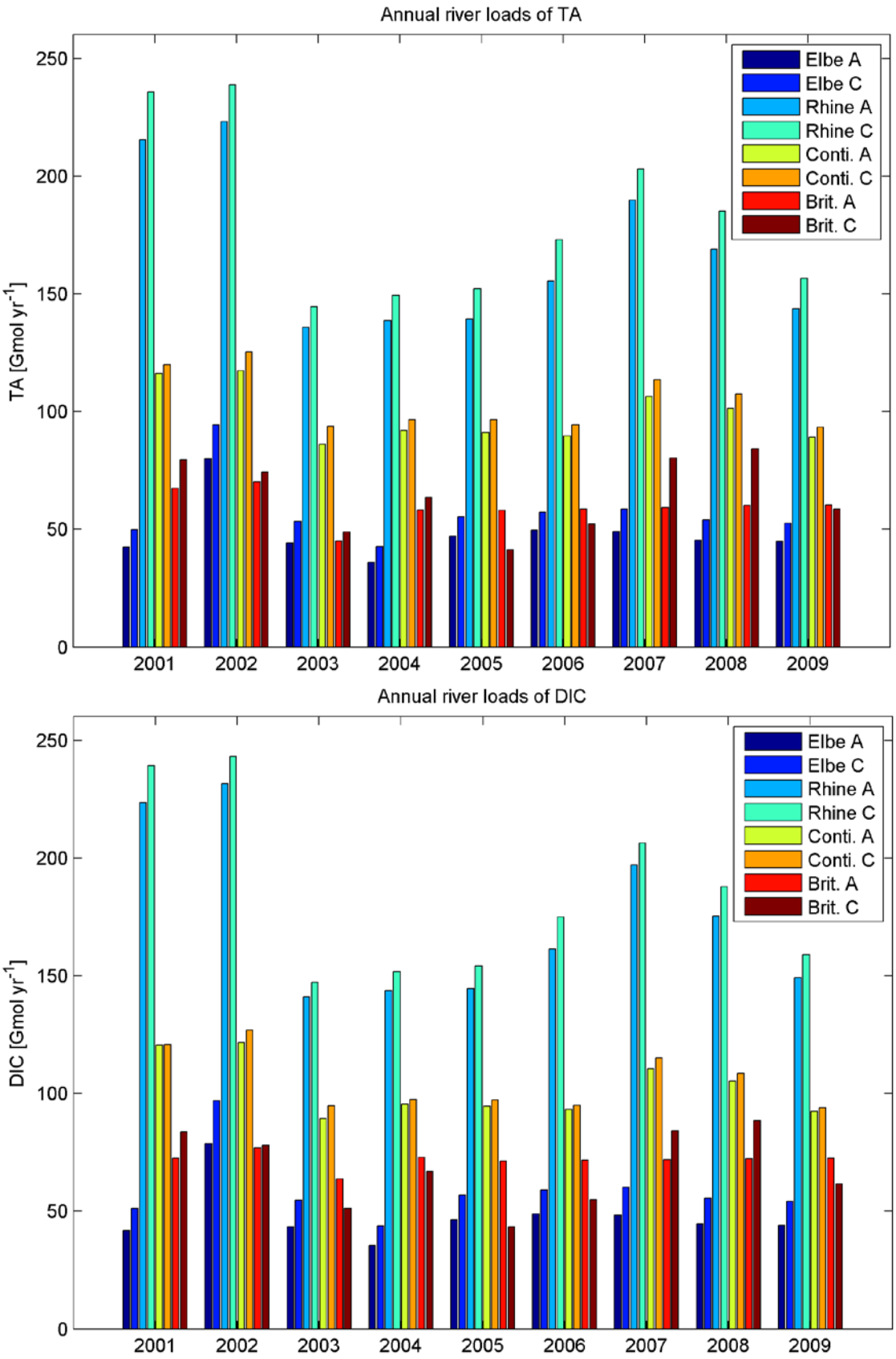

Fig. 3.4: Annual export of riverine TA and DIC in simulations A and C (and D, F) of the rivers Elbe, Rhine (both river mouths), the remaining continental rivers and the British rivers [Gmol yr^{-1}].

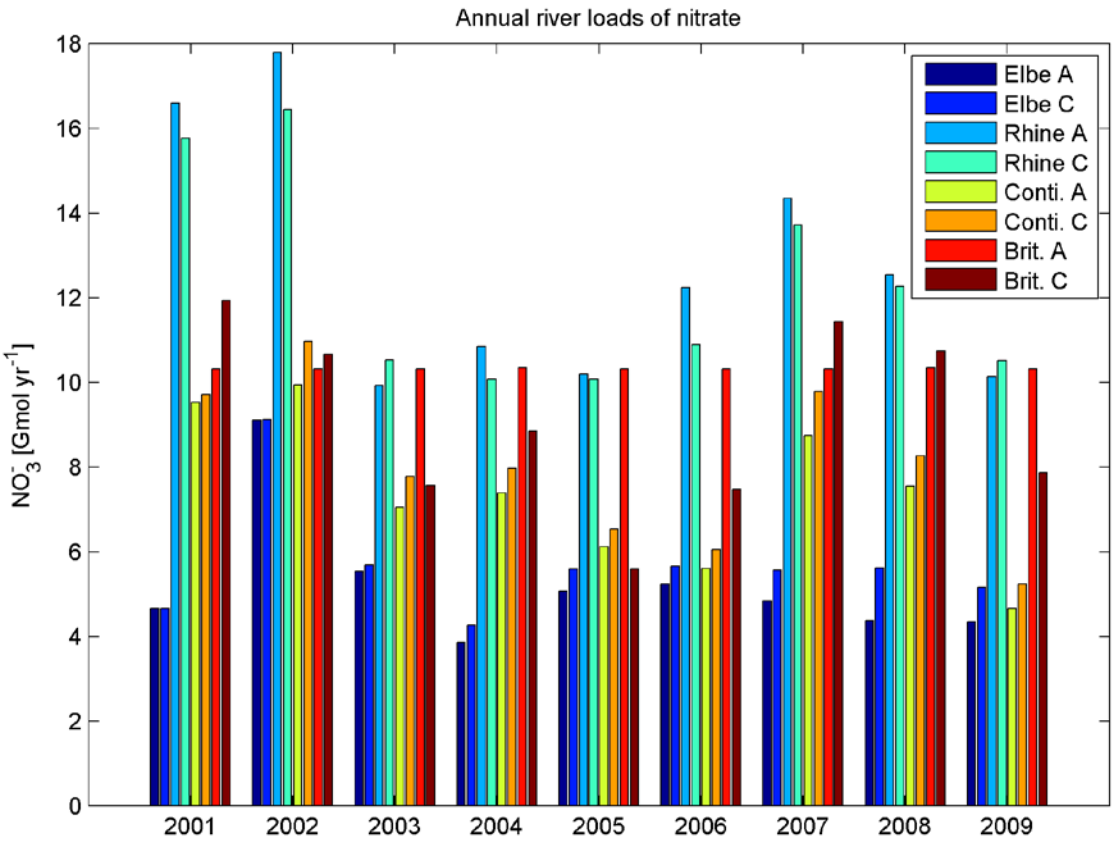

Fig. 3.5: Annual export of riverine nitrate in simulations A and C (and D, F) of the rivers Elbe, Rhine (both river mouths), the remaining continental rivers and the British rivers.

3.3 Results

3.3.1 Seasonal TA concentrations in 2008

The effects of the implemented new river input data on TA concentrations are shown in Fig. 3.6 and 3.7. Surface TA concentrations in scenario A and C are shown for February, May, August and November 2008 in Fig. 3.6. The differences between scenario B and A as well as between C and A are shown in Fig. 3.7 in order to highlight the resulting changes in TA concentrations in the German Bight. The scale in Fig. 3.7 was chosen in order to highlight differences in TA concentrations in the German Bight. As a consequence, the concentrations at the western Dutch coast were higher than the maximum value of the chosen scale in every month but these values are also mentioned in the following.

3.3.1.1 February

TA concentrations in scenario A ranged between 2275 µmol kg^{-1} at the Elbe estuary, 2345 µmol kg^{-1} at the mouth of the river Rhine and 2450 µmol kg^{-1} at the Thames estuary. TA concentrations in scenario B were about 5 to 7 µmol kg^{-1} lower at the Elbe estuary. In scenario C the TA concentrations were lower near the most rivers at the British coast except for the river Humber, where TA concentrations were up to 20 µmol kg^{-1} higher than in scenario A. This pattern of concentration differences was simulated at the British coast in every season. TA concentrations increased about 15 µmol kg^{-1} near the river Rhine. Furthermore, the TA concentrations increased about 3 to 15 µmol kg^{-1} in an area that was located east of 4°E and south of 55.5°N.

3.3.1.2 May

TA concentrations in scenario A ranged between 2275 µmol kg^{-1} at the Elbe estuary, 2350 µmol kg^{-1} in the Jade Bay (around 8.3°E and 53.5°N) and 2435 µmol kg^{-1} at the Thames estuary. TA concentrations in scenario B slightly increased about 2 to 4 µmol kg^{-1} at the northeastern part of the Dutch coast, at the Danish coast between 55°N and 55.5°N and in the Jade Bay. They decreased about 20 µmol kg^{-1} at the Elbe estuary. In scenario C the concentrations increased up to 100 µmol kg^{-1} in the direct vicinity of the river Rhine. They increased about 4 to 8 µmol kg^{-1} in an area located east of 6°E and south of 56°N. Furthermore, the TA concentrations also decreased around 6 to 100 µmol kg^{-1} near the Elbe estuary.

3.3.1.3 August

TA concentrations in scenario A ranged between 2290 µmol kg^{-1} in the northwestern part of the model domain, 2360 µmol kg^{-1} at the western part of the Dutch coast and 2380 µmol kg^{-1} at the Thames estuary. In scenario B the concentrations increased about 4 µmol kg^{-1} in the Jade Bay.

In scenario C the concentrations increased about 10 to 20 µmol kg^{-1} at the western part of the Dutch coast and about 3 to 6 µmol kg^{-1} in an area located roughly east of 4°E and south of 56°N. Furthermore, the TA concentrations also decreased around 6 to 50 mmol kg^{-1} near the Elbe estuary.

3.3.1.4 November

TA concentrations in scenario A ranged between 2280 µmol kg^{-1} in the northwestern part of the model domain and 2395 µmol kg^{-1} at the Thames estuary. In scenario B the differences in concentrations were all over below 1 µmol kg^{-1}. In scenario C the concentrations increased about up to 20 µmol kg^{-1} at the western part of the Dutch coast and up to 4 µmol kg^{-1} in an area that was located between 6°E and 8°E and between 54°N and 56°N. The TA concentrations decreased about 4 to 10 µmol kg^{-1} near the Elbe estuary.

In summary, the differences in TA concentrations were more pronounced in scenario C than in scenario A. In scenario C the TA concentrations showed a more heterogeneous pattern in the German Bight, especially in May and August. The concentrations decreased near the Elbe estuary, whereas they significantly increased west of 8°E.

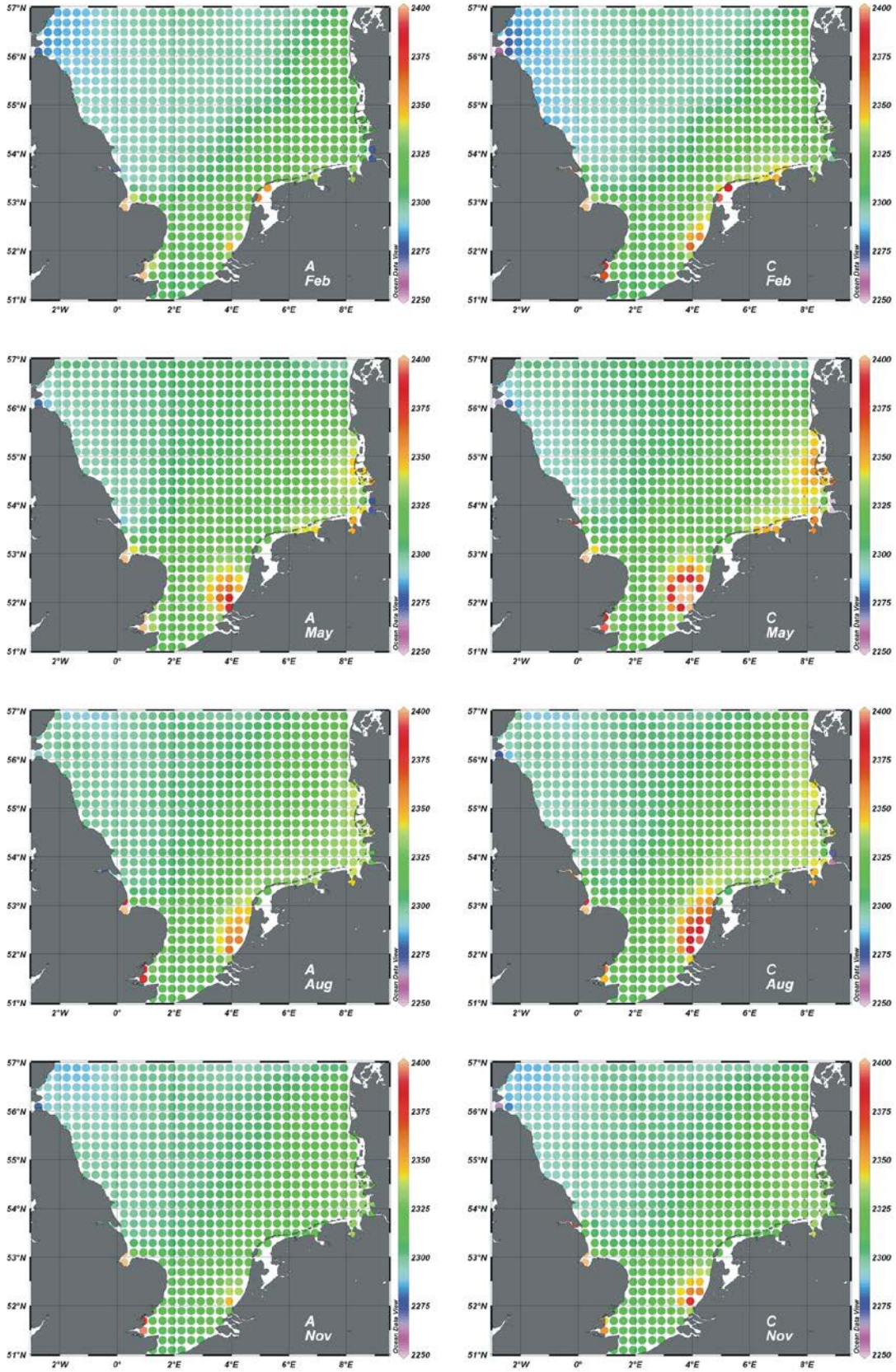

Fig. 3.6: Simulated surface TA-concentrations [µmol kg^{-1}] in scenario A and C in 2008.

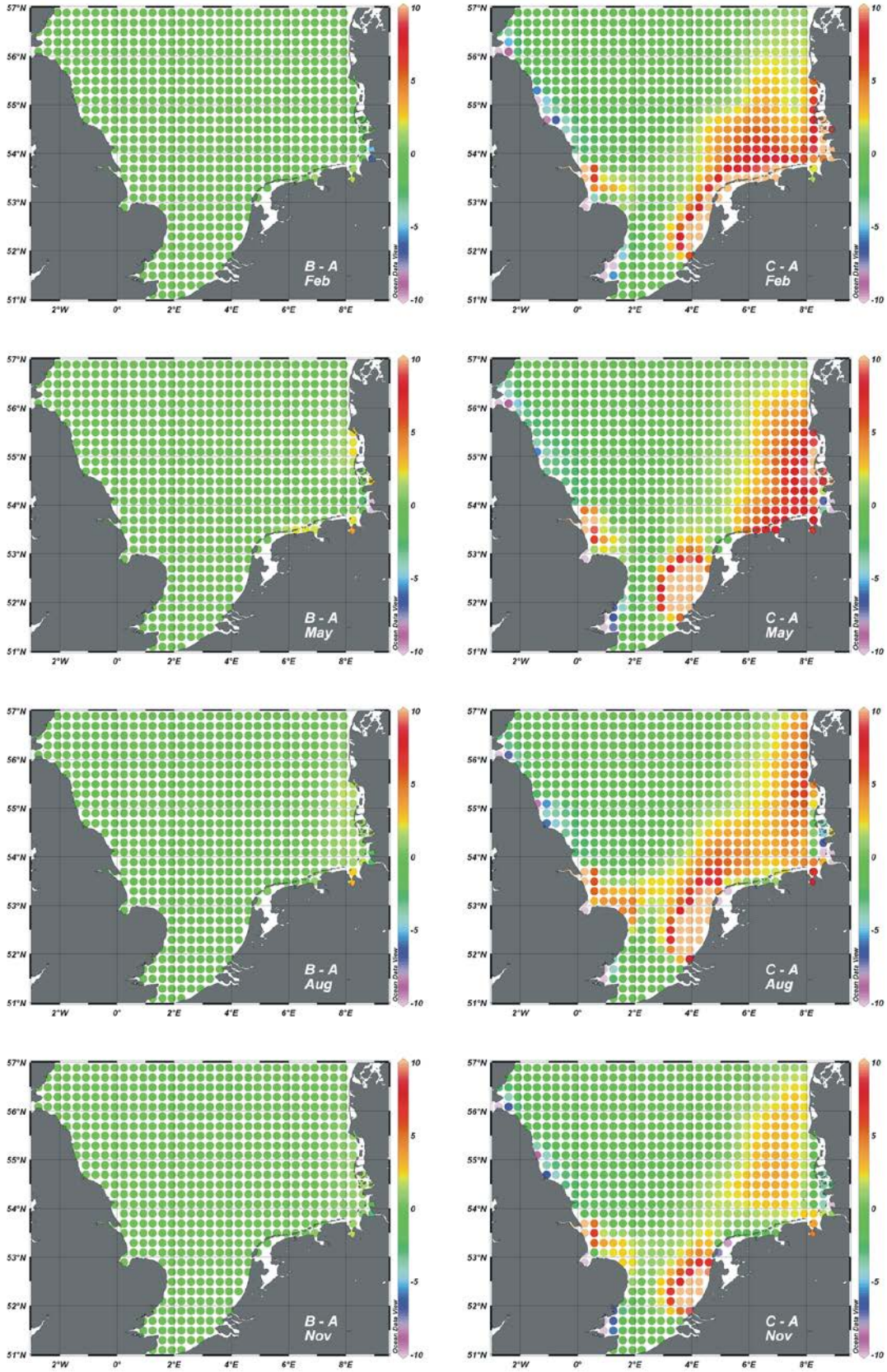

Fig. 3.7: Differences in TA-concentrations [µmol kg^{-1}] between scenario B and A as well as C and A.

3.3.2 Seasonal internal TA production in 2008

The implemented changes in river input contained changes in loads of nitrate. Hence, the internal turnover of TA is also affected. The internal turnover of TA was already explicitly discussed in chapter 2. Thus it was presented as the sum of all 17 fluxes in the chapter at hand. The differences between scenario B and A as well as between C and A are shown in Fig. 3.8 in order to highlight the resulting changes in internal TA turnover in the German Bight.

3.3.2.1 February

Changes in the internal turnover of TA were all over below 0.5 mmol m^{-2} d^{-1} in scenario B. In scenario C it increased about 0.6 mmol m^{-2} at the rivers Elbe and Wash and between 0.6 to 1.5 mmol m^{-2} d^{-1} at the river Humber.

3.3.2.2 May

In both scenarios (B and C) the internal turnover of TA increased similarly about 0.4 to 1.0 mmol m^{-2} d^{-1} in the German Bight and at the northern Dutch coast. In scenario C the internal turnover of TA increased about 1.5 mmol m^{-2} d^{-1} at the Elbe estuary, whereas it decreased at the rivers Wash and Firth of Forth about 1.4 to 2.0 mmol m^{-2} d^{-1}.

3.3.2.3 August

In scenario B the internal turnover of TA increased about 0.4 to 0.7 mmol m^{-2} d^{-1} at the Elbe estuary and along 8°E between 54°N and 55.5°N. In scenario C the internal turnover of TA increased about 0.5 to 2.0 mmol m^{-2} d^{-1} in the same areas. Additionally, it increased about 0.3 mmol m^{-2} d^{-1} at the mouth of the river Rhine. Changes at the Britsh coast ranged between -1.4 and 1.5 mmol m^{-2} d^{-1}.

3.3.2.4 November

Changes in the internal turnover of TA were all over below 0.5 mmol m^{-2} d^{-1} in scenario B. In scenario C it increased about 0.6 mmol m^{-2} d^{-1} at the Elbe estuary and it decreased up the 1.8 mmol m^{-2} d^{-1} at the river Thames.

In summary, most changes of the internal turnover of TA were located in the German Bight in May and August. In scenario A 13.12 Gmol TA yr^{-1} were internally produced in the validation area (east of 4.5°E, north of 53.5°N and south of 55.5°N) in 2008. It increased about 1.54 Gmol TA yr^{-1} in scenario B and about 1.79 Gmol TA yr^{-1} in scenario C. Nevertheless, it is remarkable that almost no changes occurred at the western Dutch coast.

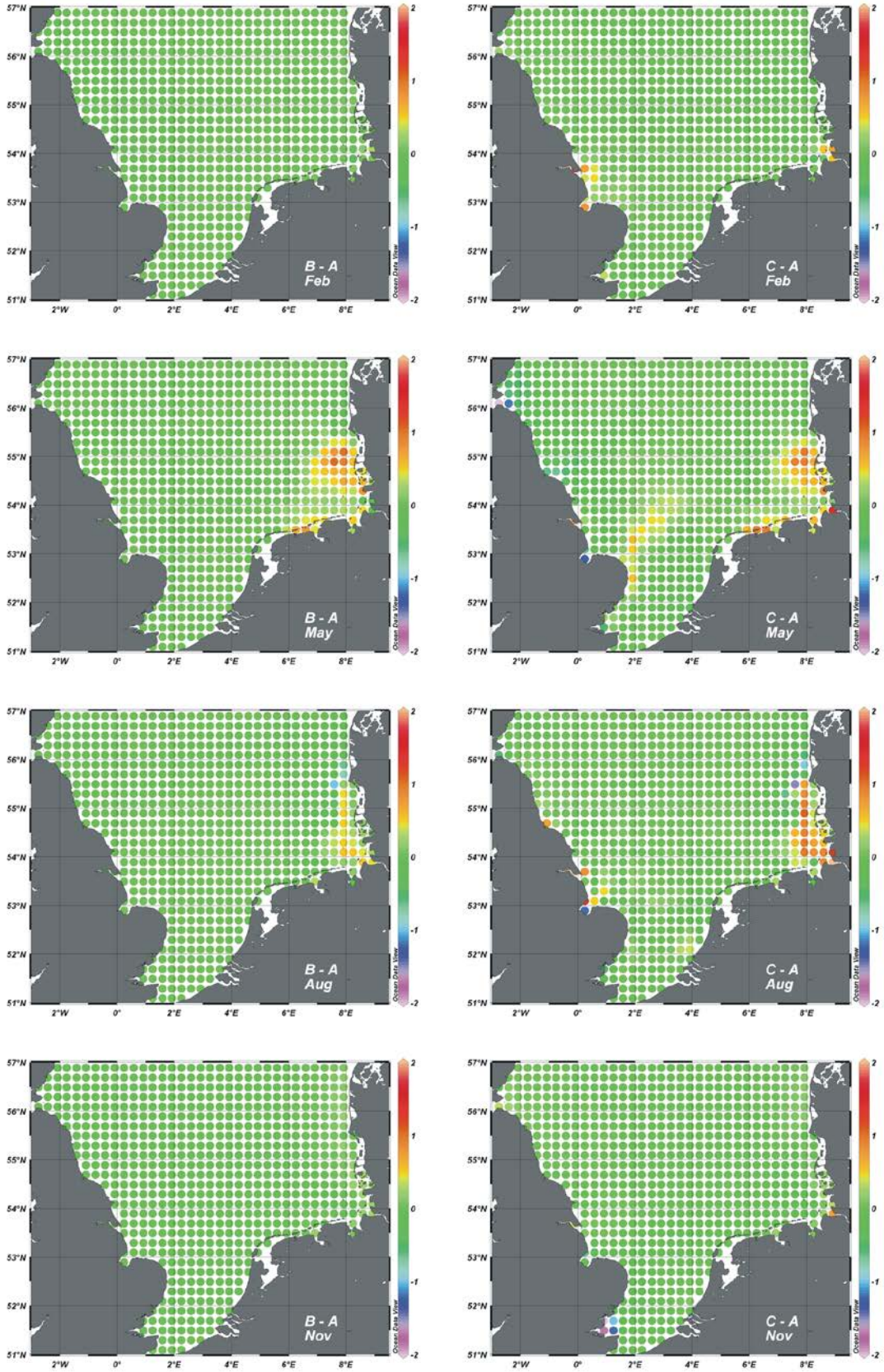

Fig. 3.8: Differences in internal turnover rates of TA [mmol m^{-2} d^{-1}] between scenario B and A as well as C and A.

3.3.3 TA originating from the river Rhine in 2008

The differences in TA concentrations between scenario A and E as well as between C and D are shown Fig. 3.9. These scenarios were conducted in order to study the impact of the river Rhine on TA concentrations in the German Bight. Furthermore, the differences in the internal turnover between these scenarios are shown in Fig. 3.10.

3.3.3.1 February

In scenario A the impact of the river Rhine on TA concentrations ranged between 4 µmol kg^{-1} near the island of Sylt and 10 µmol kg^{-1} at the river Ems (Fig. 3.9). In scenario C this impact was more pronounced in the validation area. It ranged between 7 µmol kg^{-1} in an area north of 54.5°N and south of the island of Sylt and 17 µmol kg^{-1} near the river Ems and the northern part of the Dutch coast. The internal turnover of TA that was driven by the river Rhine ranged between -1 and 1.2 mmol m^{-2} d^{-1} near the river Rhine (Fig. 3.10).

3.3.3.2 May

In scenario A the impact of the river Rhine on TA concentrations was more homogeneous than in scenario C in an area east of 6.5°E and south of 56°N (Fig. 3.9). It ranged between 7 and 8 µmol kg^{-1}, whereas it ranged between 7 µmol kg^{-1} around 6.5 °E and 12 µmol kg^{-1} near the island of Sylt and the Jade Bay. The internal turnover of TA driven by the river Rhine was most pronounced in this month (Fig. 3.10). It ranged between 3 mmol m^{-2} d^{-1} at the north western part of the Durch coast and 10 mmol m^{-2} d^{-1} near the river Rhine. Additionally, the internal turnover of TA was driven by the river Rhine about 2 to 4 mmol m^{-2} d^{-1} in the western and middle part of the validation area.

3.3.3.3 August

In both scenarios the areal extent of the impact of the river Rhine on TA concentrations was largest in this month (Fig. 3.9). In scenario A it ranged between 7 and 8 µmol kg^{-1} in most parts of the validation area and between 10 and 12 µmol kg^{-1} at the northern part of the Dutch coast. In scenario C it ranged between 8 µmol kg^{-1} in the central northern part of the validation area (around 7°E and 55°N), 11 µmol kg^{-1} near the island of Sylt and 17 µmol kg^{-1} at the northern part of the Durch coast. The internal turnover of TA was induced slightly negative by the river Rhine (-0.5 to -1.5 mmol m^{-2} d^{-1}) in the eastern and middle part of the validation area (Fig. 3.10).

3.3.3.4 November

In scenario A the impact of the river Rhine on TA concentrations ranged between 7 and 8 µmol kg^{-1} in most parts of the validation area (Fig. 3.9). In scenario C it ranged between 7 µmol kg^{-1}

at the western and northern edge of the validation area and 12 µmol kg^{-1} in an area east of 6°E and south of 55°N. The internal turnover of TA was induced about 2 mmol m^{-2} d^{-1} near the river Rhine.

In summary, the impact of the river Rhine on TA concentrations in the German Bight was more heterogeneous and more pronounced in scenario C than in scenario A. The internal turnover of TA was induced by the river Rhine similarly in both scenarios. In scenario A / C 1.21 / 1.14 Gmol TA yr^{-1} were produced internally in the validation area in 2008.

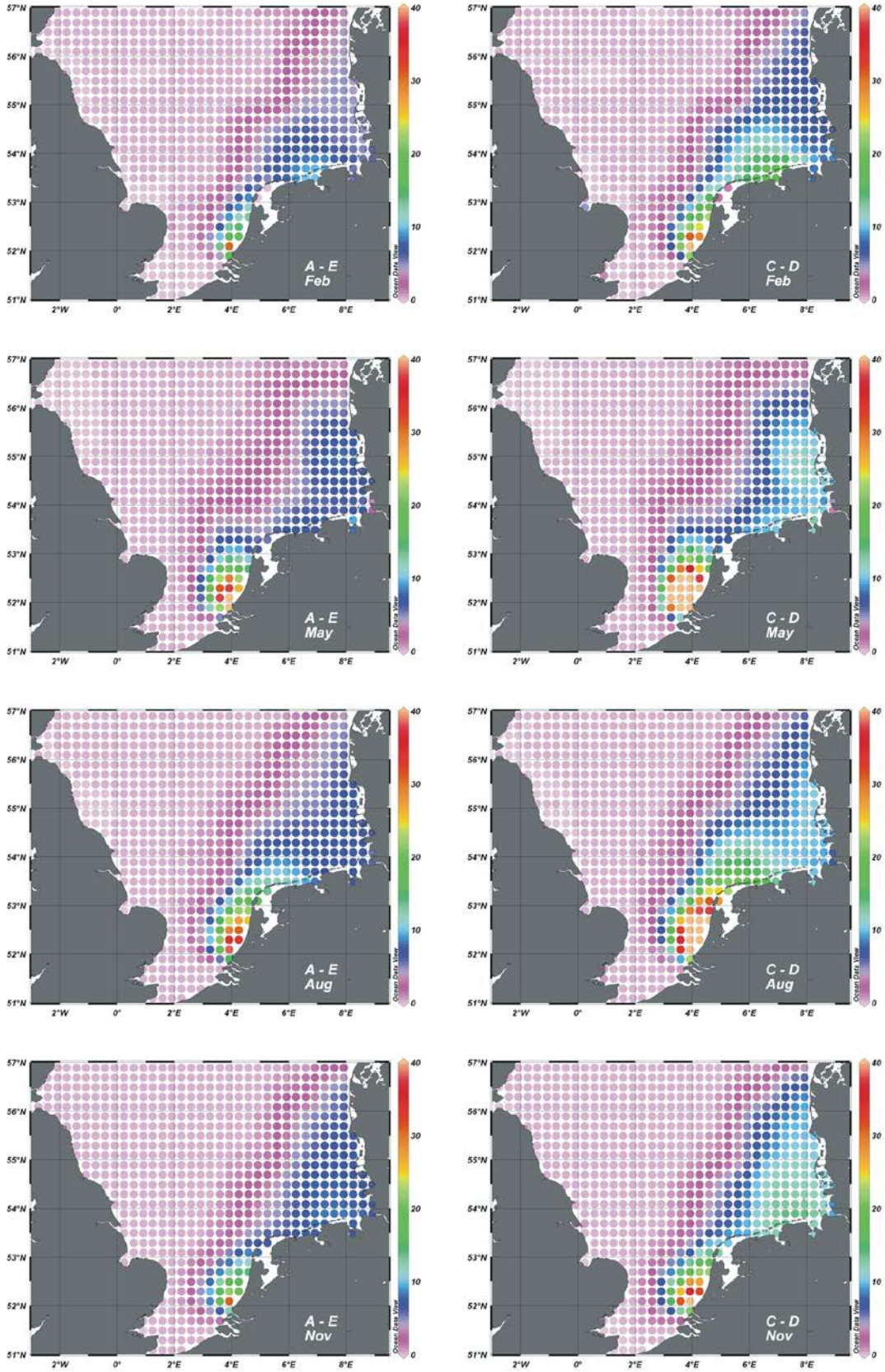

Fig. 3.9: TA that originated in the river Rhine represented by differences in TA-concentrations [µmol kg^{-1}] between scenario A and E as well as C and D.

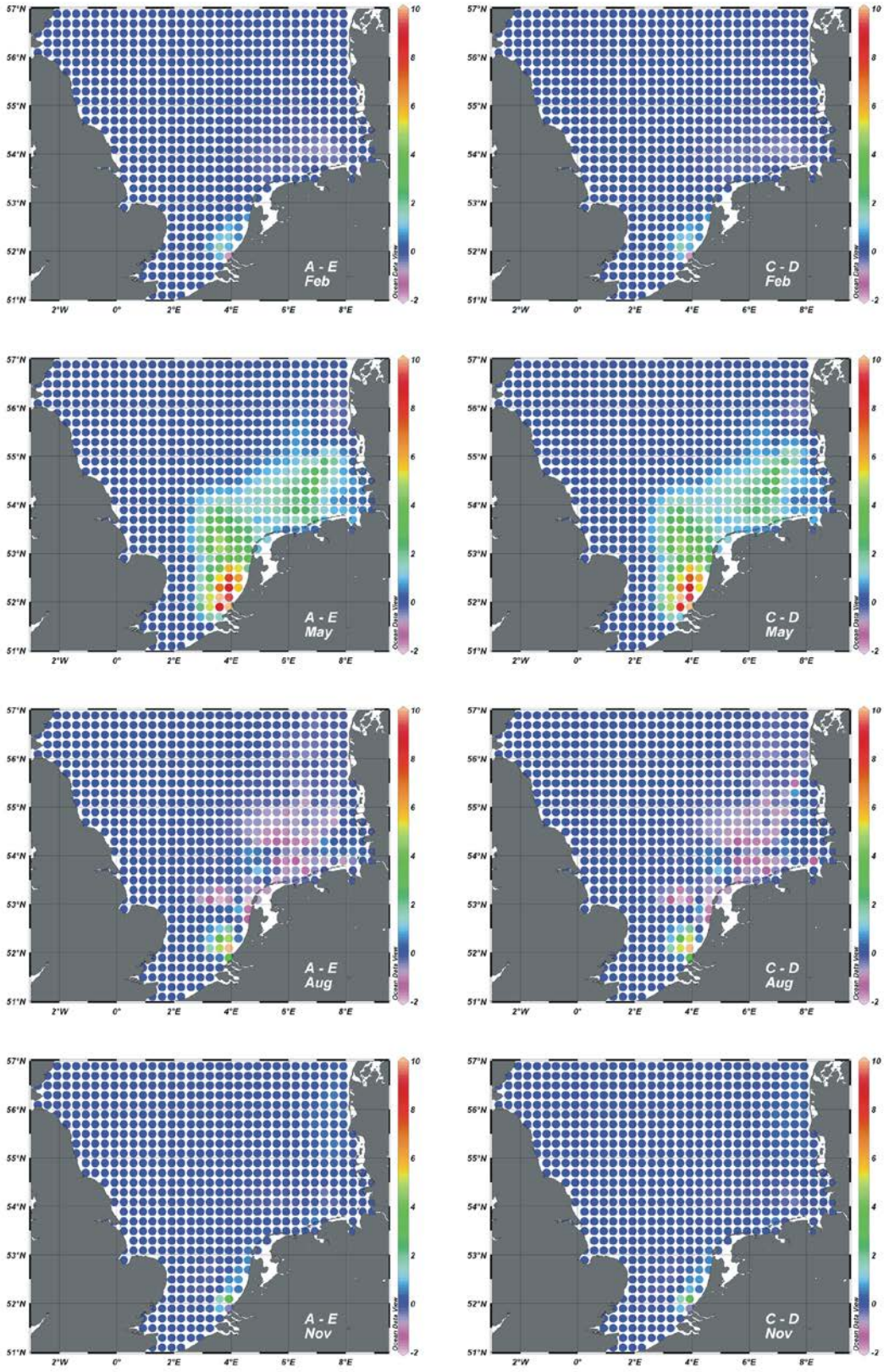

Fig. 3.10: Internal turnover rates of TA [mmol m^{-2} d^{-1}] that were induced by the river Rhine.

3.3.4 Seasonal DIC concentrations in 2008

The effects of the implemented new river input data on DIC concentrations are shown in Fig. 3.11. Surface TA concentrations in scenario A and the differences between C and A are shown for February, May, August and November 2008.

3.3.4.1 February

In scenario A the DIC concentrations ranged between 2110 µmol kg^{-1} near the English Channel and 2180 µmol kg^{-1} in the central and southern part of the German Bight. In scenario C the concentrations increased about 10 µmol kg^{-1} at the northern part of the Dutch coast and up to 30 µmol kg^{-1} near the Elbe estuary and the river Rhine.

3.3.4.2 May

In scenario A the DIC concentrations ranged between 2035 µmol kg^{-1} at the North Frisian coast and 2140 µmol kg^{-1} at the East Frisian coast. The concentrations in scenario C increased about 9 to 15 µmol kg^{-1} in the German Bight and the northern part of the Dutch coast near the river Ems. They also increased about 90 µmol kg^{-1} at the river Rhine.

3.3.4.3 August

The DIC concentrations in scenario A ranged between 1940 µmol kg^{-1} at the North Frisian and the Danish coast (between 55°N and 55.5°N) as well as in the Jade Bay and 2150 µmol kg^{-1} at the western part of the Dutch coast. The DIC-concentration in the German Bight showed a heterogeneous pattern with decreasing values from west to east. The concentrations in scenario C increased about 3 to 6 µmol kg^{-1} in the German Bight and about 25 µmol kg^{-1} at the river Rhine. They decreased about 25 to 50 µmol kg^{-1} near the Elbe estuary.

3.3.4.4 November

The DIC concentrations in scenario A ranged between 2080 µmol kg^{-1} near the English Channel and 2150 µmol kg^{-1} near the Elbe estuary. The concentrations increased in scenario C about 24 µmol kg^{-1} near the Elbe estuary and the river Rhine.

In summary, changes in DIC concentrations in the German Bight occurred especially in February and May. Only slight changes occurred in August and November.

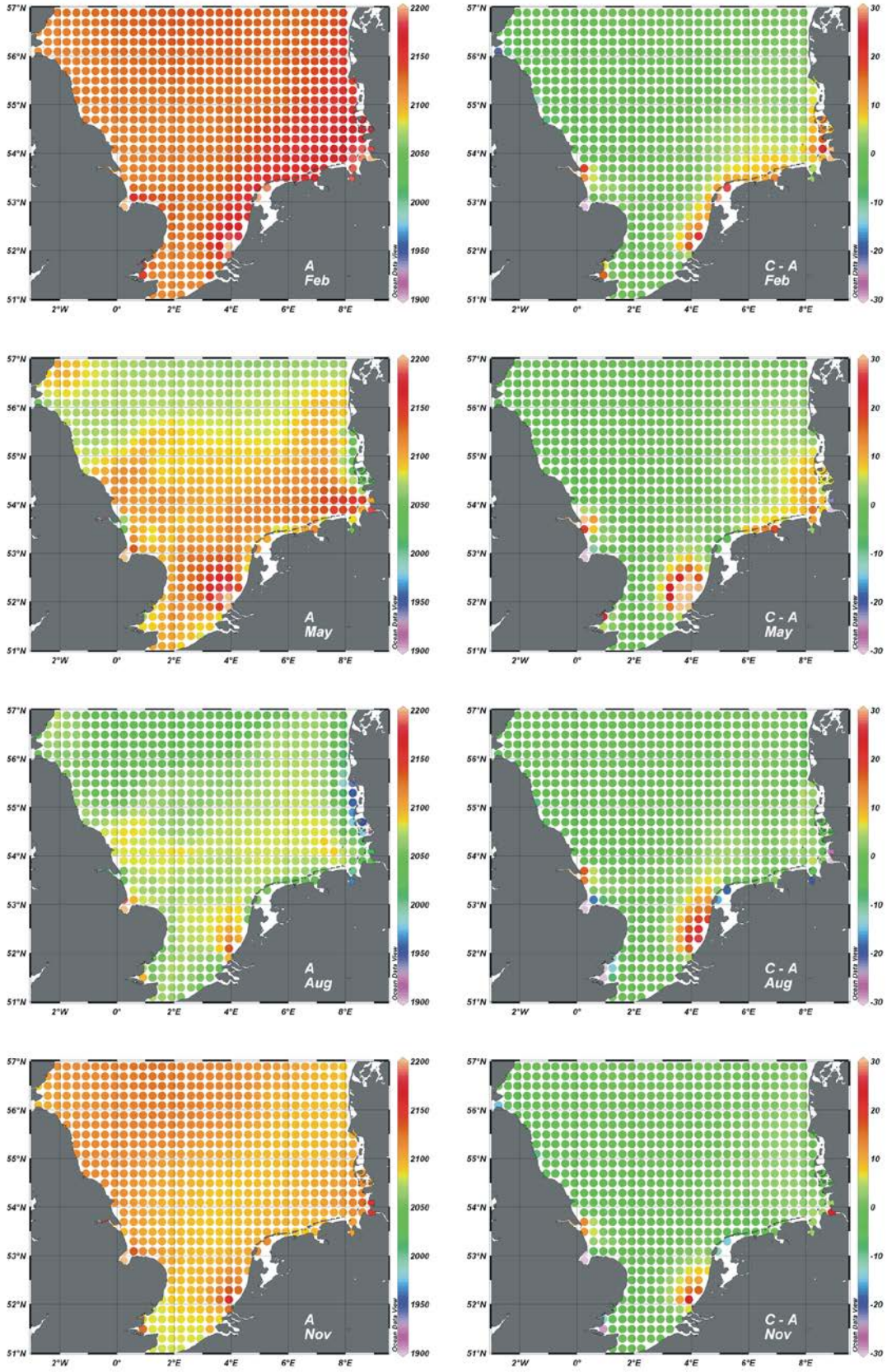

Fig. 3.11: DIC concentrations in scenario A (left) and differences in DIC concentrations [µmol kg^{-1}] between scenario C and A (right).

3.3.5 Comparison of TA and DIC concentrations with observations in 2008

The results of scenario C were compared with observations of TA and DIC in August 2008 (Salt et al., subm.). The latter revealed high TA and DIC concentrations in the German Bight (east of 7°E and south of 55°N) and around the Danish coast (around 56°N) that is shown in Fig. 3.12. The observed concentrations ranged between 2350 and 2380 µmol kg^{-1} (TA) and 2110 and 2160 µmol kg^{-1} (DIC) respectively.

The results of the conducted scenarios A – F are presented in Taylor diagrams (Taylor, 2001) in Fig. 3.13 and 3.14. Therefore, the same area was validated that was already examined in chapter 2 (east of 4.5°E, north of 53.5°N and south of 55.5°N, see Fig. 2.1). In that area observations of 10 different stations were available, each with four to six measurements at different depths (52 measured points). Measured TA and DIC concentrations of each point were compared with the modeled TA concentrations in the respective grid cells. The correlation coefficients, the standard deviations (STD) and the root mean square errors (RMSE) were calculated for each simulation.

One aim of this model development was to reduce the RMSE in order to bring the simulated TA concentrations closer to observations. The deviations from observations of scenarios A – E were represented by RMSE values around 28 µmol kg^{-1} (see Fig. 3.13). In scenario C the variation of TA concentrations in the validation area was slightly increased compared to A, which was represented by a STD of 6 µmol kg^{-1}. The STD was lowest in the scenarios without loads of the river Rhine (STD = 4 µmol kg^{-1} in D and E). The deviations from observations of simulated DIC concentrations were represented by RMSE values of 38 µmol kg^{-1} for scenarios A – C and 40 µmol kg^{-1} for scenarios D and E (Fig. 3.14). Compared to observations TA / DIC was simulated up to 50 µmol kg^{-1} / 60 µmol kg^{-1} too low in the German Bight (Fig. 3.12).

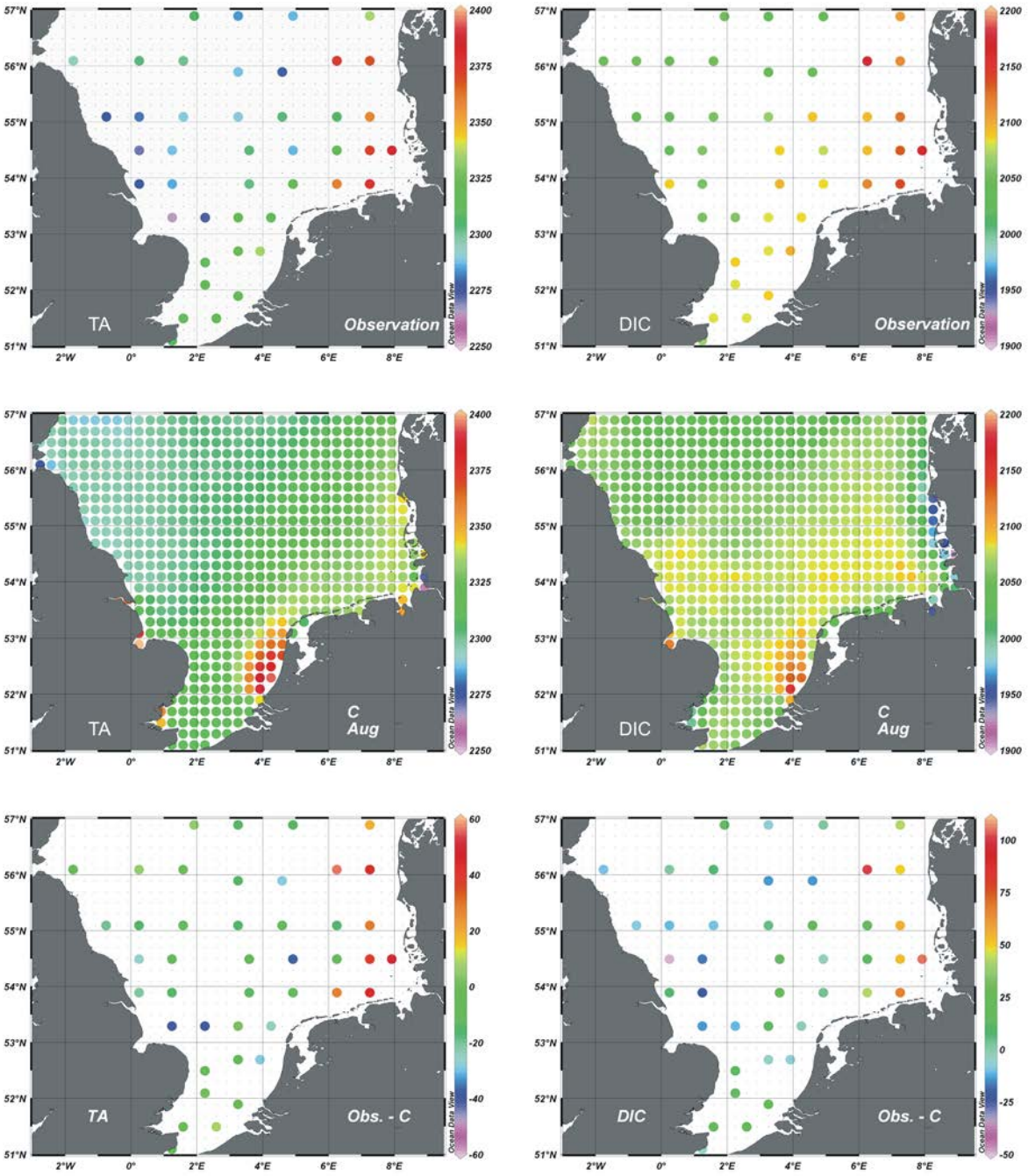

Fig. 3.12: Surface TA and DIC concentrations [µmol kg^{-1}] in August 2008 observed (top) and simulated (center, scenario C) as well as differences between observations and scenario C (bottom).

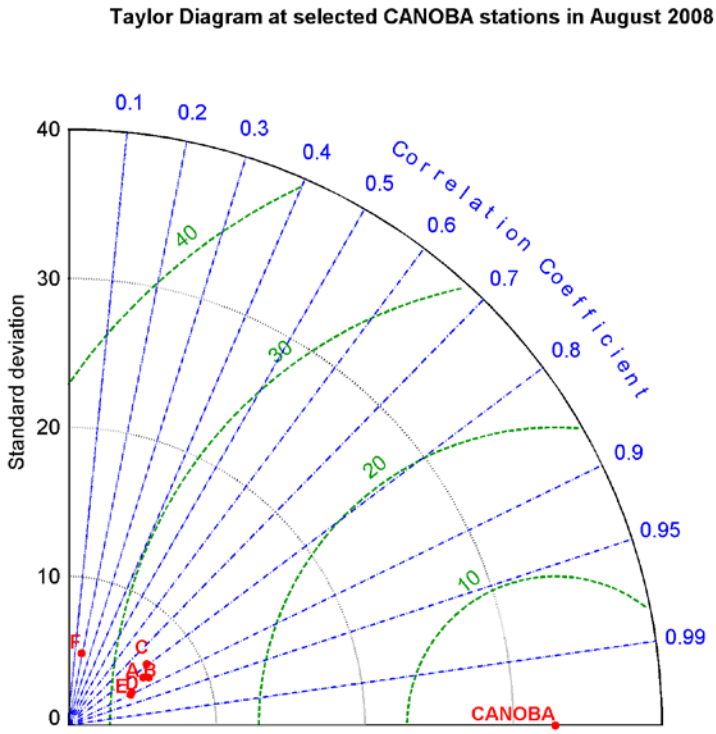

Fig. 3.13: Taylor diagram of simulated TA concentrations (A – F) compared to observed TA concentrations (52 measurements) in the validation area. Standard deviation and RMSE (green) are in µmol kg^{-1}.

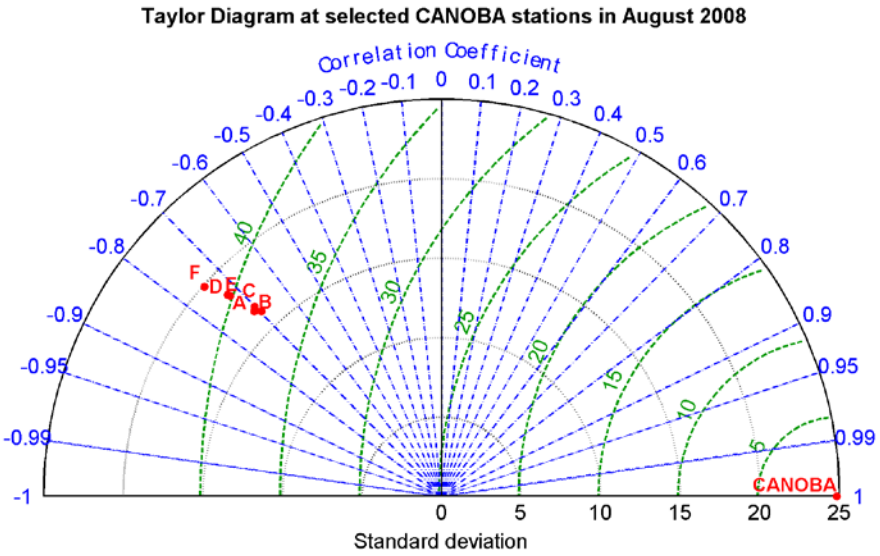

Fig. 3.14: Taylor diagram of simulated DIC concentrations (A – F) compared to observed DIC concentrations (52 measurements) in the validation area. Standard deviation and RMSE (green) are in µmol kg^{-1}.

3.4 Discussion

3.4.1 River loads and concentrations

One aim of this part of the study is to investigate whether the observed high TA concentrations could originate from rivers, especially from the Elbe estuary. River loads used in former model studies (Artioli et al., 2012, Lorkowski et al., 2012) were based on the report of Pätsch & Lenhart (2008). These TA and DIC datasets were based on measured freshwater discharges and on one concentration value for each river defined by the application of the end member approach as in Hjalmarsson et al. (2008). The data were an adequate basis for calculations of the carbonate system in the open North Sea but they lack seasonal accuracy because seasonality is only given by freshwater discharge.

The seasonal variability of TA and DIC concentrations in the Elbe estuary revealed low values in summer and higher values in winter (Tab. 3.2, Fig. 3.3). This seasonality is mainly driven by discharge with monthly mean values of about 460 $m^3\ s^{-1}$ in August and 950 $m^3\ s^{-1}$ in February (Pätsch & Lenhart, 2008). Rainfall and snowmelt in the catchment area of the Elbe estuary increase the TA and DIC mobilisation in winter and lead to the observed increased concentrations of TA and DIC in the upper estuary (Amann, 2013). This is due to the river catchment area, which is partly comprised of sedimentary carbonates (8.6%) and mixed sediments (13.5%) that are likely to contain carbonates transported via glaciers from northerly lying cretaceous marine carbonates (Amann, 2013, Lehner et al., 2008, Hartmann & Moosdorf, 2012).

Riverine TA and DIC concentrations could also be calculated by linear regressions of these parameters as a function of the logarithm of freshwater discharge. Gypens et al. (2009) assumed negative relationships between TA or DIC and the discharge in the river Scheldt that are due to dilution effects. Although this assumption is applicable for most rivers (Ludwig et al., 1996; Cai et al., 2008) it does not correspond to the positive relationships between TA or DIC and the discharge in the river Elbe that were found by Amann (2013).

Analogously to the modelled prognostic treatment of TA in this study, biogeochemical processes have also an impact on TA and DIC concentrations in the Elbe estuary. Especially nitrification can decrease TA by two mol per mol NO_3 produced. Vice versa denitrification can increase TA and Seitzinger and Kroeze (1998) estimated that about 50% of global dissolved inorganic nitrogen (DIN) river inputs are removed in estuaries by denitrification. Nevertheless, Dähnke et al. (2008) identified a change from a denitrification to a nitrification spot in the Elbe estuary that was attributed to a loss of its natural denitrification capacity due to extensive dredging and removal of sediments. Hence, the observed low TA concentrations in summer and

early fall can also be referred to the weakened denitrification capacity in the inner Elbe estuary (Amann, 2013).

Due to the scarcity of data necessary for the applications of the end member approach it was decided to use real concentrations at zero salinity in order to obtain seasonal to monthly TA and DIC concentrations for the most important rivers. This approach could lead to erroneous estimates because of potential nonconservative behaviour of chemicals in upper estuaries (Frankignoulle et al., 1996, Gypens et al., 2009). In case of the Elbe estuary Amann (2013) estimated up to 4.0 Gmol yr^{-1} additional TA and DIC that could originate from marshes (Weiss, in prep.). This would cause the main deviation of real concentrations at zero salinity from end member values.

The lack of seasonality of the TA concentrations in the dataset of Pätsch & Lenhart (2008) causes another inaccuracy if a precise TA budget is intended. Using again the example of the Elbe estuary, the TA concentration that was used for river load calculations was 2231 µmol kg^{-1} on every day. This concentration also included a certain amount of nutrients when it was determined. This could be best explained by the explicit conservative form of total alkalinity (Wolf-Gladrow, 2007) that was already mentioned in chapter 2.2.7 in this study. It means in effect that TA concentrations change due to changes in the concentrations of nutrients, mainly due to changes in nitrate. The river loads of nitrate that were calculated in the report of Pätsch & Lenhart (2008) were based on weekly concentration measurements. Variations of nitrate concentrations in the Elbe estuary can exceed up to 200 µmol kg^{-1} during the course of the year (compare Tab. 3.2) but there were no variations of concentrations considered for the calculations of TA river loads. This would not cause any problems if the determined TA concentration was calculated without any nutrients. In this case TA river loads could be easily calculated by subtracting the nitrate concentrations from the uniquely determined TA concentration value. For instance, if the corresponding nitrate concentration was 150 µmol kg^{-1}, when the TA concentration of 2231 µmol kg^{-1} was determined and the nitrate was completely taken up by phytoplankton afterwards, this would result in a TA concentration of 2381 µmol kg^{-1}. This value could be defined as “background TA” in this case. If the dataset of nitrate with weekly concentrations was used for simulations and relatively high concentrations about 300 µmol kg^{-1} occurred, this would result in a background TA concentration of 2531 µmol kg^{-1}. In fact the background TA concentration should not change if no changes due to discharge are considered (see above).

Consequently, the river load data for TA are biased because they do not keep track of changing riverine TA concentrations due to the variation of nitrate concentrations. There is an inconsistency if the datasets for TA and nitrate are used together, in order to budget riverine bulk TA and TA that could be generated by the uptake of riverine nitrate, which can hardly be

quantified. The resulting inaccuracy in the TA load of the Elbe estuary can be up to 0.4 Gmol mo^{-1} in some months, which is negligible if the carbonate system of the whole North Sea is in focus of a study (Artioli et al., 2012; Lorkowksi et al., 2012). In the study at hand the TA budget of a smaller part of the North Sea is in focus. This is the reason why it was decided to change river loads of nitrate analogously to river loads of TA in the present study. The underlying measurements of nitrate were carried out at the same places and at the same times as the TA and DIC measurements.

3.4.2 The impact of changed river loads on the TA and DIC concentrations in the German Bight

The aim of the implementation of more precise river loads was to investigate whether the observed high TA concentrations in the German Bight can originate from rivers. In the model validation the RMSE did not change from simulation A (old river loads, Pätsch & Lenhart, 2008) to simulations B and C (Fig. 3.13), which means that rivers are unlikely the origin of elevated TA concentrations in the German Bight. In comparison to A the TA and DIC concentrations mostly increased at the western part of the Dutch coast in scenario C (Fig. 3.7, 3.11). The TA and DIC concentrations slightly increased in the German Bight and the concentration patterns were more heterogeneous. This can only partly be explained by increased loads of TA and nutrients of the rivers Weser and Ems because TA concentrations in scenario B only increased about 2 µmol kg^{-1} in the German Bight (Fig. 3.7) in August. TA concentrations were about 4 µmol kg^{-1} higher (west of 8°E) in scenario C than in B. The majority of increased TA and DIC concentrations in C in that area were due to increased loads of the river Rhine (Fig. 3.9). Furthermore, the differences in concentrations between scenario C and A (Fig. 3.7) revealed similar patterns to the increased concentrations that were caused by the river Rhine in scenario C in every season (compare Fig. 3.9, left and right side). On the one hand this seems to be counter-intuitive because TA loads of the river Rhine increased similarly to TA loads of the German rivers Ems, Weser, Elbe and Eider in 2008 (Rhine +16.4 Gmol yr^{-1}, German rivers +16.3 Gmol yr^{-1} in B, +15.3 Gmol yr^{-1} in C). On the other hand TA concentrations of the river Rhine increased in scenario C compared to A, whereas the TA concentrations of the Elbe estuary decreased. Hence, the effect of dilution by freshwater discharge on simulated TA concentrations increased near the Elbe estuary, whereas it decreased near the river Rhine.

3.4.3 Introduction of effective river loads (Riv_{eff})

The effective river load (Riv_{eff}) was defined in order to quantify the combined effects of river load and freshwater discharge on TA concentration in the respective model grid cell. Riv_{eff} enables a comparison of the impact of river input and internal processes on TA concentration changes.

The annual TA river loads (TA_{lo}) that discharged directly into the validation area (rivers Elbe, Weser, Ems and Eider) were 78.2 Gmol yr^{-1} in scenario A and an additional 15.3 Gmol yr^{-1} in scenario C (93.5 Gmol yr^{-1}) in 2008. Internal processes accounted for a TA production of 14.9 Gmol yr^{-1} (including atmospheric nitrogen input) in the validation area in C, which was almost equal to the additional river loads. In order to combine the effects of river loads and dilution, the freshwater discharge in the validation area has to be considered additionally, which was 41.11 km^3 yr^{-1} in 2008. Following a simple mass balance calculation the flushing of the respective grid cells with river input resulted in a decrease of TA concentrations if the riverine concentration was lower than the concentration in the respective grid cell. This effect was defined as TA_{fl} and it could be figured out if the amount of TA was calculated that was flushed out of the grid cells with river input due to the freshwater discharge (Fig. 3.15). It was calculated from concentration changes caused by the additional volume of freshwater discharge so that it could be distinguished from advection due to currents. TA_{fl} in the validation area was 96.7 Gmol yr^{-1} in 2008. Thus, an effective river input (Riv_{eff}) could be defined as the difference of TA_{lo} and TA_{fl} in Gmol yr^{-1}.

$$Riv_{eff} = TA_{lo} - TA_{fl} \qquad (3.1)$$

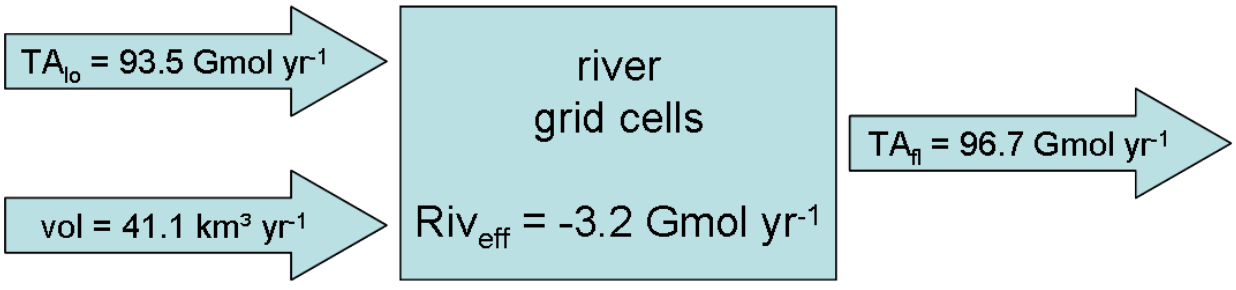

Fig. 3.15: Schematic description of the effective river input (Riv_{eff}) in the validation area (sum of rivers Elbe, Weser, Ems and Eider).

The effective river input was -3.2 Gmol TA yr^{-1} in scenario C (-2.2 Gmol TA yr^{-1} in scenario A) and was remarkably lower than TA that was produced internally (14.9 Gmol TA yr^{-1}).

Moreover, it is pointed out that the riverine input in the validation area has an annual dilution effect. This is in marked contrast to the river Rhine that has an effective river input of 23.9 Gmol TA yr^{-1} in scenario C (10.6 Gmol TA yr^{-1} in scenario A). Compared to scenario A Riv_{eff} of the German rivers decreased about 1.0 Gmol TA yr^{-1} due to the implemented changes in river input. Opposed to this, Riv_{eff} of the river Rhine increased about 13.3 Gmol TA yr^{-1}. This is why the impact on TA concentrations of the river Rhine was more pronounced even in the German Bight than the impact of the German rivers. Certainly, this depends also on hydrodynamic conditions in the North Sea. Clockwise flow patterns, which can occur especially in spring, can reduce the impact of the river Rhine on TA concentrations in the German Bight (Lenhart & Pohlmann, 1997). The impact of different hydrodynamical conditions will be discussed in chapter 4.

3.4.4 Temporal progress of Riv_{eff} and internal turnover of TA

The cumulative temporal progress of Riv_{eff} and the internal turnover of TA (sum of $F_1 - F_{17}$) are presented in Fig. 3.16. The Riv_{eff} decreased steadily in scenario A, whereas it decreased from February to November in scenario C and increased in December and January. The progress of Riv_{eff} in scenario C was in accordance with the implemented new TA concentrations of the Elbe estuary (Fig. 3.3). Low TA concentrations in the Elbe estuary induced a stronger decrease of Riv_{eff} in scenario C than in scenario A in summer, although the effects of unchanged concentrations of the remaining German rivers were included in Riv_{eff}.

The temporal progress of the internal turnover of TA has already been discussed in chapter 2. However, the implemented changes in river loads also included changes in river loads of nutrients. Most effects of changed nutrient loads on TA concentrations were similar in scenarios B and C (Fig. 3.8), thus most changes in the internal turnover rate were due to the increased river loads of German rivers. The internal turnover rates of scenario A and C were similar until April (Fig. 3.16). Differences first occurred near the island of Sylt and the northern Dutch coast in May, when nitrate or phosphate became the limiting factor at the end of a phytoplankton bloom (Lorkowski et al., 2012). At that time the increased availability of nutrients induced an enhanced uptake of nitrate and primary production. More organic material induced additional denitrification so that TA was produced irreversibly. This effect lasted until August and resulted in 1.79 Gmol TA that got additionally produced mainly in the German Bight (Fig. 3.8).

The implemented changes in loads of the river Rhine mostly affected loads of TA and thus direct changes of TA concentrations in 2008. Nitrate loads of the river Rhine did not differ much from scenario A in 2008 but they differed more in other years (Fig. 3.5). Nevertheless, the total amount of internally produced TA that was induced by the river Rhine in the validation

area was 1.14 Gmol yr^{-1}, which was 0.07 Gmol yr^{-1} lower than in scenario A. Considering the whole model domain an internal TA production of 11.4 Gmol yr^{-1} was induced by loads of the river Rhine in scenario C (12.0 Gmol yr^{-1} in A), which is comparable to loads of nitrate in 2008 (12.5 Gmol yr^{-1} in A and 12.3 Gmol yr^{-1} in C).

In summary, the effect of the river Rhine and the pooled effect of the German rivers can be distinguished due to their different impact on TA concentrations. The effective TA river input of the river Rhine is significantly higher than the pooled effective river input of the German rivers. Thus, the river Rhine affects concentration changes of TA more directly, whereas the German rivers affect changes of TA concentrations mainly indirectly by loads of nutrients.

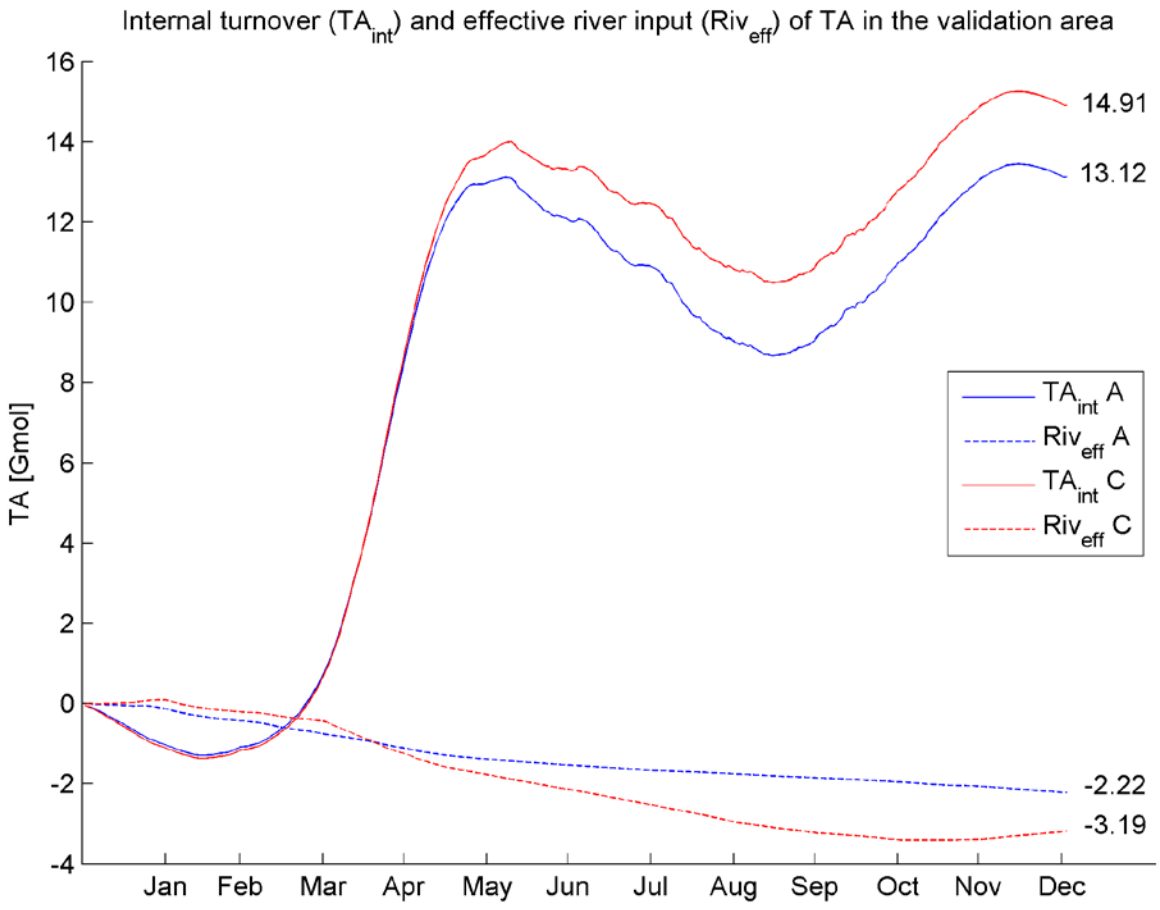

Fig. 3.16: Cumulative temporal progress of internal turnover of TA (TA_{int}) and effective river input (Riv_{eff}) of TA in the validation area [Gmol].

3.5 Conclusion

Experiments with more precise estimates of river loads and the consideration of dilution effects due to freshwater discharge showed that observed high TA concentrations in the German Bight in summer unlikely originate directly from rivers. Although river loads of nutrients fuel the internal processes that generate TA, they only contribute partly to observed high concentrations in August, because the majority of internally produced TA was converted in April and May. A precise localisation of TA and DIC sources is important in order to understand the evolution of the carbonate system in the German Bight through rising atmospheric CO_2 concentrations and climate change. Under recent conditions rivers play a secondary role in the carbonate system of the German Bight in summer. This may change if increasing / decreasing precipitation in the catchment area of the Elbe estuary or the river Rhine would increase / decrease the riverine TA concentration and thus the effective river input of TA. Also a more extensive dredging and removal of sediments in the Elbe estuary could lead to decreasing denitrification and thus more nitrate that enters the German Bight. If the additional nitrate would be denitrified entirely after entering the German Bight, this would not lead to increased TA exports from the German Bight, because the nitrate concentration would not change the background concentration of TA. Nevertheless, changes in river loads of nutrients or organic material can change the primary production and remineralisation in the German Bight. If more organic material would be remineralised under anoxic conditions e.g. in tidal mud flats this could potentially increase the export rates of TA in the Wadden Sea.

4 Alkalinity generation in the Wadden Sea as a major driver of the carbonate system in the southern North Sea

4.1 Introduction

Anaerobic degradation of organic material is the most important biogeochemical process in marginal seas that irreversibly produces net alkalinity. Hu and Cai (2011) estimated the contribution of anaerobic processes in global ocean margins on oceanic net alkalinity budget to be in the order of 4 - 5 Tmol TA yr^{-1} that include continental shelves and oxygen minimum zones. Additionally, they estimated another 0.1 - 1.1 Tmol TA yr^{-1} originating from pyrite burial in coastal habitats.

The dependency of the carbon fluxes in the North Sea on TA especially on the TA produced in the Wadden Sea was debated by Thomas et al. (2004) and Thomas et al. (2009). The Wadden Sea facilitates approximately 7 – 10% of the annual CO_2 uptake of the North Sea. They calculated in a first approximation about 72.5 Gmol TA yr^{-1} originating in the Wadden Sea based on observations in the southern North Sea in 2001 and 2002. They reveal a larger seasonal amplitude than could be explained by riverine TA alone, especially in summer. These findings were confirmed in the previous chapters of this study. Neither seasonal variations in riverine TA concentrations nor enhanced eutrophication can cause the observed high TA concentrations in summer.

The irreversible generation of net TA in the Wadden Sea depends on reaction products that either resist or escape re-oxidation by oxygen. The first main process is denitrification, which generates molecular nitrogen (N_2) that can escape to the atmosphere. Jensen et al. (1996) estimated about 100 Gmol N yr^{-1} denitrified in the Wadden Sea. This amount is supposed to yield 99 Gmol yr^{-1} of net TA (Chen and Wang, 1999; Thomas et al. 2009). The second main process is sulphate reduction that generates H_2S. It can either be buried as pyrite or escape to the atmosphere if sediments are exposed to air at low tide (Kristensen et al., 2000). These processes have been estimated in a range of 6 – 13 Gmol S yr^{-1} in the Wadden Sea (Kristensen et al., 2000; de Beer et al., 2005), which is equal to a production of 12 – 26 Gmol TA yr^{-1}.

The aim of this chapter is to check the estimations of Thomas et al. (2009) and to have a closer look at TA produced in the Wadden Sea and on seasonal and interannual variabilites of TA concentrations in the German Bight. In the context of anthropogenic and climate change a distinct allocation of TA sources is necessary to investigate the evolution of the carbonate system in the North Sea. The TA generation in the Wadden Sea underlies the effects of changes in the production of organic matter and accelerating sea level rise. The North Frisian Wadden Sea will be more affected by sea level rise due to its larger tidal basins (van Beusekom et al., 2012), which results in a loss of intertidal areas. Thus, a further distinction of different Wadden Sea export areas is necessary for a more precise allocation of TA sources.

In contrast to other modelling studies of the carbonate system of the Northwest European shelf (Lorkowski et al., 2012; Artioli et al., 2012) sources and sinks of TA and DIC were implemented into the model that identify the dynamic behaviour of the Wadden Sea as an area of effective production and decomposition of organic material. The respective exchange rates were calculated by using measured pelagic DIC and TA concentrations in the Wadden Sea and modelled tidal water mass exchange.

As a first step simulations of different scenarios of Wadden Sea export rates are conducted and compared to the results of selected scenarios of the previous chapters and with observations from August 2008 (Salt et al., subm.). Afterwards seasonal differences in TA and DIC concentrations in the German Bight are examined.

As a second step the seasonal and interannual variabilities of TA and DIC concentrations in the German Bight were investigated for the years 2001 – 2009. Additionally, different hydrodynamic stream patterns and flushing times in the validation area were assumed in order to examine their impact on seasonal and interannual variabilities.

4.2 Methods

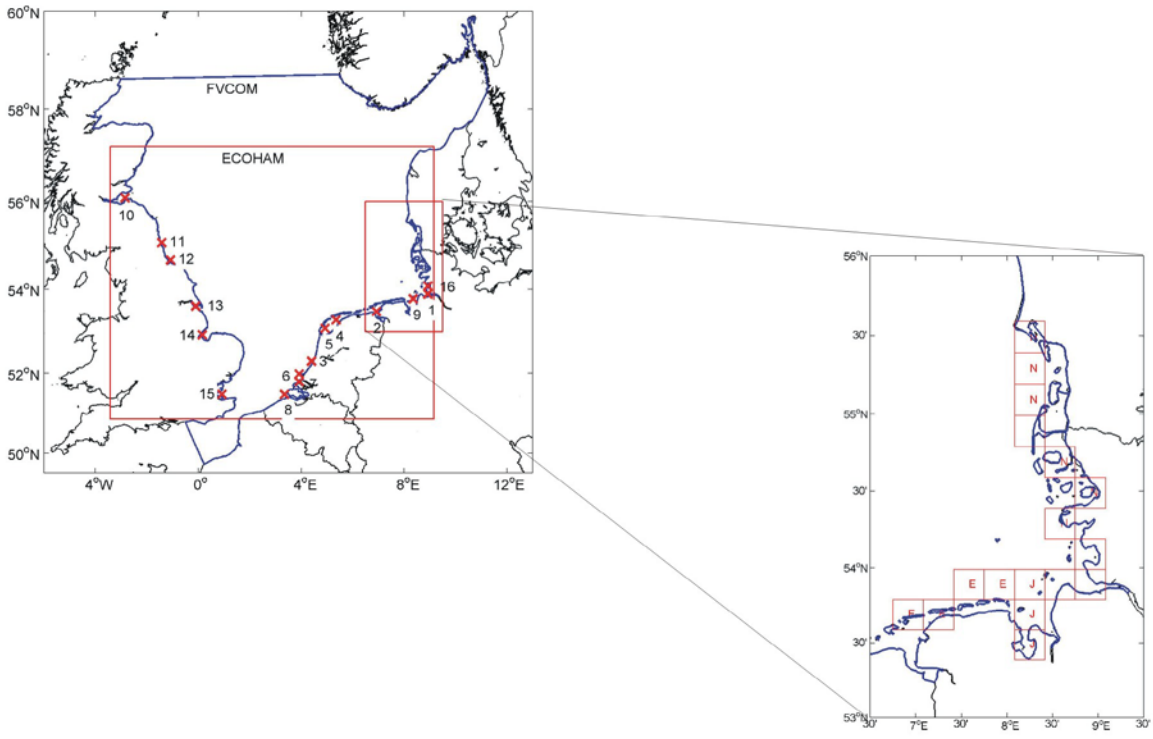

Figure 4.1: Model domains of ECOHAM (red) and FVCOM (blue), positions of rivers 1 – 16 (left, see table 4.2) and the Wadden Sea export areas grid cells (right).

4.2.1 Implementation of Wadden Sea dynamics

The Wadden Sea system of the southern North Sea extends from Den Helder (the Netherlands) in the West to Esbjerg (Denmark) in the North over a length of 450 km covering an area of about 9500 km^2 (Ehlers, 1994). A chain of barrier islands forms the boundary between the Wadden Sea and the open North Sea. Deep inlet channels between the islands enable water and material exchange with the open North Sea. The entire Wadden Sea system is characterised by semidiurnal tides with a tidal range between 1.5 m in the most westerly part and 4 m in the estuaries of the rivers Weser and Elbe (Streif, 1990).

The biogeochemical dynamics and the corresponding influence on the adjacent southern North Sea were discussed by van Beusekom (2012). In the study at hand the exchange of TA and DIC between North Sea and Wadden Sea was investigated. Therefore controlled sinks and sources for TA and DIC were implemented for some of the south-eastern cells of the North Sea grid (Fig. 4.1). The cells with adjacent Wadden Sea were separated into three exchange areas: the East Frisian and the North Frisian Wadden Sea as well as the Jade Bay, distinguished by “E”, “N” and “J” (Fig. 4.1, right side).

The Wadden Sea area itself was not resolved by the model. Two parameters were determined in order to quantify the TA and DIC loads from the Wadden Sea into the North Sea.

1) Concentration changes of pelagic TA and DIC in the Wadden Sea during one tide,

2) Water mass exchange between the back-barrier islands and the open sea during one tide

Measured concentrations of TA and DIC as well as modelled water mass exchange rates of the export areas served as a basis for the calculated exchange. Measured concentrations were provided by Winde (2013) and modelled water mass exchange rates were provided by Grashorn (2013).

The daily Wadden Sea exchange of TA and DIC was calculated in the following way:

$$wad\_flu = \frac{wad\_sta * wad\_exc}{vol} \quad (4.1)$$

Differences in measured concentrations in the Wadden Sea during rising and falling water levels were temporally interpolated and summarized as *wad_sta* [mmol m^{-3}]. Modelled daily Wadden Sea exchange rates of water masses (tidal prisms during falling water level) were defined as *wad_exc* [m^3 d^{-1}], and the volume of the corresponding North Sea grid cell was *vol* [m^3]. *wad_flu* [mmol m^{-3} d^{-1}] were the daily concentration changes of TA and DIC in the respective North Sea grid cells.

In fact, some amounts of the tidal prisms return without mixing with North Sea water, and calculations of Wadden Sea export should therefore consider flushing times in the respective back-barrier areas. Since differences in measured concentrations between rising and falling water levels were used, this effect is already assumed to be represented in the data. This approach enabled the use of tidal prisms without consideration of any flushing times.

4.2.1.1 Wadden Sea - measurements

The flux calculations for simulations were carried out representatively in tidal basins of the East and North Frisian Wadden Sea (Spiekeroog Island, Sylt-Rømø) as well as in the Jade Bay. For the present study seawater samples were used taken by Winde (2013) on tidal cycles during different seasons. The mean concentrations of TA and DIC during rising and falling water levels and the respective differences (ΔTA and ΔDIC) are given in Tab. 4.1. Measurements in August 2002 were taken from Moore et al. (2011). The Δ-values were used as *wad_sta* and linearly interpolated between the times of observations for the simulations. Of course, the linear

progress of the Δ-values did not represent the natural behaviour perfectly, especially if only few data are available. As a consequence, possible short events of high TA and DIC export rates could potentially be missed that occurred in periods outside the observation periods.

Table 4.1: Mean TA and DIC concentrations [µmol kg^{-1}] during rising and falling water levels and the respective differences (Δ-values) that were used as wad_sta in (4.1). Areas are the North Frisian (NF), the East Frisian (EF) Wadden Sea and the Jade Bay (JB).

Area	Date	TA (rising)	TA (falling)	ΔTA	DIC (rising)	DIC (falling)	ΔDIC
NF	29.04.2009	2343	2355	12	1983	2106	123
	17.06.2009	2328	2332	4	2170	2190	20
	26.08.2009	2238	2252	14	2077	2105	28
	05.11.2009	2335	2333	-2	2205	2209	4
JB	20.01.2010	2429	2443	14	2380	2392	12
	21.04.2010	2415	2448	33	2099	2132	33
	26.07.2010	2424	2485	61	2159	2187	28
	09.11.2010	2402	2399	-3	2302	2310	8
EF	03.03.2010	2379	2393	14	2313	2328	15
	07.04.2010	2346	2342	-4	2068	2082	14
	17./18.05.2011	2445	2451	6	2209	2221	12
	20.08.2002	2377	2414	37	2010	2030	20
	01.11.2010	2423	2439	16	2293	2298	5

A statistical analysis of uncertainties of ΔTA and ΔDIC was not possible, because only concentrations were considered measured with a delay of 2 hours compared to low tide and high tide. This was done in order to obtain representative concentrations of rising and falling water levels. As a consequence, only 2 - 3 measurements for each location and season were considered for calculations of ΔTA and ΔDIC, which made a statistical analysis of uncertainties impossible.

4.2.1.2 Wadden Sea – modelling the exchange rates

Grashorn (2013) performed the hydrodynamic computations of exchanged water masses (*wad_exc*) with FVCOM (Chen, 2003) by adding up the cumulative seaward transport during falling water level (tidal prisms) between the back-barrier islands that were located near the respective ECOHAM cells with adjacent Wadden Sea area. These values are given in Tab. 4.2 for each ECOHAM cell in the respective export areas. The definition of the first cell N1 and the

last cell E4 is in accordance to the clockwise order in Fig. 4.1 (right side). For the sake of clarity a more detailed description of the calculations is given in the appendix (A9).

Table 4.2: Daily Wadden Sea runoff to the North Sea at different export areas.

Position	wad_exc [10^6 m³ d^{-1}]
N1	273
N2	1225
N3	1416
N4	1128
N5	4038
N6	18
J1 - J3	251
E1	380
E2	634
E3	437
E4	857

4.2.2 Simulations

The years 2001 to 2009 were simulated with 3 spin up years in 2000. 7 different scenarios (A - G) were conducted as described below. The respective Wadden Sea export rates are shown in Fig. 4.2. Simulations of previous chapters (A – C) are also shown here in order to highlight the effects of Wadden Sea export rates on TA and DIC concentrations in the German Bight.

A:

This scenario was the same as it was already shown in the previous chapters (scenario A): The prognostic treatment of TA was implemented and constant river concentrations for TA and DIC (Pätsch & Lenhart, 2008; Lorkowski et al., 2012) were used. Interannual and seasonal variations of TA and DIC river loads were proportional to freshwater discharges.

B:

This scenario was the same like scenario C in the previous chapter: Loads of TA and DIC were calculated more precisely for the main continental rivers. For that reason monthly variations of riverine TA and DIC concentrations as well as new nitrate concentrations were integrated for the main continental rivers.

C:

This scenario was the same like scenario F in the previous chapter: The setup of simulation B was used but without the impact of internal fluxes on TA. Note that only the impact on TA was switched off and not the respective fluxes itself.

D:

This was the first simulation where the Wadden Sea was implemented as described above. Summer export rates for the East Frisian Wadden Sea were based on concentration differences that were calculated from linear interpolation of measurements that have been conducted in March, April and November 2010 and May 2011 (Tab. 4.1). This scenario could be seen as minimum assumption for Wadden Sea export rates of TA and DIC because there was no summer measurement of TA concentration for the East Frisian Wadden Sea.

E:

Since this study focuses on TA concentrations in summer the data set of TA concentrations in the East Frisian Wadden Sea was extended with data measured there in August 2002. As expected, these data showed higher differences in TA concentrations of rising and falling water levels than in simulation D. This simulation could be seen as a medium assumption for Wadden Sea export rates.

F:

The same concentration differences that were measured in the Jade Bay were also used for the East Frisian Wadden Sea. This simulation represented a maximum assumption for Wadden Sea export.

G:

The impact of internal fluxes (F_1 – F_{17}) was compared with Wadden Sea export of TA. Therefore, the setup of simulation E was used without the impact of internal fluxes on TA. Note that only the impact on TA was switched off and not the respective fluxes itself.

Tab. 4.3: Summary of the main features of simulations A – G: "Prognostic TA" is the concentration change of TA due to internal processes (see chapter 2). "River configuration" means the implementation of all described changes in chapter 3. "Wadden Sea export" means an estimate of the exported amount of TA and DIC. "EF Wadden Sea data" is a description of the data source for the East Frisian Wadden Sea (see above for more details).

Simulation	prognostic TA	River configuration	Wadden Sea export	EF Wadden Sea data
A	enabled	**unchanged**	no	-
B	enabled	changed	no	-
C	**disabled**	changed	no	-
D	enabled	changed	**minimum**	**no summer conc.**
E	enabled	changed	**medium**	summer conc.
F	enabled	changed	**maximum**	**Jade Bay data**
G	**disabled**	changed	**medium**	summer conc.

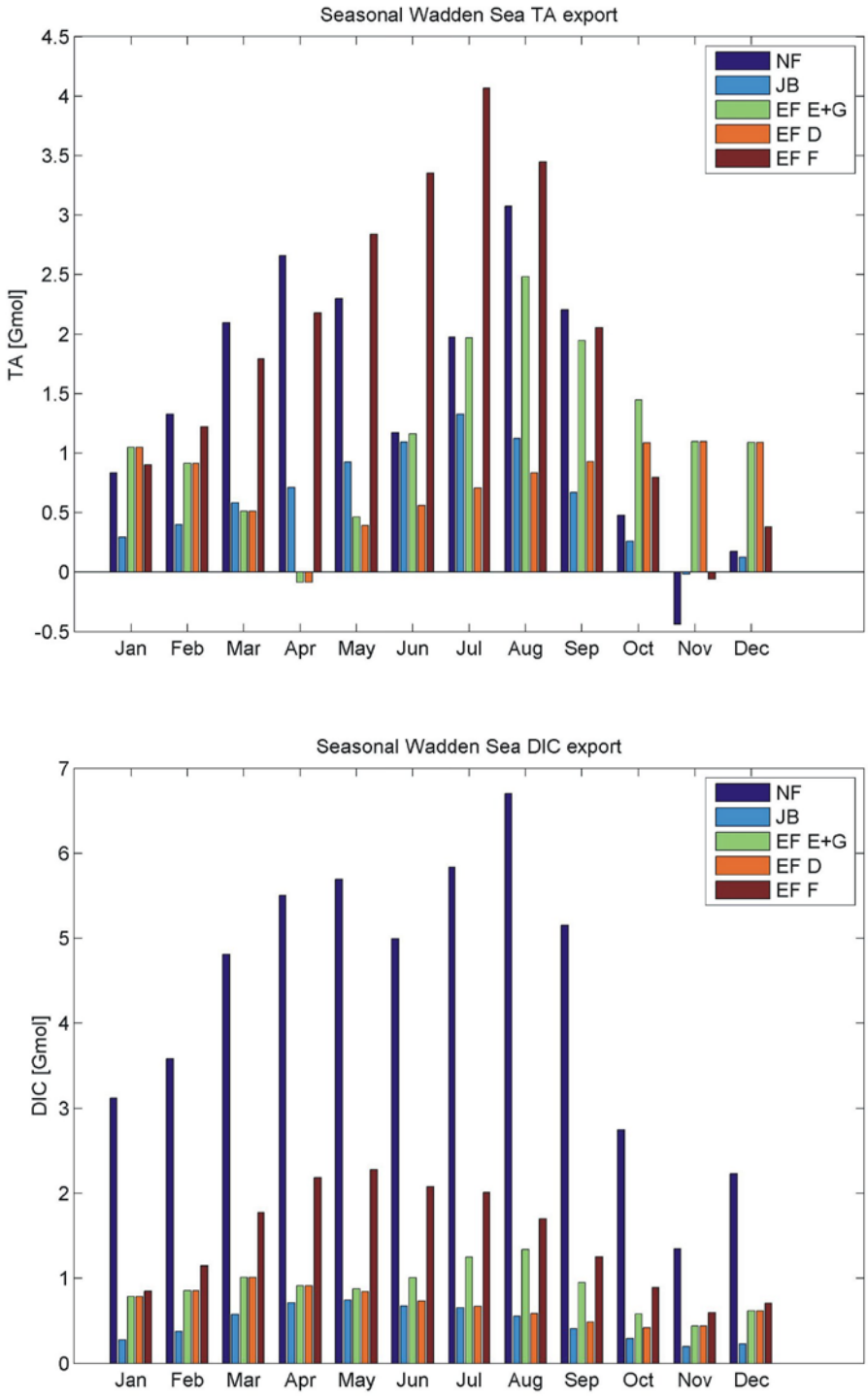

Figure 4.2: Monthly Wadden Sea export of DIC and TA [Gmol mon^{-1}] at the North Frisian coast (NF), East Frisian coast (EF) and the Jade Bay in simulations D – G.

4.3 Results

4.3.1 Model validation - TA concentrations in summer 2008

The results of simulations A – G were compared with observations of TA in August 2008 (Salt et al., subm.). The latter revealed high TA concentrations in the German Bight (east of 7°E and south of 55°N) and around the Danish coast (around 56°N) as shown in Fig. 4.3. The observed concentrations in these areas ranged between 2350 and 2380 µmol kg^{-1}. These findings were in accordance with observed TA concentrations in August / September 2001 (Thomas et al., 2009). TA concentrations in other parts of the observed domain ranged between 2270 µmol kg^{-1} near the British coast (53°N – 56°N) and 2330 µmol kg^{-1} near the Dutch coast and the Channel.

In order to give a statistical overview the results of simulations A to G were also presented and compared in a Taylor diagram (Taylor, 2001) in Fig. 4.4. Therefore, an area was focused (validation area), which was located east of 4.5°E, north of 53.5°N and south of 55.5°N (Fig. 2.1). In that area observations of 10 different stations were available, each with four to six measurements at different depths (52 measured points). Measured TA concentrations of each point were compared with the modeled TA concentrations in the respective grid cells. The correlation coefficients, the standard deviations (STD) and the root mean square errors (RMSE) were calculated for each simulation. One aim of this model development was to reduce the RMSE in order to bring the simulated TA concentrations closer to observations.

TA concentrations in simulation A ranged between 2290 µmol kg^{-1} in the north western part of the model domain, 2360 µmol kg^{-1} at the western part of the Dutch coast and 2380 µmol kg^{-1} at the Thames estuary at the British coast (see Fig. 4.3). In comparison with observations and the other simulations, A had the lowest variations in TA-concentrations in the validation area with 2320 µmol kg^{-1} at the Elbe estuary and 2340 µmol kg^{-1} in the Jade Bay. The deviation of A from observations was represented by a RMSE of 28 µmol kg^{-1} (see Fig. 4.4).

In simulation B the TA concentrations showed a more heterogeneous pattern with a maximum value of 2390 µmol kg^{-1} at the western part of the Dutch coast and in the river mouth of the Wash estuary at the British coast. A minimum value of 2260 to 2270 µmol kg^{-1} was simulated at the mouths of the rivers Elbe and Firth of Forth. The TA concentration pattern in the German Bight was also more heterogeneous than in simulation A because higher concentrations of 2350 µmol kg^{-1} and 2340 µmol kg^{-1} were simulated at the Jade Bay and in the central part of the German Bight. The deviation of B from observations was represented by a RMSE of 28 µmol kg^{-1} (Fig. 4.4). Compared to A the variation of TA concentrations in the validation area was slightly increased which is represented by a STD of 5 µmol kg^{-1}.

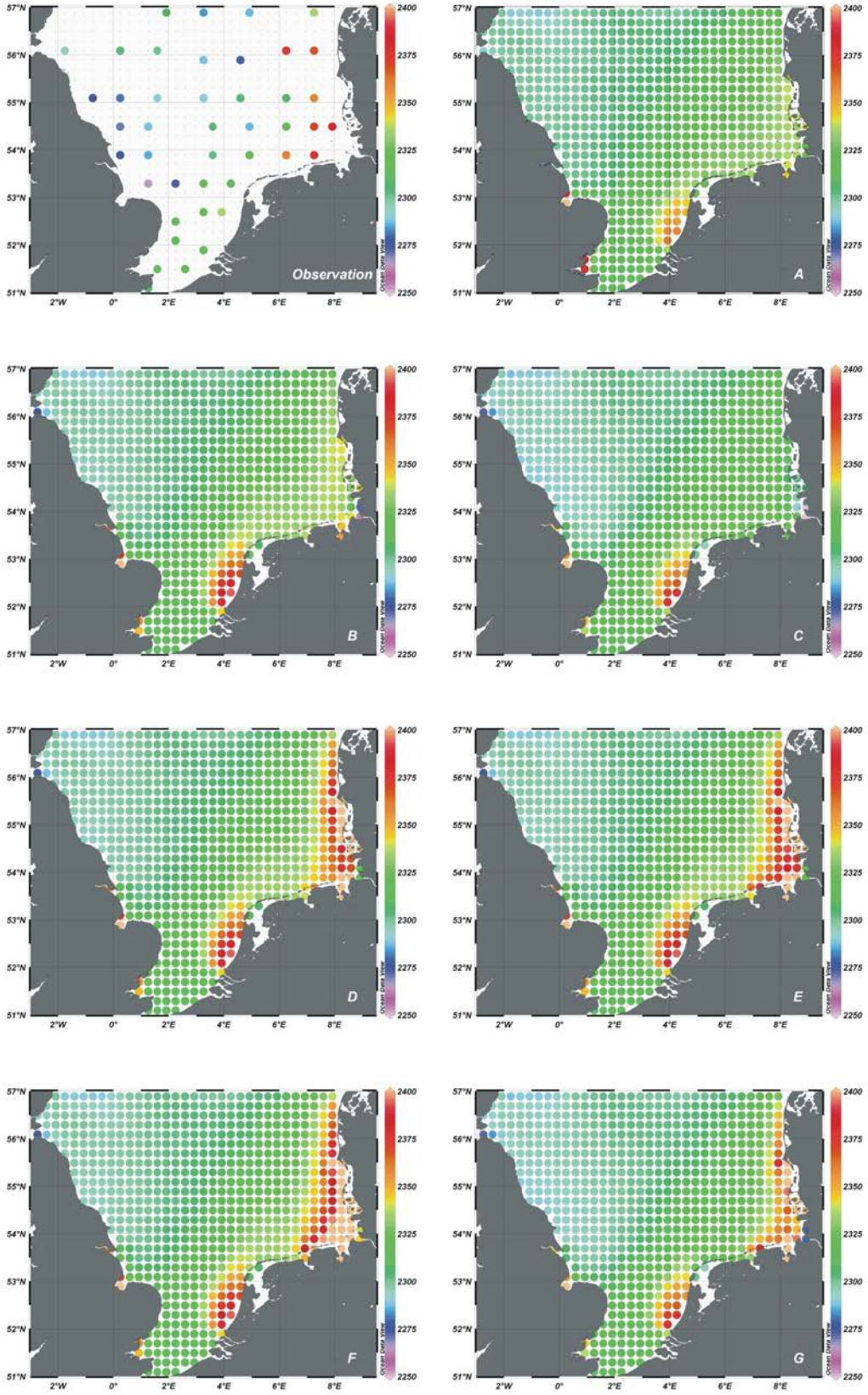

Figure 4.3: Surface TA-concentrations [µmol kg^{-1}] in August 2008 observed and simulated (A – G).

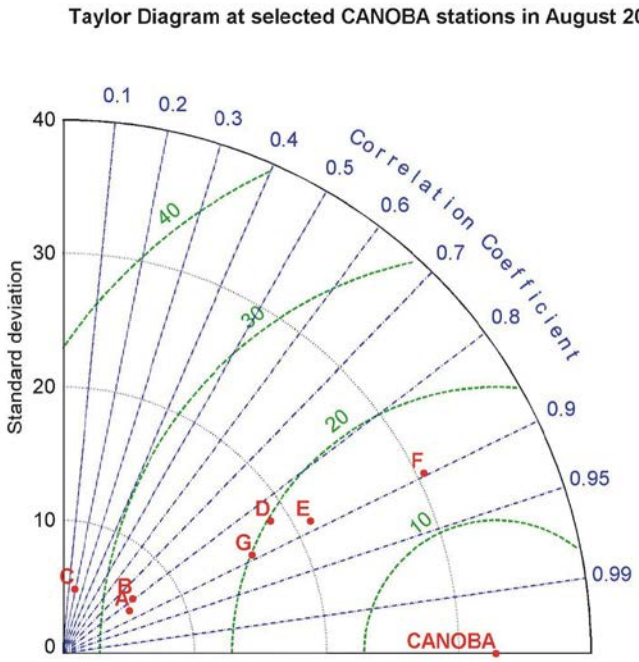

Figure 4.4: Taylor diagram of simulated TA-concentrations (A – G) compared to observed TA-concentrations (52 measurements) in the validation area.

In comparison to simulation B TA concentrations in simulation C showed only slightly lower values in the western and middle part of the model domain (Fig. 4.3). The largest differences occurred at the Danish coast between 55°N and 56°N and in the German Bight, especially in the Jade Bay. TA was simulated 20 µmol kg^{-1} to 40 µmol kg^{-1} lower in these areas. The deviation from observation was highest in C and was represented by a RMSE of 33 µmol kg^{-1}.

The simulations D – F were based on different assumptions of Wadden Sea export quantities of TA and DIC as described above. The major differences in TA concentrations of these scenarios compared to B were presented in Fig. 4.7 (left side). These differences occurred east of 6.5°E. TA was simulated similarly in D – F at the Danish coast (north of 55°N). In this area the concentration was about 20 to 150 µmol kg^{-1} higher than in simulation B. The main differences between these scenarios occurred in the central part of the German Bight (54°N, 8°E). Depending on the respective scenario, the TA concentrations were simulated about 20 to 90 µmol kg^{-1} higher than in B. With increasing Wadden Sea export (from D to F) the effect of elevated concentrations spread further to the west especially near the East Frisian coast. Compared to A and B it was possible to increase the variations (STD) with rising export values of TA (18 µmol kg^{-1} in D, 21 µmol kg^{-1} in E and 30 µmol kg^{-1} in F). It was also possible to bring the simulations closer to observation which was represented by decreasing RMSE values (20 µmol kg^{-1} in D, 17 µmol kg^{-1} in E and 15 µmol kg^{-1} in F).

In simulations E and G the same TA export quantities were assumed but the impact of internal processes on TA concentrations was switched off in G. TA in G was simulated 20 to 40 µmol kg^{-1} lower than in E. The deviation of G from observation was represented by a RMSE of 20 µmol kg^{-1}.

4.3.2 Model validation - DIC concentrations in summer 2008

Analogously to TA the simulations were compared with observations of DIC concentrations in summer 2008 (Salt et al., subm.). They also revealed high values in the German Bight (east of 7 °E and south of 55°N) and around the Danish coast (around 56°N) which is shown in Fig. 4.5. The observed concentrations in these areas ranged between 2110 and 2160 µmol kg^{-1}. Observed DIC concentrations in other parts of the model domain ranged between 2020 µmol kg^{-1} in the north western part and 2110 µmol kg^{-1} at the Dutch coast.

The DIC concentrations in simulations A – C ranged between 1940 µmol kg^{-1} at the North Frisian and the Danish coast (between 55°N and 55.5°N) as well as in the Jade Bay and 2150 µmol kg^{-1} at the western part of the Dutch coast (Fig. 4.5). The DIC concentrations in the German Bight showed a heterogeneous pattern with decreasing values from west to east. In comparison to B lower DIC concentrations in C occurred at the river mouth of the river Elbe, at the southern part of the Jade Bay, at the North Frisian coast and at the Danish coast. DIC-concentrations in these areas were around 20 µmol kg^{-1} lower than in B. Less differences about 10 µmol kg^{-1} occurred in an area between 54°N to 55°N and 6°E to 8°E. The deviations from observation of A and B were indicated by RMSEs of 38 µmol kg^{-1} (see Fig. 4.6). The deviation from observation was highest in C represented by a RMSE of 42 µmol kg^{-1}.

Analogously to TA, the differences in DIC concentrations of the simulations D – F compared to B were presented in Fig. 4.7 (right side). These differences occurred east of 6.5°E. DIC was also simulated similarly in D – F at the Danish coast (north of 55°N). In this area DIC was up to 200 µmol kg^{-1} higher than in B. Differences between these scenarios occurred in the central part of the German Bight (54°N, 8°E). Depending on the respective scenario the DIC concentrations were simulated about 20 to 60 µmol kg^{-1} higher than in B. With increasing Wadden Sea export of DIC the effect of elevated concentrations spread further to the west, especially near the East Frisian coast. Compared to B the variations decreased, which was indicated by lower STDs (7 µmol kg^{-1} in D, 8 µmol kg^{-1} in E and 13 µmol kg^{-1} in F). The simulated DIC-concentrations were brought closer to the observation, which was represented by decreasing RMSE values (25 µmol kg^{-1} in D, 24 µmol kg^{-1} in E and 20 µmol kg^{-1} in F).

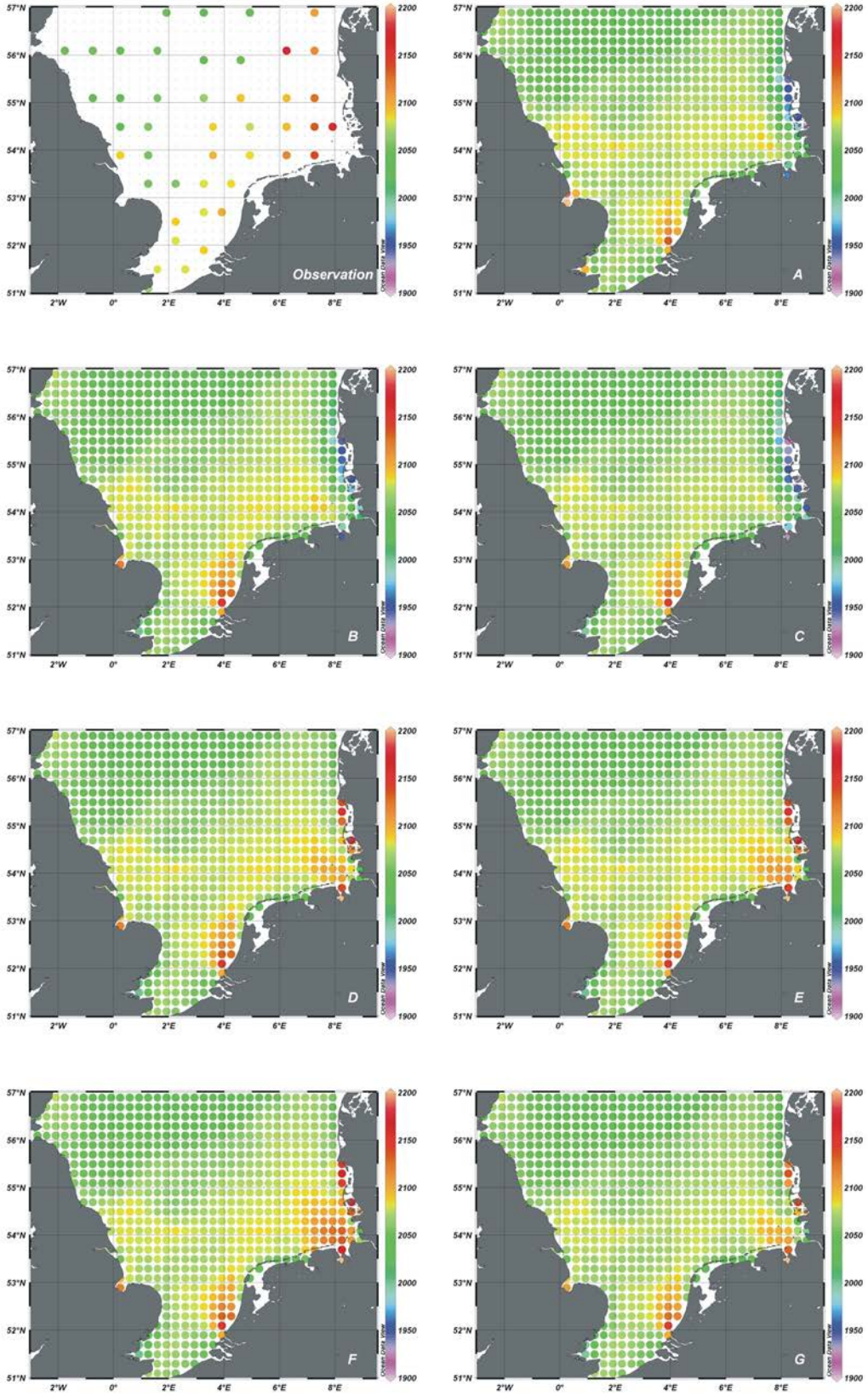

Figure 4.5: Surface DIC-concentrations [µmol kg^{-1}] in August 2008 observed and simulated (A – G).

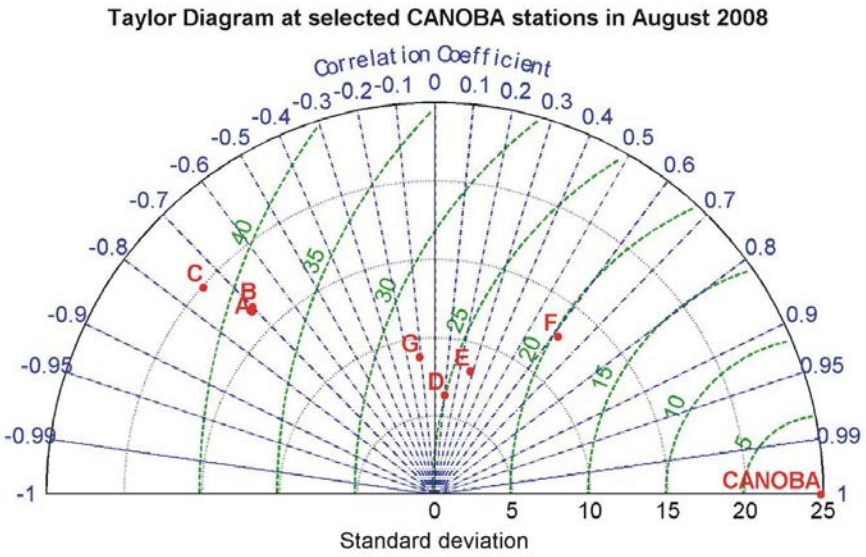

Figure 4.6: Taylor diagram of simulated DIC-concentrations (A – G) compared to observed TA-concentrations (52 measurements) in the validation area.

In simulations E and G the same TA and DIC export quantities were assumed but the impact of internal processes on TA concentrations was deactivated in G. Differences between these two scenarios occurred analogously to C. The deviation from observation of G was represented by a RMS of 27 µmol kg^{-1}.

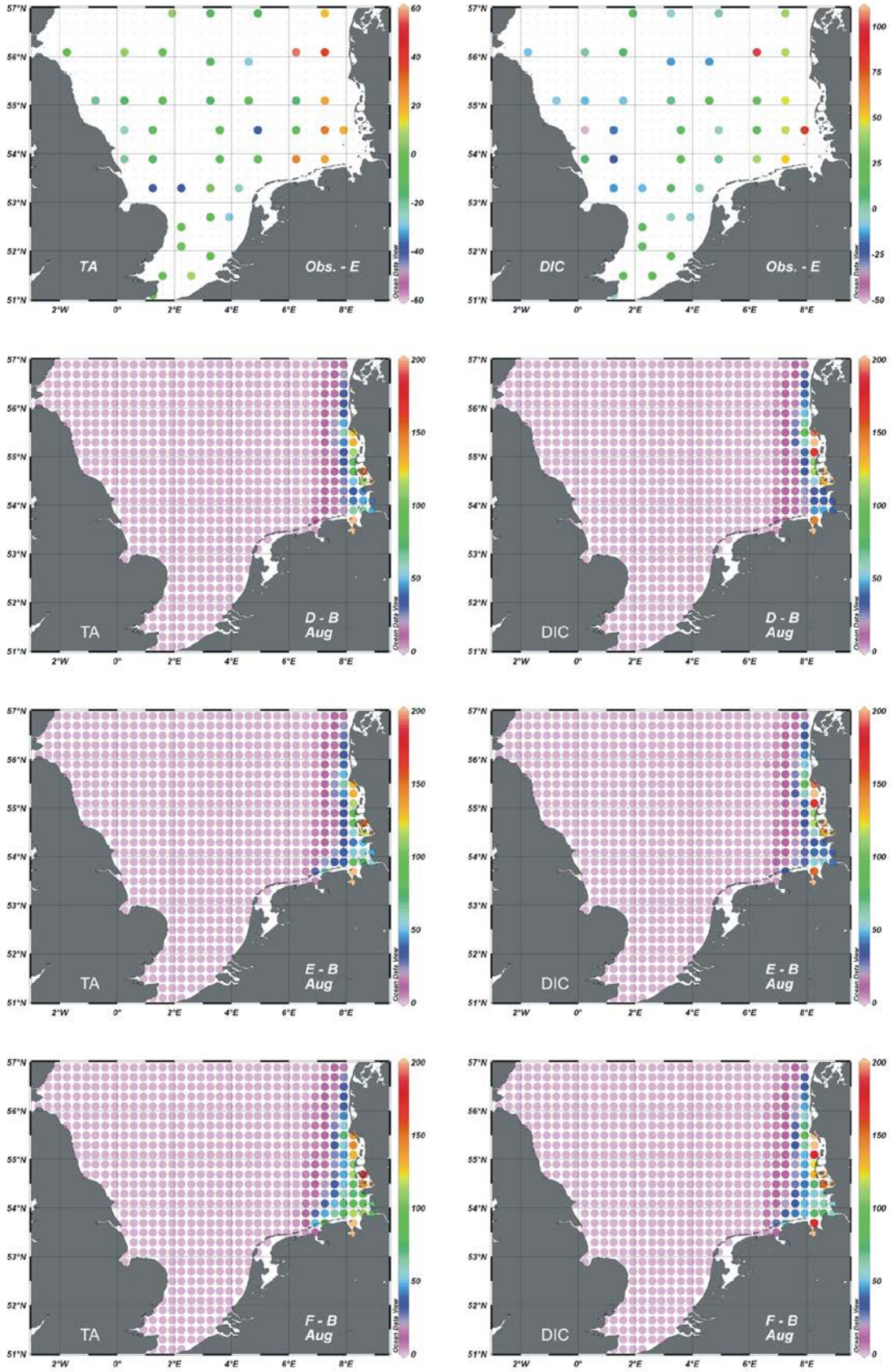

Figure 4.7: Differences between observations and scenario E [µmol kg^{-1}] as well as increases in TA and DIC concentrations [µmol kg^{-1}] due to Wadden Sea exports represented by differences in scenarios (D, E, F) and scenario B.

4.3.3 Seasonal and interannual variability of TA concentrations

The years 2001 to 2009 were simulated for all scenarios A to G. Monthly mean concentrations of TA were calculated in the validation area and are shown in Fig. 4.8. Mean concentrations of surface TA in the validation area measured in August and November 2001, February and May 2002, August 2005 and August 2008 were also shown in Fig. 4.10. It should be mentioned here, that it was decided to show only measured surface data in order not to weight positions with greater depths and thus more measurements. Therefore, the image of the measurements (observations) in Fig. 4.8 is supposed to give an overview of measured seasonality and interannual variability and should be compared to simulations A – G only in a qualitative way. The lowest values were measured in November 2001 (2313 µmol kg^{-1}) and in February 2002 (2304 µmol kg^{-1}). In August, measured mean values of concentrations ranged from 2330 µmol kg^{-1} in 2005 to 2337 µmol kg^{-1} in 2008.

The highest TA-concentration in simulation A was about 2335 µmol kg^{-1} and occurred in August 2001. The lowest concentrations in each year were about 2310 to 2315 µmol kg^{-1} and occurred in February and March. Summer concentrations in the years 2002 to 2007 were in the range of 2325 to 2330 µmol kg^{-1} and the highest values in the respective years.

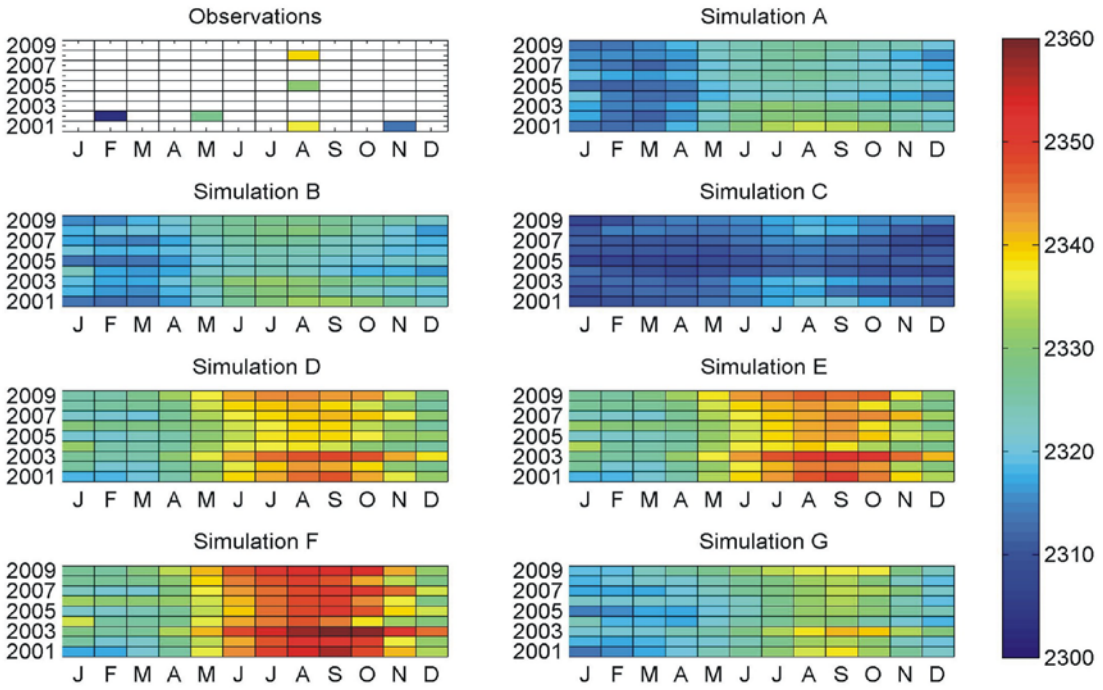

Figure 4.8: Observed mean surface concentrations and simulated monthly mean concentrations of TA [µmol kg^{-1}] in the validation area.

In comparison to A the TA-concentrations in simulation B showed about 2 µmol kg^{-1} higher values in the winter months. TA-concentrations in A were about 2 – 3 µmol kg^{-1} higher in summer 2001 than in B.

Simulation C was calculated similar to B but without impact of internal processes on TA. The concentrations in simulation C showed the lowest variability of all simulations. They ranged between 2300 µmol kg^{-1} in winter, spring and autumn and 2322 µmol kg^{-1} in August 2001, 2003 and 2008. The years 2004 to 2007 showed even lower variabilities.

The lowest TA concentrations in the Wadden Sea scenarios (simulations D – F) occurred in January and February 2001 with 2315 µmol kg^{-1}. The highest concentrations in these scenarios occurred in September 2003 with 2348 µmol kg^{-1} in D, 2354 µmol kg^{-1} in E and 2360 µmol kg^{-1} in F. In comparison to B the winter and spring TA concentrations in D – F were about 10 µmol kg^{-1} higher. The main differences occurred in summer and autumn. Depending on the scenario the TA concentrations were simulated about 18 to 30 µmol kg^{-1} higher in that time. Thus, the seasonal variabilities were increased. Additionally, the results of D – F also showed high interannual variabilities in summer and autumn. Summer concentrations ranged between 2338 to 2348 µmol kg^{-1} in D, 2340 to 2354 µmol kg^{-1} in E and 2343 to 2360 µmol kg^{-1} in F.

Simulation G was calculated similar to E but without impact of internal processes on TA. The concentrations in G showed the lowest variability of all Wadden Sea scenarios. They ranged between 2313 µmol kg^{-1} in January 2001 and 2342 µmol kg^{-1} in September 2003. Compared to simulation C the TA concentrations showed a higher interannual variability, especially in summer when values of 2338 to 2342 µmol kg^{-1} occurred.

4.3.4 Seasonal and interannual variability of DIC concentrations

Analogously to TA, mean surface DIC concentrations that were measured in the validation area are shown in Fig. 4.9. The lowest values occurred in August and ranged from 2080 to 2110 µmol kg^{-1}. The highest value was 2150 µmol kg^{-1} and was measured in February 2002.

The years 2001 to 2009 were simulated for all scenarios A to G. Monthly mean concentrations of DIC were calculated in the validation area and are shown in Fig. 4.9. In all simulations the concentrations increased from October to March and decreased from April to September.

Maximum values of 2140 to 2155 µmol kg^{-1} in simulation A occurred every year in March and minimum values of 2045 to 2060 µmol kg^{-1} in September. The highest interannual variability occurred in April with concentrations between 2125 to 2150 µmol kg^{-1} in 2004 and 2006 respectively. Generally, the DIC concentrations in simulation B showed a similar pattern as in A

but with up to 10 µmol kg^{-1} higher values in February and March. During the whole simulation period the DIC concentrations in C were 5 to 10 µmol kg^{-1} lower than in B.

As well as in the previous simulations the lowest DIC concentrations in the Wadden Sea scenarios (D – F) occurred in September and the highest concentrations occurred in March. Compared to B the overall DIC concentration was elevated in every Wadden Sea scenario. Depending on the scenario the concentrations were up to 10 µmol kg^{-1} higher in March and between 30 to 40 µmol kg^{-1} higher in September. The differences among the Wadden Sea scenarios were highest in August 2007, September 2002 and September 2007, when the DIC concentrations were up to 25 µmol kg^{-1} higher in F than in D. Analogously to the comparison of simulations B and C the DIC concentrations in G were 5 to 10 µmol kg^{-1} lower than in E.

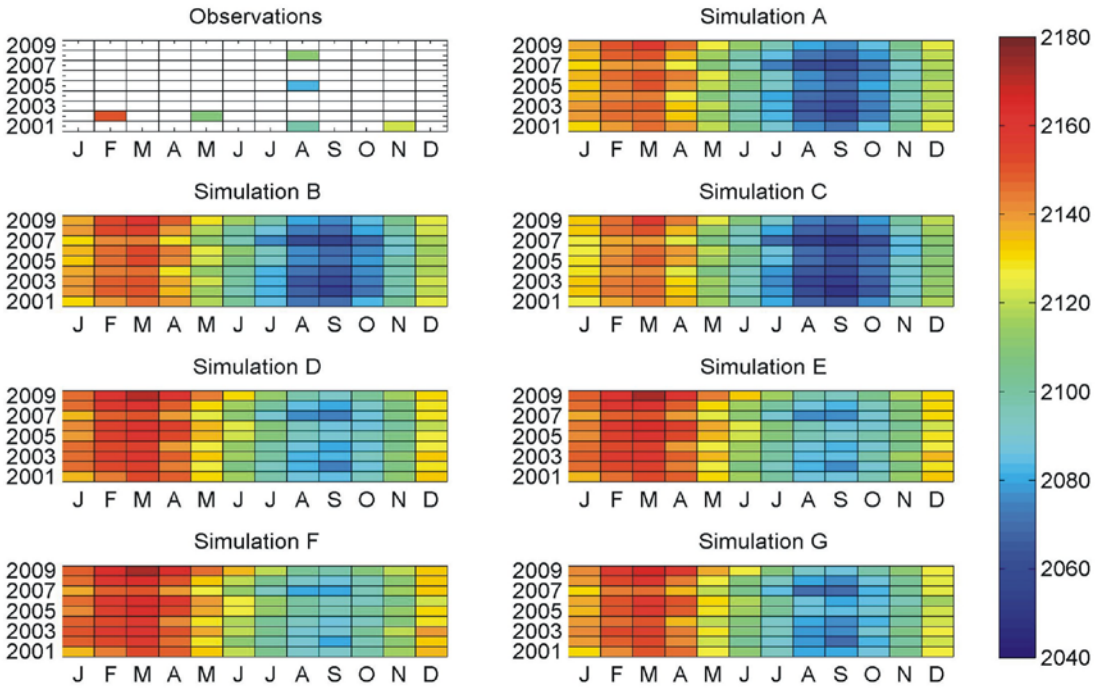

Figure 4.9: Observed mean surface concentrations and simulated monthly mean concentrations of DIC [µmol kg^{-1}] in the validation area.

4.3.5 Hydrodynamic conditions and flushing times

The calculations of Wadden Sea TA export in Thomas et al. (2009) were based on several assumptions concerning riverine input of bulk TA and nitrate, atmospheric deposition of nitrogen, water column inventories of nitrate and the exchange between the Southern Bight and the adjacent North Sea (Lenhart et al., 1995). The latter was computed by considering that the water in the Southern Bight is flushed with water of the adjacent open North Sea at time scales of six weeks. In the study at hand, flushing times in the validation area in summer and winter are presented for the years 2001 to 2009 in Fig. 4.10. Additionally, typical monthly flow patterns of the model area are in excerpts presented in Fig. 4.11. They were chosen in order to show which patterns occurred in 2008 and which patterns occurred when flushing times in summer were highest (2003 and 2006).

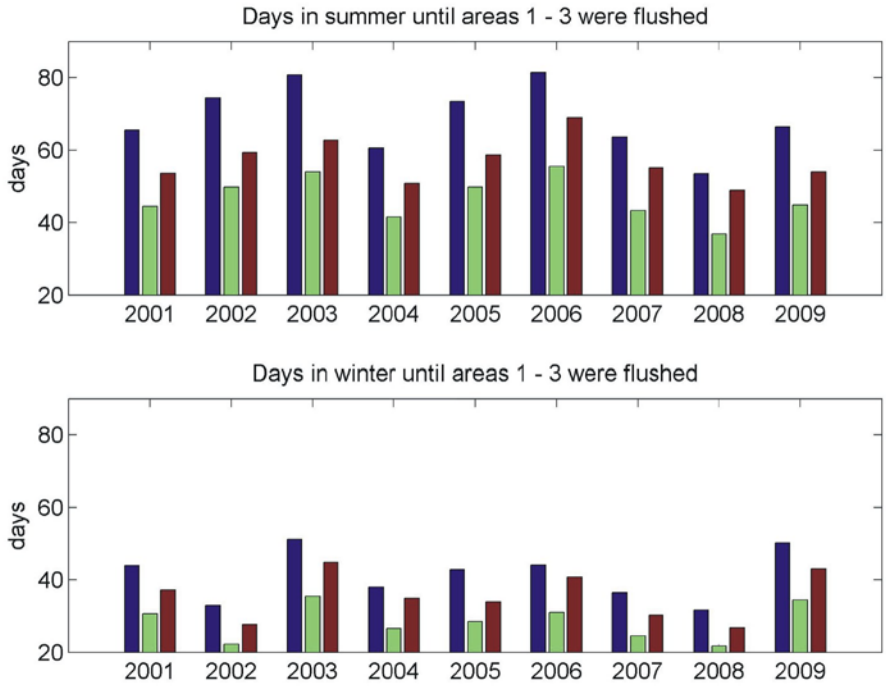

Figure 4.10: Flushing times in the validation area in summer (June to August) and winter (January to March). The whole validation area is represented in blue, green is the western part of the validation area (4.5°E to 7°E) and red is the eastern part (east of 7°E).

The flushing times were calculated by dividing the total volume of the respective areas 1 – 3 by the total inflow into the areas m^3 $(m^3\ s^{-1})^{-1}$. Flushing times were consistently higher in summer than in winter. Summer values in the whole validation area ranged from 54 days in 2008 to 81 days in 2003 and 2006, whereas the winter values in the same area ranged from 32 days in 2008 to 51 days in 2003 and 2009. The flushing times in the western and eastern part of the validation

area were smaller. Flushing times in the western part were consistently shorter than in the eastern part. These differences ranged from 5 days in winter 2002 to 14 days in summer 2006 and 2008. The interannual variabilities of all areas were higher in summer than in winter.

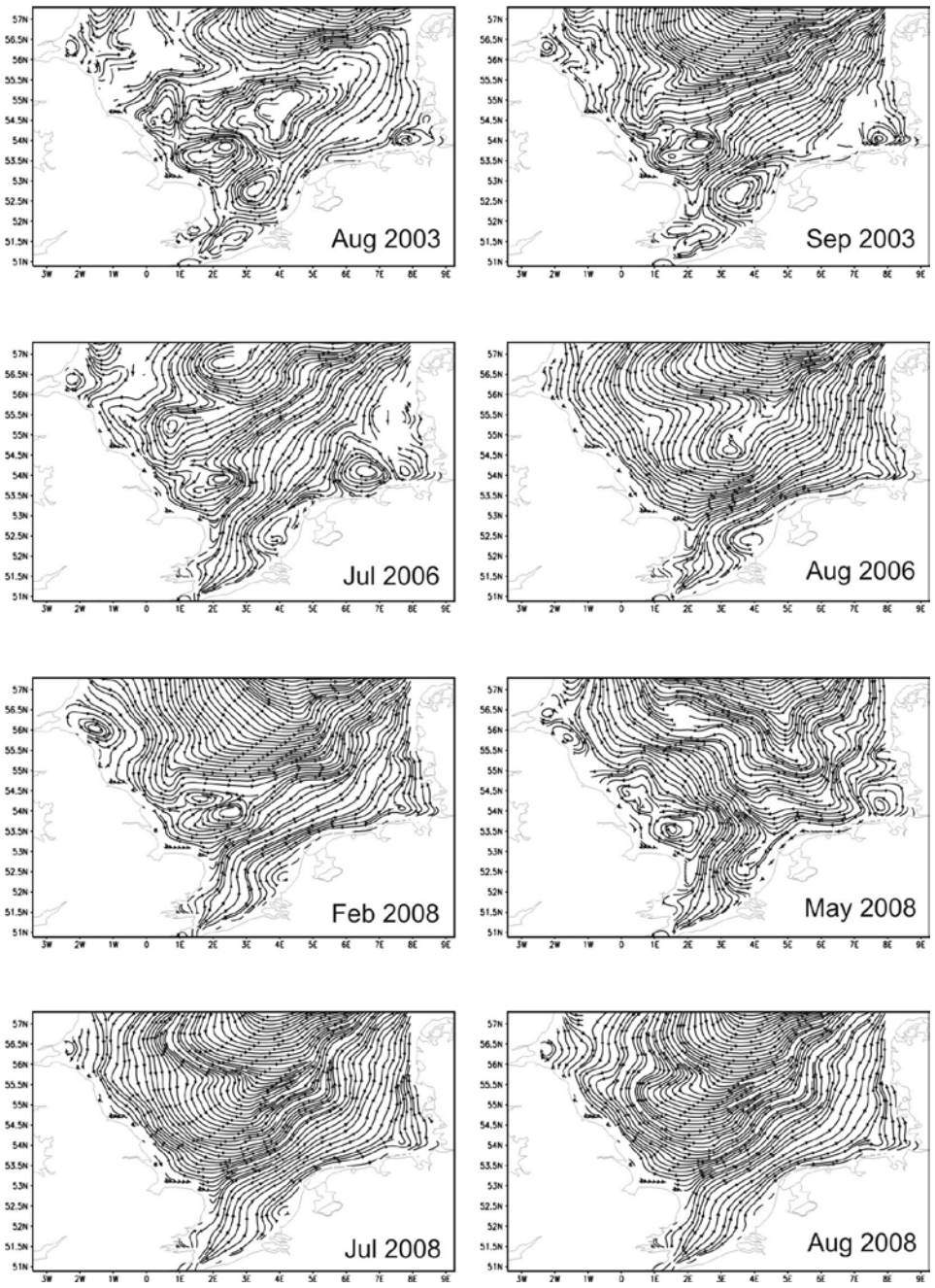

Figure 4.11: Different patterns of streamlines in the model.

The patterns of streamlines showed in general an anticlockwise flow direction. A clockwise flow direction, like to be seen in the eastern part of the model domain in August 2003 and May 2008 could occur especially in April and May in other years that were not shown here. A clockwise flow direction in the eastern part in summer occurred only in August 2003 during the simulation period. Other effects that could occur in summer (see September 2003 and July

2006) were slow flow rates in the eastern part of the model domain and the appearance of circling flow patterns in the German Bight. Simulated annual means of the passage through the English Channel ranged between 0.054 Sv in 2003 and 0.125 Sv in 2002.

4.4 Discussion

The aim of this study is to specify the estimations of Thomas et al. (2009) who calculated about 72.5 Gmol yr^{-1} TA originating from the Wadden Sea. These calculations were based on observations from the CANOBA dataset in 2001 and 2002. The observed high TA concentrations in the south eastern North Sea also occurred in August 2008 (Salt et al.,subm.) and were used for model validation in this study. Former modelling studies of the carbonate system of the North Sea (Artioli et al., 2012, Lorkowski et al., 2012) did not consider the Wadden Sea as a source of TA and DIC. They showed good to reasonable agreement to observations from the CANOBA dataset in large parts of the North Sea in 2001 / 2002 (Thomas et al., 2009). Nevertheless, focussing on the German Bight, especially on summer measurements east of 7°E, the observed high TA concentrations could not be simulated satisfactorily. In the study at hand it was possible to identify the Wadden Sea as an important TA source for the German Bight and it was possible to recalculate the estimations of Thomas et al. (2009) and to obtain an annual Wadden Sea TA export rate of 40 Gmol yr^{-1}. Additionally, it was possible to define the most important river loads more precisely in order to get a more exact budget of TA and DIC in the German Bight. All steps that were required to calculate the budget are discussed in the following.

4.4.1 Wadden Sea exchange rates of TA and DIC

The Wadden Sea is an area of effective decomposition of organic material (van Beusekom et al., 2012) that originates from land and from the North Sea (Thomas et al., 2009). Anaerobic degradation of organic matter generates TA and increases the CO_2 buffer capacity of seawater. In this study modelled Wadden Sea export rates of TA and DIC were based on concentration measurements during tidal cycles in the years 2009 to 2011 (Tab. 4.1) and on calculated tidal prisms from a two day-period that were representative as annual mean values. From these data three different scenarios of different Wadden Sea export rates in the East Frisian Wadden Sea were simulated (simulations D – F). Certainly, this method contained uncertainties referred to the seasonality due to the fact that differences in concentrations during falling and rising water levels were linearly interpolated. These interpolated values were based on four to five measurements in the three export areas that were conducted in different years. Consequently, it was not aimed to reproduce the exact TA and DIC concentrations in the years 2001 to 2009. The simulations should be seen as possible scenarios if Wadden Sea export rates were considered. Nevertheless, the implementation of Wadden Sea export rates enabled a better reproduction of observed high TA concentrations in the German Bight in summer (compare simulations D – F in Fig. 4.4 and 4.7). The primary processes that could contribute to the TA generation in the Wadden Sea have been discussed in the study of Thomas et al. (2009) and

were identified as denitrification, sulphate reduction or processes that are coupled to sulphate reduction and other processes.

4.4.1.1 Denitrification

Denitrification in the Wadden Sea is driven by organic material decomposition and allochthonous nitrate supply. Taking CH_2O as a short form for the organic material without consideration of nitrogen or phosphorus content, the denitrification process reads:

$$5CH_2O + 4H^+ + 4NO_3^- \Rightarrow 2N_2 + 5CO_2 + 7H_2O \quad (4.2)$$

Approximately 20% of nitrate that is denitrified within the Wadden Sea originates from rivers (Beusekom & de Jonge, 2002; Seitzinger et al., 2006). The remaining nitrate can be supplied by smaller rivers, groundwater discharge and the adjacent North Sea (Slater & Capone, 1987).

4.4.1.2 Sulphate reduction

Sulphate reduction generates H_2S that can escape to the atmosphere when sediments are exposed at low tide (Kristensen et al., 2000):

$$2CH_2O + SO_4^{2-} + 2H^+ \Rightarrow 2CO_2 + H_2S + 2H_2O \quad (4.3)$$

Furthermore, H_2S can also be buried as pyrite (FeS_2) in the sediment (4.4) if reduced iron is available from iron reduction (4.5). Sulphur (S) can be considered as a product of incomplete sulphate reduction (Hu and Cai, 2011):

$$Fe^{2+} + H_2S + S \Rightarrow FeS_2 + 2H^+ \quad (4.4)$$

$$CH_2O + 4FeOOH + 8H^+ \Rightarrow 4Fe^{2+} + CO_2 + 7H_2O \quad (4.5)$$

A third process that can produce TA in the Wadden Sea is methane oxidation by sulphate reduction (Wolf-Gladrow, 2007):

$$CH_4 + SO_4^{2-} \Rightarrow HCO_3^- + HS^- + H_2O \quad (4.6)$$

Considering (4.3) it gets clear that TA increases by 2 mol per 1 mole of decreasing sulphate. Reaction (4.4) leads to no change in TA because the consumption of iron cancels the TA produced due to iron reduction (4.5). Thomas et al. (2009) showed that the South Eastern Bight

act as a sink for TA during autumn and winter, which can be attributed to the reoxidation of pyrite (Luff & Moll, 2004; de Beer et al., 2005).

All these fluxes can hardly be estimated by the model or by TA measurements alone. Only if DIC variations in the Wadden Sea were taken into account some numbers can be found (see next paragraph).

4.4.1.3 Other Processes

The net effect of evaporation and precipitation in the Wadden Sea has to be considered, too. Although these processes are balanced in the German Bight, enhanced evaporation can occur in the Wadden Sea due to increased heating during low tide around noon. Onken & Riethmüller (2010) estimated an annual negative freshwater budget in the Hörnum Basin based on long-term hydrographic time series from observations in a tidal channel. From this data a mean salinity difference between flood and ebb currents of approximately -0.02 PSU can be considered. This would result in an increasing TA concentration by 1 µmol kg^{-1}, which is the range of the inaccuracy of measurements. Furthermore, the enhanced evaporation interferes with effects of groundwater input into the Wadden Sea. Hence, this effect can only hardly be derived from salinity differences between flood and ebb tides. As a consequence, the effect of additional nutrient input via groundwater discharge into the Wadden Sea remains unclear.

Certainly, aerobic degradation also occurs in the Wadden Sea, which results in a reduction of TA by 17 mol for the regeneration of 106 mol of organic carbon if a C:N:P ratio of 106:16:1 is assumed (Thomas et al., 2009).

4.4.2 TA / DIC ratios during the course of the year

The Wadden Sea export rates in this study were calculated as bulk exports. The underlying processes were not simulated explicitly but the ratios of exported TA and exported DIC can give hints about the dominant processes (Chen & Wang, 1999; Thomas et al. 2009). Aerobic degradation of organic material results in a reduction of TA due to increasing nitrate and increasing DIC and is indicated by a TA / DIC ratio of -0.16. Denitrification is indicated by a TA / DIC ratio of 1 and processes related to sulphate reduction are indicated by a TA / DIC ratio of 2. The respective export rates and ratios of the export rates TA / DIC for the different export areas are shown in Fig. 4.12.

The TA / DIC ratio in the North Frisian Wadden Sea (NF) ranged most of the time between 0 and 0.5. Aerobic degradation of organic material and denitrification were the dominant processes here. The ratio got negative in autumn, which was due to a negative ΔTA value and thus a consumption of TA (compare Tab. 4.1). The sediment got swirled up due to increasing wind speed and buried pyrite could get reoxidated. The DIC export rate had also its minimum in autumn, which was due to a decreasing supply of organic material in that time.

The TA / DIC ratios of the Jade Bay and the East Frisian Wadden Sea in simulation F were the same. The ratio was about 1 between January and May. The ratio ranged between 1.5 and 2 between May and September, when sulphate reduction, pyrite burial and methane oxidation by sulphate reduction became the dominant processes. The ratio decreased to -0.5 in autumn, when aerobic degradation and reoxidation of pyrite occurred, which was also due to increasing wind and reoxidation of the sediment. The DIC export rate had its minimum in autumn again due to decreasing supply of organic matter.

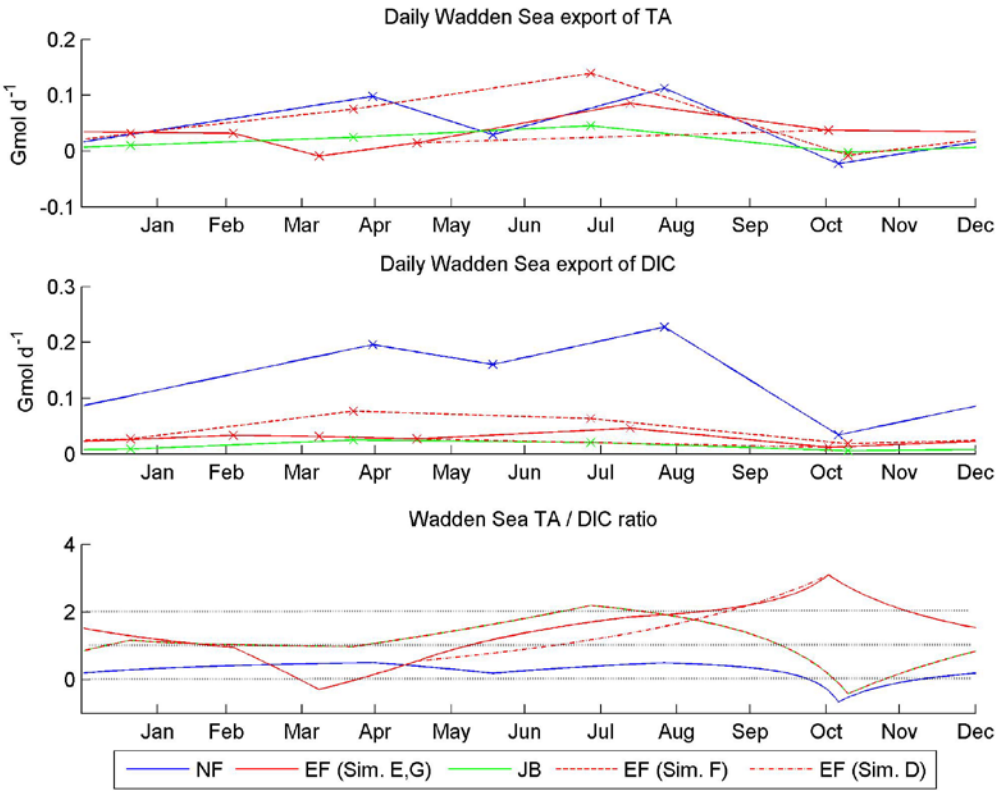

Figure 4.12: Daily Wadden Sea export rates of TA and DIC [Gmol d^{-1}] and the TA / DIC ratio of the export rates in the North Frisian (NF) and East Frisian (EF) Wadden Sea as well as in the Jade Bay (JB). Different scenarios of Wadden Sea export rates are indicated according to the respective simulations (D – G). The times of concentration measurements are indicated with x.

The TA / DIC ratio of the East Frisian Wadden Sea in simulations D, E and G was about 1 in January and February, when denitrification dominated. A slightly negative value occurred at the beginning of April when aerobic degradation of organic matter dominated. Between April and August the ratio increased to 2. Anaerobic degradation became dominant. Denitrification dominated until June in simulations E and G and until July / August in simulation D. Afterwards the ratios increased up to 3 in autumn mainly due to relatively high ΔTA values (16 µmol kg^{-1}) compared to ΔDIC values (5 µmol kg^{-1}) (compare Tab. 4.1). This was due to dominating processes related to sulphate reduction. The maximum ratio of 3 could be due to a short-term effect of iron reduction that influenced the measurements of TA concentrations. Iron reduction leads to a high generation of TA on short time scales because reduced iron can be rapidly reoxidised.

Derived from these data, the North Frisian Wadden Sea export area showed another pattern than the East Frisian Wadden Sea and the Jade Bay export areas. Aerobic degradation of organic matter played a key role in the North Frisian Wadden Sea during the whole course of the year. The DIC export rates indicated that most organic matter got degraded there, which was also due to the fact that the daily exchanged water masses in the North Frisian Wadden Sea (8.1 km^3 d^{-1}) were 3.5 times higher than in the East Frisian Wadden Sea (2.3 km^3 d^{-1}) and 10 times higher than in the Jade Bay (0.8 km^3 d^{-1}) (compare Tab. 4.2). However, TA export rates of the North Frisian and the East Frisian Wadden Sea were in the same range. Regional differences in organic matter dynamics in the Wadden Sea were discussed by van Beusekom et al. (2012). Organic matter turnover is driven by the import from the North Sea but different eutrophication effects are mainly related to the shape and size of a tidal basin. Van Beusekom et al. (2012) proposed that wider tidal basins with a large distance between barrier islands and mainland generally have a lower eutrophication status than narrower tidal basins. This leads to a "dilution" effect of the imported organic matter in wider tidal basins. In this study aerobic degradation of organic matter dominated in the North Frisian Wadden Sea, where the size of the tidal basins and the distance between barrier islands and mainland are larger. This indicated less eutrophication than in the East Frisian Wadden Sea, where anaerobic degradation of organic matter dominated.

4.4.3 Dominating anaerobic processes in the Wadden Sea

The calculated daily export rates of TA and the corresponding TA / DIC ratios enabled an association of exported TA to the underlying processes. Negative TA / DIC ratios were assigned to aerobic degradation of organic matter. TA / DIC ratios between 0 and 1 were completely allocated to denitrification, whereas ratios between 1 and 2 were proportionally allocated to denitrification and sulphate reduction related processes. Ratios greater than 2 were completely allocated to sulphate reduction processes, although iron reduction may have caused this high ratio. The amount of TA that was produced due to these processes is presented in Tab. 4.4. Certainly, these figures can only be interpreted as a coarse approach to the underlying processes because it is doubtful that no sulphate reduction takes place in any parts of the North Frisian Wadden Sea or that no denitrification takes place in the East Frisian Wadden Sea or the Jade Bay in summer. Nevertheless, these figures can be compared with other studies.

Kristensen et al. (2000) and de Beer et al. (2005) estimated the Wadden Sea sulphate reduction in a range of 6 to 13 Gmol yr^{-1}, which corresponds to a TA production of 12 to 26 Gmol yr^{-1}. Considering the fact that the West Frisian Wadden Sea at the northern Dutch coast is not yet included into the model the numbers are in acceptable accordance with 8.5 to 15.5 Gmol TA yr^{-1} that was produced in this model due to sulphate reduction related processes (Tab. 4.4).

Data obtained by Jensen et al. (1996) were extrapolated to about 100 Gmol N yr^{-1} that gets denitrified in the entire Wadden Sea (Thomas et al., 2009), which would correspond to a TA production rate of about 99 Gmol yr^{-1}. This amount exceeds the calculation in the study at hand by a factor of 3 to 4 (26.6 to 33.4 Gmol yr^{-1}). The difference could not only be explained by the missing West Frisian Wadden Sea as an additional source of TA in the model. It is likely that most of the estimated 100 Gmol N yr^{-1} are part of coupled ammonification, nitrification and denitrification, which does not change net TA (Hu and Cai, 2011). Analogously to the internal processes in the model only the denitrification of allochthonous nitrate can change net TA. This is also applicable for the Wadden Sea. Furthermore, in terms of TA turnover the effect of coupled ammonification, nitrification and denitrification is not only restricted to the same place in the sediment in the Wadden Sea. These processes can also be seen as coupled in terms of net TA production in a tidal basin if they take place in the same tidal basin. As a consequence, the production of net TA caused by denitrification can only hardly be calculated from direct measurements of denitrification rates.

On a regional scale, Deek et al. (2012) calculated denitrification from own measurements to be about 1 Gmol N yr^{-1} in the North Frisian Wadden Sea, which is remarkably lower than the amount derived from TA / DIC ratios (18.36 Gmol N yr^{-1}) in Tab. 4.4. Although Deek et al. (2012) stated that their calculation may be a lower estimate of denitrification in the North

Frisian Wadden Sea, this deviation is most likely due to the calculation of TA / DIC ratios. The underlying TA and DIC concentrations were measured near the outlet of the Sylt-Rømø bight, a tidal basin where the above mentioned processes can take place at different locations simultaneously. Hence, the measured concentrations were influenced by denitrification but also by aerobic degradation on the one side and sulphate reduction related processes on the other side. The TA / DIC ratios of the last two processes can interfere and result in TA / DIC ratios between 0 and 2. This leads to potentially overestimated rates of denitrification in Tab. 4.4. Thus, it should be pointed out that a detailed nitrogen budget of the Wadden Sea cannot be derived from this TA / DIC ratios.

Nevertheless, the regional differences in the Wadden Sea have different impacts on the carbonate system in the German Bight. High TA / DIC ratios indicate an increased buffer capacity for atmospheric CO_2, whereas the low TA / DIC ratios of the North Frisian Wadden Sea indicate an additional export of excess DIC. This leads to an increased acidification effect in the German Bight.

Table 4.4: TA that was produced irreversibly due to aerobic degradation of organic matter, denitrification and sulphate reduction related processes in the North Frisian Wadden Sea (NF), the Jade Bay and in the East Frisian Wadden Sea in simulations D – G.

Process	NF	JB	EF (Sim. E, G)	EF (Sim. F)	EF (Sim. D)
Aerobic	-0.51	-0.03	-0.11	-0.08	-0.11
Denitrification	18.36	3.70	4.91	11.35	4.49
Sulphate red.	0.00	3.82	9.24	11.71	4.70
Sum	17.85	7.49	14.04	22.98	9.08

4.4.4 The impact of exported TA and DIC on the North Sea

In this study it was possible to relate the observed high TA and DIC concentrations mainly to TA and DIC export rates from the Wadden Sea (Fig. 4.3 – 4.7). Three different scenarios indicated a minimum, medium and maximum estimate of Wadden Sea export rates. TA concentrations could be better reproduced than DIC concentrations, which was mainly due to the higher sensitivity of DIC to modelled biology. Nevertheless, from a present point of view the Wadden Sea is the main driver of TA concentrations in the German Bight. Future forecast studies of the evolution of the carbonate system in the German Bight have to put another focus on the Wadden Sea and its determining processes.

In this context the Wadden Sea evolution due to future sea level rise is the most important factor. The balance between sediment supply from the North Sea and sea level rise is a general precondition for the persistence of the Wadden Sea (Flemming and Davis, 1994; Van Koningsveld et al., 2008). An accelerating sea level rise could lead to a deficient sediment supply from the North Sea and shift the balance at first in the largest tidal basins and at last in the smallest basins (CPSL, 2005; Van Goor et al., 2003). The share of intertidal flats as potential sedimentation areas is larger in smaller tidal basins (van Beusekom et al., 2012), whereas larger basins have a larger share of subtidal areas. Thus, assuming an accelerating sea level rise, large tidal basins will turn into lagoons, while tidal flats may still exist in smaller tidal basins. This effect could decrease the overall Wadden Sea export rates of TA, because sediments would no longer be exposed to the atmosphere and the products of sulphate reduction would reoxidate in the water column immediately. Moreover, sedimentary exchange in the former intertidal flats would only be diffusive and no longer advective due to hydraulical gradients during ebb tides, when parts of the sediment get unsaturated with water. During these sedimentological changes the composition of sediments can also change. If sediments become sandier, aerobic degradation of organic matter would become more dominant. The North Frisian Wadden Sea would be more affected by a rising sea level because there the tidal basins are larger than the tidal basins in the East Frisian Wadden Sea and even larger than the in the inner Jade Bay.

The Wadden Sea export of TA and DIC is driven by the turnover of organic material. Decreasing anthropogenic eutrophication can lead to decreasing phytoplankton biomass and production (Cadée & Hegeman, 2002; van Beusekom et al., 2009). Thus, the natural variability of the North Sea primary production becomes more important in determining the organic matter turnover in the Wadden Sea (McQuatters-Gollop et al. (2007); McQuatters-Gollop & Vermaat (2011)). Moreover, despite the assumption of decreasing overall TA export rates from the Wadden Sea the impact of the North Frisian Wadden Sea on the carbonate system of the German Bight could potentially change due to a change of tidal prisms and thus a change in imported organic matter. If less organic matter gets remineralised in the North Frisian Wadden less DIC would be exported to the North Sea.

In the context of climate change, processes that have impact on the freshwater budget of tidal mud flats can become more important. An increasing discharge of small rivers and groundwater into the Wadden Sea could increase nutrient loads and the production of organic matter. Evaporation could also increase due to increased warming and become a more important process than today (Onken & Riethmüller, 2010).

Concluding, in the course of climate change the North Frisian Wadden Sea will be affected first by sea level rise, which will result in decreased TA and DIC export rates due to less turnover of

organic matter there. This could lead to an increased buffering of atmospheric CO_2 in the German Bight. Furthermore, if the other parts of the Wadden Sea will be affected by sea level rise, the TA export rates will further decrease and thus the buffer capacity in the German Bight will decrease, too. Overall, less organic matter will be remineralised in the Wadden Sea.

4.4.5 TA budgets and variability of TA concentrations in the German Bight

Modelled TA and DIC concentrations in the German Bight showed a high interannual and seasonal variability (Fig. 4.8, 4.9). Overall, the TA variability was more sensitive to Wadden Sea export rates than the DIC variability because the latter was also dominated by biology and atmospherical exchange. However, the implementation of Wadden Sea DIC export rates enabled a better reproduction of observed DIC concentrations, too.

It is obvious to associate the TA variability with the variabilities of the different sources. In order to calculate a realistic budget, simulation E was considered to be the most probable scenario because it was based on the most measurements in the East Frisian Wadden Sea. Annual and seasonal budgets of TA sources and sinks are shown in Tab. 4.5. The budget could not be perfectly closed because in every year a difference between sources and sinks occurred that ranged between 0.77 and 1.78 Gmol yr^{-1}. The relative error was always smaller than 1 % but could not be referred to a single process. Other estimates showed that the error increased with the total number of fluxes included in a budget calculation. Since 17 fluxes were included in the prognostic treatment of TA it was likely that the difference was due to these inaccuracies. Nevertheless, the error is smaller than every process considered for TA calculation and should thus not change the results of this study significantly.

River loads ranged from 77.76 to 152.14 Gmol yr^{-1} and had the highest variability of all TA sources in the validation area. As already explained in chapter 3 it is difficult to compare the river loads itself with internal processes and Wadden Sea exchange rates without consideration of freshwater discharge. For this purpose an effective river input was introduced in chapter 3.4.3 that enabled a direct comparison of river loads, dilution of TA due to freshwater discharge, Wadden Sea exchange rates and the internal processes. If the annual means of the amounts of all sources were compared, a relative ranking of the processes could be derived. 68 % of all TA concentration changes in the validation area were due to Wadden Sea export rates, 23 % were due to internal processes and 9 % were due to effective river input of bulk TA. Certainly, this ranking depends mainly on the characteristics of the Elbe estuary. The river Rhine had an effective river input of 28 Gmol yr^{-1} in 2008, which would have a much grater impact on TA concentration changes than the Elbe estuary.

Table 4.5: Annual TA budgets in the validation area of the years 2001 to 2009 and seasonal budgets in 2008 from January to March, April to June, July to September and October to December [Gmol]. The Wadden Sea source of TA is referred to simulation E. Riv_{eff} was introduced in chapter 3.4.3. Flow is the amount of TA that passes the validation area. Negative values indicate an export from the validation area to the adjacent North Sea. Δcontent indicates the difference of the TA contents of the last and the first time steps of the simulated year or quarter.

	Wadden Sea	Int. processes	River loads	Riv_{eff}	Flow	ΔContent
2001	39.38	13.19	86.98	-5.15	-4.09	136.37
2002	39.38	20.11	152.14	-7.03	-288.82	-75.42
2003	39.38	15.75	90.68	-3.83	-124.59	22.15
2004	39.44	12.54	77.76	-4.46	-39.75	90.79
2005	39.39	12.34	88.70	-5.12	-128.21	12.99
2006	39.39	11.31	87.90	-5.52	-98.98	40.43
2007	39.39	12.38	109.51	-5.16	-166.98	-4.22
2008	39.44	14.93	93.48	-4.45	-105.95	42.97
2009	39.39	10.14	83.14	-4.99	-190.23	-56.86
Jan - Mar	8.08	0.87	42.14	-0.87	-60.92	-9.83
Apr - Jun	10.41	12.47	25.69	-1.97	-6.92	41.65
Jul - Sep	16.76	-2.32	9.58	-1.34	59.93	83.94
Oct - Dec	4.19	3.91	16.08	-0.27	-98.04	-72.79

On seasonal time scales the internal processes got more important from April to June (50%) and from October to December (47%). The impact of effective river input was smaller than 10% in every quarter. The Wadden Sea TA export rates had an impact of 82% on TA concentration changes in the validation area from January to March and from July to September.

The sum of Wadden Sea exchange rates, internal processes and effective river loads was highest in 2002 (52.46 Gmol yr^{-1}) and lowest in 2009 (44.54 Gmol yr^{-1}). However, the highest TA concentrations were simulated in summer 2001, 2009 and especially in summer 2003 (Fig. 10, simulation E). In simulation G (like simulation E but without impact of internal processes on TA concentrations) the same pattern could be reproduced. Thus, the interannual variability was not driven by temporal changes of the internal processes and the Wadden Sea export rates were similar in every year. The high interannual variability of summer concentrations could only be driven by hydrodynamic differences between the years. Flushing times were higher in summer than in winter (Fig. 4.10) in every year, which increased the amount of exported TA that accumulated in the validation area. They were also more variable in summer than in winter, but high TA concentrations could not only be derived from the presented flushing times. Changes in stream patterns also caused high interannual differences in summer TA concentrations (Fig. 4.11). Distinct anticlockwise stream patterns defined the hydrodynamic conditions in every

winter. Summer stream patterns were in most years weaker especially in the German Bight (compare Fig. 4.11 September 2003, July 2006). In August 2003 a clockwise pattern was found, which led to further accumulation of TA in the water masses. This could explain the highest concentrations in summer 2003.

One aim of this study was to recalculate the Wadden Sea TA export rates calculated by Thomas et al. (2009). They estimated that 72.5 Gmol TA yr^{-1} were produced in the Wadden Sea. Their calculations were based on measurements in 2001 and 2002. The presented model was validated with data measured in August 2008 (Salt et al., subm.) but the measurements were conducted at the same positions. High TA concentrations in the German Bight could be observed in summer 2001 and in summer 2008. Due to the scarcity of data the West Frisian Wadden Sea could not be considered in the simulations but the amount of exported TA from that area could potentially be in the same range as from the East Frisian Wadden Sea (10 to 14 Gmol yr^{-1}). In the TA budgeting in Tab. 4.5 simulation E was most representable with an annual export of about 39.4 Gmol yr^{-1} from the Wadden Sea. With additional export from the West Frisian Wadden Sea the overall Wadden Sea export could be 53.4 Gmol yr^{-1} at the maximum. Thus, the TA export from the Wadden Sea calculated in this study is 19.1 to 33.1 Gmol yr^{-1} lower compared to the study of Thomas et al. (2009). This is mainly due to the flushing time that was assumed by Thomas et al. (2009). They considered the water masses to be flushed within six weeks (Lenhart et al., 1995). Flushing times calculated in the study at hand were significantly longer and more variable in summer. Since the Wadden Sea export calculated by Thomas et al. (2009) was defined as a closing term of the TA budget, underestimated summerly flushing times led to an overestimation of the exchange with the adjacent North Sea.

4.5 Conclusion

We presented a budget calculation of TA sources in the larger German Bight and related 68% of the annual TA concentration changes to Wadden Sea exports of TA. The impact of riverine bulk TA is less important in the German Bight due to the comparatively low TA concentrations in the Elbe estuary. Nevertheless, the rivers are sources of allochthonous nitrate, which is the main source for net TA generation due to denitrification.

The evolution of the carbonate system in the German Bight under future anthropogenic or climate change scenarios depends on the fate of the Wadden Sea. The amount of TA and DIC that is exported from the Wadden Sea depends on the amount of organic matter that gets imported to and degraded in the Wadden Sea. Decreasing riverine nutrient loads can lead to decreasing phytoplankton biomass and production (Cadée & Hegeman, 2002; van Beusekom et al., 2009). However, further offshore natural dynamics can override the effects of riverine nutrient loads (van Beusekom et al., 2012).

In the context of sea level rise, the North Frisian Wadden Sea will potentially be more affected by a loss of intertidal areas than the East Frisian Wadden Sea (van Beusekom et al., 2012). However, this effect can reduce the turnover of organic material in the Wadden Sea, which can counteract the effect of increased TA production due to a stimulated organic matter production.

In this study it was possible to quantify the effect of different TA sources on TA concentrations in the German Bight. Derived from TA / DIC ratios (Fig. 4.12) the different Wadden Sea export areas can have contrary effects on the carbon budget of the German Bight in terms of release or uptake of CO_2. Thomas et al. (2004) estimated that the Wadden Sea facilitates approximately 7 – 10% of the annual CO_2 uptake of the North Sea so it is worth to study future scenarios of CO_2 uptake driven by the Wadden Sea in the light of climate change.

5 Final discussion

The main aim of this study is to investigate the impact of anaerobic processes on TA in the southern North Sea and to calculate the amount of TA that is exported from the Wadden Sea into the North Sea. The observed high TA concentrations in the German Bight cannot be reproduced without consideration of the Wadden Sea as a source for TA. Although the calculation of Wadden Sea TA export by Thomas et al. (2009) reveal 40 Gmol yr^{-1} instead of 73 Gmol yr^{-1} it remains the most important TA source if the effective river loads are considered. A simple consideration of bulk river loads without implication of freshwater discharge neglects the possibility of TA dilution by river input and overestimates the riverine impact on TA concentrations.

During the recent study several questions arose that are answered in the following:

Which processes dominate the TA turnover (production – consumption) in the southern North Sea?

Hu & Cai (2011) stated that only the denitrification of allochthonous nitrate can produce net TA. However, TA can be already produced prior to denitrification due to the uptake of nitrate by phytoplankton. This can be confirmed in chapter 2, because only the nitrate-related processes in the model show a significant imbalance at the end of the year that is accountable for TA production. Although the ammonium-related processes show high rates, they are mostly balanced during the course of the year and lead only to minor TA production or consumption. Calcite-related processes can explain TA production or consumption on seasonal time scales in the model, but they are mostly balanced at the end of the year.

What are the temporal and spatial deviations between the amount of denitrification and actually produced TA?

The deviations between denitrification and actually produced TA (TA turnover) are high in large parts of the validation area. There are significant differences between denitrification and TA turnover during the course of the year but they converge at the end of the year. High concentrations of TA measured at a certain place and time can hardly be related to

denitrification, because TA is likely produced prior to denitrification. However, the source of nitrate plays an important role in this assumption. In case denitrification is mainly fuelled by pelagic nitrate invading the sediment this would also produce TA but this case cannot be reproduced in the model. Although studies showed that denitrification in the North Sea (without the Wadden Sea) is mainly fuelled by nitrification in the upper sediment layer (Raaphorst et al., 1990; Seitzinger & Giblin, 1996), it remains an open question whether denitrification is at least partly fuelled directly by pelagic nitrate in some parts of the North Sea. This would decrease the deviations at places where denitrification exceeds TA turnover.

At which spatial scales is it adequate to use denitrification rates as an estimate for TA production in the North Sea?

It is shown in this study that denitrification is only partly applicable as a proxy for annual TA production, which was also under debate by Hu & Cai (2011). Thomas et al. (2009) considered benthic denitrification in the entire North Sea (excluding the Wadden Sea) to correspond to a TA release of about 119 Gmol yr^{-1}. This accounts for 15% of the potential annual CO_2 uptake if a Revelle factor of 11 is considered. If the majority of the allochthonous nitrogen in this area is denitrified the estimate has to be corrected in terms of atmospheric nitrogen deposition and riverine TON input. Thomas et al. (2009) considered simulated denitrification rates calculated by Pätsch & Kühn (2008), who included riverine TON input of about 10 – 15 Gmol yr^{-1} and additional atmospheric nitrogen deposition of about 27 Gmol N yr^{-1} in their simulation. Hence, the net TA production in the entire North Sea (excluding the Wadden Sea) is about 40 Gmol yr^{-1} lower than calculated by Thomas et al. (2009). It has to be mentioned here that the model domain examined by Pätsch & Kühn (2008) included a larger area compared to the presented model domain. Hence, they used higher amounts of atmospheric nitrogen deposition and riverine TON input for their calculations.

Can enhanced river loads of nutrients induce a significantly higher TA turnover that can explain observations of high TA concentrations in the German Bight?

River loads of nutrients and TA turnover correlate well (R^2=0.82) in the German Bight. In the study at hand it was not possible to reproduce the observed high TA concentrations in years with comparatively high river loads of nutrients without consideration of Wadden Sea exports. Nevertheless, the internal turnover of TA is the second most important driver of TA concentrations in the southern North Sea.

Can seasonal variations in river loads of bulk TA be the origin of observed high TA concentrations in the German Bight?

It is possible to increase the seasonal variability of TA in the German Bight by including variations in riverine TA concentrations. Nevertheless, these changes do not lead to significantly higher TA concentrations in the German Bight. Artioli et al. (2012) related high TA concentrations to river loads in the German Bight, although they could not reproduce the observations there. In the current study it is shown that the effect of rivers on TA concentrations in the German Bight is low if dilution by riverine freshwater discharge is also considered.

Do loads of the river Rhine affect TA concentrations or the TA turnover in the German Bight significantly?

The level of TA concentrations in the German Bight is influenced significantly by the river Rhine after new river loads were implemented into the model. TA turnover in the German Bight is not affected by the river Rhine significantly. In Fig. 2.12 it seems that TA and DIC concentrations near the outlet of the river Rhine are calculated too high in simulations compared to observations. However, it should be mentioned here that the plume of the river Rhine can proceed alongside of the western Dutch coast (Hoppema, 1990), so it is likely that the plume was not sampled during the observations due to the fixed positions of the measurement stations.

What is the dominant driver of TA concentrations in the southern North Sea and what drives their interannual variability?

The Wadden Sea has the largest impact on TA concentrations in the German Bight on an annual time scale. Of course this influence is lower if the entire North Sea is considered but its impact is still significant. In spring the impact of internal TA turnover on TA concentrations is higher than the impact of the Wadden Sea due to the occurrence of phytoplankton blooms and the associated enhanced nutrient uptake. Nevertheless, differences in flushing times and the occurrence of weak meteorological blocking situations can lead to enhanced accumulation of simulated TA in the German Bight and thus increase the interannual variability especially in summer.

Are there regional differences in TA exported from the Wadden Sea into the North Sea?

Van Beusekom et al. (2012) stated that the eutrophication status of a tidal basin depends on its size. The distance between mainland and barrier islands is generally higher in the North Frisian Wadden Sea than in the East Frisian Wadden Sea, which might explain the differences between

North Frisian Wadden Sea and East Frisian Wadden Sea in the simulations. Calculations based on the measurements in the Wadden Sea show that sulphate reduction related processes exceed denitrification in the Jade Bay and in the East Frisian Wadden Sea, whereas about 18 Gmol TA yr^{-1} is produced only by denitrification in the North Frisian Wadden Sea (see chapter 4). The calculations of TA produced by sulphate related processes are in acceptable accordance with literature values (Kristensen et al., 2000; de Beer et al., 2005) but calculations of TA related to denitrification in the Wadden Sea bear uncertainties. Based on the measurements from Jensen et al. (1996), Thomas et al. (2009) estimated an annual denitrification rate of about 100 Gmol N yr^{-1} in the whole Wadden Sea, whereas Deek et al. (2012) calculated denitrification from their own measurements to be about 1 Gmol N yr^{-1} in the northern part of the Wadden Sea. Both figures differ significantly from calculations in chapter 4, but it should be pointed out that no nitrogen budget of the Wadden Sea could be derived from the presented TA / DIC ratios. The calculation of 18 Gmol TA yr^{-1} produced by denitrification in the North Frisian Wadden Sea is likely to be interfered by aerobic processes and sulphate reduction related processes. Denitrification in the Wadden Sea can also exceed TA production due to the coupling of nitrification and denitrification. In this case, the coupling is not limited to the same place in the sediment. These processes can also be coupled in terms of net TA production if they take place in the same tidal basin. Furthermore, also Deek et al. (2012) stated that their calculation may be a lower estimate of denitrification in the Wadden Sea.

5.1 Final budgeting of TA production in the North Sea and conclusion

Thomas et al. (2009) estimated that anaerobic organic matter degradation irreversibly facilitates about 20 – 25% of the CO_2 uptake of the North Sea. Their calculation is based on 119 Gmol TA yr^{-1} generated in the North Sea due to denitrification and on 73 Gmol TA yr^{-1} originated in the Wadden Sea. As it is shown above only 79 Gmol TA yr^{-1} can be attributed to denitrification in the North Sea and also the exported TA from the Wadden Sea is lower than previously estimated by Thomas et al. (2009). Thus, on the basis of a simple proportional calculation the revised budget implies that anaerobic organic matter degradation facilitates only up to 15% of the annual CO_2 uptake of the North Sea. Thomas et al. (2009) also calculated the potential CO_2 uptake resulting from global denitrification (Seitzinger et al., 2006) to be 15 Tmol yr^{-1}. In the current model study only 66% of denitrified nitrogen also produces net TA. Hence, on the basis of a simple proportional calculation the global estimated CO_2 uptake induced by denitrification in ocean margins could be reduced to 10 Tmol yr^{-1}.

The calculations of Wadden Sea export rates of TA and DIC in this study were based on measurements conducted at one place for each of the three exchange areas. This reveals uncertainties because the measurements were extrapolated to large areas of the Wadden Sea. The calculations in this study were more precise than the first estimates by Thomas et al. (2009) but interannual variabilites of the Wadden Sea export could not be resolved. Nevertheless, it is shown that the Wadden Sea is an important driver of the carbonate system in the southern North Sea and it is worth investigating its dynamics and further evolution. Future model studies of the carbonate system in the southern North Sea may try to parameterize organic matter degradation in the Wadden Sea fuelled by the southern North Sea and the resulting Wadden Sea export rates of TA, DIC and nutrients. An even more precise model study can aim to simulate the Wadden Sea itself coupled to the southern North Sea. This approach would enable a distinct spatiotemporal budgeting of the major biogeochemical processes in the Wadden Sea.

Appendix

A Data used for calculations of the Dutch rivers and river loads in the years 2001 - 2009

A1: Data provided by waterbase.nl used for calculations of the Dutch river Noordzeekanaal at station Ijmuiden.

	Data given by waterbase.nl					Calculated values	
date	HCO_3^-[µmol l^{-1}]	pH	S[PSU]	T[°C]	NO_3^-[µmol l^{-1}]	DIC[µmol l^{-1}]	TA[µmol l^{-1}]
22.01.2007	3607	8.1	6.4	9.9	188.6	3751	3814
19.02.2007	3443	7.9	6.0	8.4	172.9	3568	3556
19.03.2007	3279	8.0	7.8	10.5	236.4	3410	3453
19.04.2007	3279	8.1	7.8	17.1	101.4	3445	3558
10.05.2007	3279	8.1	10.4	16.6	70.0	3466	3609
11.06.2007	3115	7.9	8.1	21.5	67.1	3254	3315
09.07.2007	3115	7.8	5.7	21.2	87.1	3236	3239
06.08.2007	3279	8.0	5.4	22.3	97.1	3419	3486
03.09.2007	2951	7.8	9.9	21.8	75.0	3083	3125
01.10.2007	3115	7.8	9.3	18.5	102.1	3246	3272
26.11.2007	3279	8.0	11.4	10.6	89.3	3427	3502
27.12.2007	2787	7.9	9.0	8.3	140.0	2895	2907
21.01.2008	3607	7.9	7.8	9.0	122.9	3744	3750
18.02.2008	3279	8.0	7.1	7.7	172.1	3402	3426
17.03.2008	3279	8.0	8.0	8.6	182.1	3407	3444
14.04.2008	2787	8.4	7.0	11.5	120.7	2976	3149
13.05.2008	2787	9.4	6.6	18.1	72.1	4899	7091
09.06.2008	3115	7.6	9.3	21.1	70.0	3252	3223
07.07.2008	3115	8.0	10.7	23.1	65.0	3298	3435
04.08.2008	2951	7.8	2.9	22.0	60.0	3056	3029
01.09.2008	2787	7.7	7.4	21.2	104.3	2902	2893
27.10.2008	3279	8.2	8.3	15.9	94.3	3472	3629
24.11.2008	3279	7.9	3.0	13.1	129.3	3389	3363
22.12.2008	3770	7.9	8.5	7.1	123.6	3915	3917
19.01.2009	3607	7.8	9.2	7.1	137.9	3750	3724
16.02.2009	3607	7.7	4.9	6.3	159.3	3766	3667
16.03.2009	3443	8.1	9.2	8.1	152.1	3594	3676
14.04.2009	3443	7.9	8.5	13.7	132.1	3582	3615
11.05.2009	3115	8.3	8.3	16.4	95.7	3338	3542
08.06.2009	3115	7.9	7.8	19.6	75.7	3248	3298
06.07.2009	3279	8.0	9.3	22.9	40.7	3458	3583
03.08.2009	2787	8.0	8.5	23.2	60.7	2934	3035
31.08.2009	2787	8.0	10.1	22.9	53.6	2946	3063
08.10.2009	2787	7.9	10.8	20.1	79.3	2922	2995
23.11.2009	2623	7.9	9.7	13.2	103.6	2732	2766
21.12.2009	3279	7.9	7.9	9.8	147.9	3405	3415

A2: Data provided by waterbase.nl used for calculations of the Dutch river Nieuwe Waterweg at station Maassluis.

	Data given by waterbase.nl					Calculated values	
date	HCO_3^- [µmol l^{-1}]	pH	salinity [PSU]	T [°C]	NO_3^- [µmol l^{-1}]	DIC [µmol l^{-1}]	TA [µmol l^{-1}]
24.01.2007	2295	8.0	1.7	7.8	257.1	2366	2341
21.02.2007	2623	7.6	1.7	7.4	246.4	2775	2643
21.03.2007	2951	8.1	0.5	8.8	192.9	3031	2998
18.04.2007	3115	8.3	2.6	14.5	200.0	3236	3309
15.05.2007	2951	7.8	1.7	16.0	142.1	3057	2999
13.06.2007	2295	8.0	1.5	21.1	152.1	2365	2361
11.07.2007	2623	7.8	0.8	18.7	157.1	2717	2656
08.08.2007	2623	8.0	1.2	21.4	157.9	2700	2691
05.09.2007	2787	8.0	0.8	19.0	125.7	2866	2844
03.10.2007	2787	7.8	1.3	15.5	162.1	2888	2827
28.11.2007	2623	7.5	1.2	7.1	220.7	2819	2636
27.12.2007	3279	7.6	0.8	3.8	214.3	3503	3295
23.01.2008	2787	7.5	0.4	7.8	245.7	3016	2797
20.02.2008	2787	7.8	2.3	5.3	234.3	2901	2824
19.03.2008	2623	7.8	0.7	8.3	245.7	2733	2646
16.04.2008	2787	8.0	0.7	10.2	222.1	2870	2828
14.05.2008	2623	8.3	0.6	18.9	155.7	2695	2719
11.06.2008	2623	7.8	1.6	21.7	150.7	2714	2673
09.07.2008	2951	7.9	3.8	20.8	126.4	3056	3064
06.08.2008	2623	7.9	2.1	22.5	121.4	2709	2697
03.09.2008	2787	7.9	4.9	19.8	111.4	2892	2909
01.10.2008	2623	8.0	4.2	15.6	114.3	2717	2737
26.11.2008	2951	8.1	0.8	7.5	179.3	3033	3003
23.12.2008	2787	8.0	0.9	6.1	222.1	2874	2826
21.01.2009	3115	8.2	1.6	3.3	193.6	3202	3195
18.02.2009	2623	8.0	0.9	4.6	247.9	2707	2658
18.03.2009	2623	8.0	0.4	8.0	253.6	2704	2653
15.04.2009	2787	8.2	1.3	14.1	163.6	2867	2883
13.05.2009	2787	8.2	2.6	15.5	150.7	2885	2930
10.06.2009	2787	8.1	3.7	17.9	115.7	2892	2939
08.07.2009	2787	8.0	2.9	22.5	112.9	2884	2907
05.08.2009	2623	7.9	2.1	21.6	125.7	2709	2696
02.09.2009	2623	7.9	5.5	20.4	100.7	2725	2749
28.10.2009	2623	8.0	3.9	12.0	157.1	2712	2719
25.11.2009	2787	8.1	1.6	10.6	202.9	2868	2862
22.12.2009	2623	7.8	2.6	4.2	225.0	2731	2659

A3: Data provided by waterbase.nl used for calculations of the Dutch river Haringvliet at station Haringvlietsluis.

	Data given by waterbase.nl					Calculated values	
date	HCO_3^- [µmol l^{-1}]	pH	salinity [PSU]	T [°C]	NO_3^- [µmol l^{-1}]	DIC [µmol l^{-1}]	TA [µmol l^{-1}]
30.01.2007	2295	8.0	0.3	6.3	268.6	2375	2309
27.02.2007	2459	7.8	0.3	7.5	261.4	2584	2468
27.03.2007	2623	8.2	0.3	8.5	199.3	2686	2649
24.04.2007	2787	9.1	0.3	13.7	210.7	2919	3044
22.05.2007	2787	8.4	0.3	16.3	150.7	2842	2842
19.06.2007	2787	8.2	0.3	20.5	132.9	2848	2826
17.07.2007	2459	8.0	0.3	19.5	167.1	2529	2480
14.08.2007	2623	8.1	0.3	20.0	112.1	2687	2652
11.09.2007	2623	8.2	0.3	17.6	161.4	2681	2657
09.10.2007	2951	8.0	0.3	14.6	150.7	3040	2973
06.11.2007	2623	8.0	0.3	10.9	190.7	2707	2641
04.12.2007	2623	7.7	0.3	6.7	225.7	2792	2631
03.01.2008	2459	7.7	0.3	3.2	212.1	2632	2466
26.02.2008	2623	7.9	0.3	5.8	247.1	2735	2635
26.03.2008	2459	7.8	0.3	6.8	232.9	2586	2468
22.04.2008	5246	8.1	0.3	11.2	212.9	5386	5291
20.05.2008	2787	8.1	0.3	16.8	132.9	2857	2815
15.07.2008	2787	8.1	0.3	18.6	126.4	2856	2816
12.08.2008	2623	8.2	0.3	19.7	120.7	2680	2659
09.09.2008	2623	8.2	0.3	17.1	122.9	2681	2656
07.10.2008	2787	8.1	0.3	13.5	122.1	2859	2812
04.11.2008	2787	8.2	0.3	10.1	140.0	2852	2816
30.12.2008	2623	8.3	0.3	3.0	225.7	2682	2651
27.01.2009	2951	8.4	0.3	2.5	217.1	3011	2989
24.02.2009	2787	8.0	0.3	4.8	248.6	2887	2802
24.03.2009	2459	8.1	0.3	8.3	222.9	2528	2478
21.04.2009	2623	8.3	0.3	14.3	177.1	2677	2662
19.05.2009	2787	8.2	0.3	15.0	145.0	2850	2820
16.06.2009	2787	8.3	0.3	17.8	146.4	2844	2832
14.07.2009	2623	8.4	0.3	20.4	105.0	2676	2681
11.08.2009	2623	8.3	0.3	21.3	119.3	2677	2670
08.09.2009	2131	8.4	0.3	17.9	100.0	2174	2175
06.10.2009	2623	8.3	0.3	15.2	107.1	2677	2663
03.11.2009	2787	8.2	0.3	11.4	97.9	2851	2817
29.12.2009	2459	8.1	0.3	2.6	231.4	2536	2475

A4: Data provided by waterbase.nl used for calculations of the Dutch river Scheldt at station Schaar van Ouden Doel.

	Data given by waterbase.nl					Calculated values	
date	HCO_3^- [µmol l^{-1}]	pH	salinity [PSU]	T [°C]	NO_3^- [µmol l^{-1}]	DIC [µmol l^{-1}]	TA [µmol l^{-1}]
22.01.2007	3443	7.8	5.4	9.1	363.6	3574	3529
05.02.2007	3443	7.8	4.6	8.0	345.7	3575	3518
07.03.2007	3607	7.6	2.1	9.3	362.1	3802	3639
04.04.2007	3279	7.8	4.8	10.8	361.4	3402	3360
29.05.2007	3443	7.9	9.8	18.0	247.9	3598	3664
25.06.2007	3443	7.7	10.6	20.8	199.3	3593	3604
23.07.2007	3443	7.7	9.3	20.6	264.3	3589	3590
20.08.2007	3279	7.7	9.3	20.5	265.7	3418	3419
17.09.2007	3443	7.7	10.3	19.0	194.3	3590	3592
15.10.2007	3607	7.7	10.0	16.4	223.6	3758	3746
14.11.2007	3770	7.9	8.8	11.3	206.4	3921	3947
12.12.2007	3443	7.7	2.5	8.7	293.6	3597	3485
07.01.2008	3770	7.9	5.8	5.7	325.0	3907	3880
04.02.2008	3934	7.9	4.8	7.4	368.6	4074	4042
31.03.2008	3607	7.8	1.8	8.9	352.9	3747	3654
28.04.2008	3607	7.9	5.5	12.9	320.7	3738	3739
26.05.2008	3607	7.9	7.4	17.6	240.7	3755	3796
23.06.2008	3279	7.8	7.2	19.4	265.0	3411	3422
21.07.2008	3443	7.8	9.0	19.3	215.7	3588	3616
20.08.2008	3443	7.6	8.5	20.2	212.9	3593	3551
17.09.2008	3279	8.0	9.6	18.1	222.9	3442	3542
13.10.2008	3443	7.8	10.0	16.0	219.3	3587	3608
10.11.2008	3443	8.3	10.8	11.8	225.7	3689	3913
08.12.2008	3934	7.8	4.9	7.3	294.3	4086	4021
19.01.2009	3770	8.0	8.5	3.9	270.0	3912	3933
02.02.2009	3934	7.9	4.9	3.8	307.9	4077	4029
02.03.2009	3770	7.7	4.6	6.4	325.0	3938	3831
01.04.2009	3934	8.0	4.4	9.7	352.1	4070	4075
25.05.2009	3607	7.9	8.4	17.6	240.0	3760	3813
24.06.2009	3607	7.9	9.8	19.5	200.0	3774	3850
22.07.2009	3770	7.7	11.3	21.5	177.1	3938	3959
18.08.2009	3279	7.9	12.9	22.3	167.9	3458	3572
14.09.2009	2787	7.8	13.0	19.3	150.0	2917	2968
12.10.2009	3443	7.8	12.9	16.8	162.1	3597	3643
09.11.2009	3443	7.8	13.1	12.3	139.3	3590	3614
07.12.2009	3770	7.8	8.5	9.4	234.3	3919	3898

A5: Data provided by waterbase.nl used for calculations of loads from the Ijseelmeer (west and east) at station Vrouwezand.

	Data given by waterbase.nl					Calculated values	
date	HCO_3^- [µmol l^{-1}]	pH	salinity [PSU]	T [°C]	NO_3^- [µmol l^{-1}]	DIC [µmol l^{-1}]	TA [µmol l^{-1}]
10.01.2007	2459	8.3	0.4	7.5	80.7	2512	2489
06.02.2007	2787	8.6	0.4	4.9	119.3	2841	2849
06.03.2007	2623	8.4	0.3	6.8	229.3	2675	2662
03.04.2007	2787	8.7	0.3	9.3	225.0	2848	2877
02.05.2007	2787	8.7	0.3	14.6	182.9	2853	2892
26.06.2007	1967	8.7	0.3	18.3	35.7	2017	2050
24.07.2007	1557	8.9	0.3	19.0	15.7	1613	1664
21.08.2007	1557	8.9	0.3	18.8	5.0	1613	1663
18.09.2007	1639	8.9	0.3	15.3	0.7	1694	1741
16.10.2007	2459	9.0	0.3	13.4	37.1	2553	2638
13.11.2007	2295	8.5	0.3	7.6	0.7	2339	2340
11.12.2007	2787	8.5	0.4	6.2	137.1	2840	2838
08.01.2008	2951	8.5	0.3	2.6	174.3	3008	2999
05.02.2008	3115	8.5	0.3	4.6	217.1	3175	3169
04.03.2008	2787	8.6	0.3	6.1	175.0	2841	2852
01.04.2008	1803	8.7	0.3	6.7	247.1	1841	1857
27.05.2008	2951	8.5	0.3	14.8	143.6	3010	3021
24.06.2008	2295	8.7	0.4	17.4	78.6	2352	2389
22.07.2008	1607	8.6	0.4	16.0	22.1	1641	1657
19.08.2008	1574	8.9	0.3	17.9	33.6	1629	1678
16.09.2008	1213	8.8	0.4	16.0	15.0	1247	1275
14.10.2008	1967	8.6	0.3	12.9	17.1	2008	2024
11.11.2008	2295	8.6	0.3	8.8	60.0	2341	2353
09.12.2008	2459	8.4	0.3	3.6	62.9	2509	2492
22.01.2009	2951	8.5	0.4	1.4	153.6	3008	2997
03.02.2009	2951	8.5	0.4	0.2	140.0	3008	2995
03.03.2009	1803	9.0	0.4	4.3	167.1	1858	1903
01.04.2009	1967	8.8	0.4	7.5	105.0	2014	2043
25.05.2009	1803	8.9	0.4	17.0	78.6	1865	1920
23.06.2009	1066	9.0	0.4	17.3	25.0	1110	1155
22.07.2009	1607	8.8	0.3	19.3	21.4	1655	1694
19.08.2009	820	9.1	0.4	20.2	2.1	865	915
14.09.2009	1197	9.1	0.4	16.5	6.4	1257	1320
13.10.2009	1803	8.6	0.4	12.1	0.7	1841	1854
10.11.2009	2131	8.4	0.4	8.6	0.7	2173	2165
08.12.2009	2295	8.3	0.4	6.8	37.1	2345	2322

A6: Values of TA, DIC and nitrate concentrations [µmol kg^{-1}] of rivers with improved river loads, calculated from A1 – A6 (new river loads) and river loads used in chapter 2. New river loads were introduced in chapter 3.2.2.

River parameter	Chapter 2 (mean for NO_3)	New river loads introduced in chapter 3												
		Jan	Feb	Mar	Apr	May	Jun	Jul	Aug	Sep	Oct	Nov	Dec	average
Elbe TA	2231	2380	2272	2293	2083	2017	1967	1916	1768	1988	2156	2342	2488	2139
Noordzeekanaal TA	2580	3762	3550	3524	3441	4748	3278	3419	3183	3027	3299	3210	3413	3488
Nieuwe Waterweg TA	2580	2778	2708	2765	3006	2883	2658	2876	2695	2834	2761	2834	2927	2810
Haringvliet TA	2580	2588	2635	2532	3666	2826	2829	2659	2660	2496	2816	2758	2585	2754
Scheldt TA	3832	3781	3863	3708	3725	3758	3626	3722	3514	3367	3666	3825	3801	3696
Ijsselmeer TA	2580	2829	3005	2472	2259	2611	1864	1672	1419	1445	2172	2286	2551	2215
Elbe DIC	2195	2415	2319	2362	2179	2093	2025	1956	1853	2018	2200	2428	2512	2197
Noordzeekanaal DIC	2678	3748	3579	3470	3334	3901	3252	3331	3136	2977	3214	3183	3405	3378
Nieuwe Waterweg DIC	2678	2861	2794	2823	2991	2879	2657	2886	2706	2828	2773	2907	3036	2845
Haringvliet DIC	2678	2673	2735	2600	3661	2850	2846	2687	2681	2512	2859	2803	2670	2798
Scheldt DIC	3971	3798	3909	3829	3737	3704	3592	3705	3490	3316	3648	3733	3868	3694
Ijsselmeer DIC	2678	2824	3008	2458	2234	2576	1826	1636	1369	1399	2134	2285	2565	2193
Elbe NO_3	201	247	330	277	225	193	161	129	103	112	157	267	164	197
Noordzeekanaal NO_3	133.4	150	168	190	118	79	71	64	73	78	92	107	137	111
Nieuwe Waterweg NO_3	180.5	232	243	231	195	150	140	132	135	113	145	201	220	178
Haringvliet NO_3	177.4	233	252	218	200	143	144	133	117	128	127	143	228	172
Scheldt NO_3	283.5	320	341	347	345	243	221	219	215	189	202	190	274	259
Ijsselmeer NO_3	99.8	136	159	190	192	135	46	20	14	7	18	20	79	85

A7: Annual loads of TA, DIC and nitrate in the Elbe estuary, the river Rhine, the remaining continental rivers and the British rivers. "Old" values were used in chapter 2 for simulations, "new" value were introduced in chapter 3. All values are in Gmol yr^{-1}.

		2001	2002	2003	2004	2005	2006	2007	2008	2009	average
TA	Elbe old	42.50	79.98	44.17	36.06	47.12	49.74	49.07	45.40	44.77	48.76
	Elbe new	49.80	94.32	53.46	42.65	55.31	57.23	58.72	53.93	52.70	57.57
	Rhine old	215.34	223.21	135.81	138.59	139.23	155.40	189.86	168.91	143.82	167.80
	Rhine new	235.73	238.81	144.55	149.45	152.08	172.99	203.03	185.23	156.60	182.05
	Cont. Rivers old	116.17	117.34	86.11	91.99	91.15	89.77	106.53	101.43	89.10	98.84
	Cont. Rivers new	119.97	125.43	93.83	96.60	96.44	94.41	113.43	107.52	93.35	104.55
	Brit. Rivers old	67.41	70.08	44.95	58.19	58.11	58.71	59.30	60.14	60.46	59.71
	Brit. Rivers new	79.59	74.26	48.80	63.63	41.29	52.31	80.31	84.26	58.62	64.79
DIC	Elbe old	41.81	78.69	43.45	35.47	46.36	48.94	48.28	44.66	44.05	47.97
	Elbe new	51.17	96.91	54.77	43.80	56.85	59.07	60.19	55.44	54.20	59.16
	Rhine old	223.52	231.69	140.96	143.84	144.52	161.29	197.07	175.33	149.29	174.17
	Rhine new	239.18	243.14	147.33	151.82	154.20	174.97	206.41	187.81	158.94	184.87
	Cont. Rivers old	120.55	121.74	89.32	95.50	94.61	93.13	110.51	105.25	92.46	102.56
	Cont. Rivers new	120.79	127.02	94.85	97.47	97.23	95.03	115.07	108.57	94.04	105.56
	Brit. Rivers old	72.52	77.10	63.82	72.88	71.41	71.68	71.96	72.38	72.51	71.81
	Brit. Rivers new	83.55	77.96	51.23	66.80	43.36	54.92	84.31	88.46	61.55	68.02
Nitrate	Elbe old	4.65	9.10	5.53	3.86	5.06	5.24	4.83	4.37	4.35	5.22
	Elbe new	4.65	9.12	5.68	4.27	5.59	5.66	5.56	5.61	5.16	5.70
	Rhine old	16.59	17.79	9.93	10.84	10.19	12.23	14.34	12.54	10.13	12.73
	Rhine new	15.76	16.44	10.52	10.08	10.07	10.89	13.71	12.26	10.51	12.25
	Cont. Rivers old	9.52	9.94	7.05	7.39	6.12	5.60	8.74	7.55	4.65	7.40
	Cont. Rivers new	9.71	10.96	7.78	7.96	6.53	6.05	9.78	8.26	5.24	8.03
	Brit. Rivers old	10.32	10.32	10.32	10.34	10.32	10.32	10.32	10.34	10.32	10.32
	Brit. Rivers new	11.92	10.65	7.56	8.85	5.59	7.46	11.42	10.74	7.86	9.12

A8: Annual loads of ammonium, phosphate and total organic nitrogen (TON) in the Elbe estuary, the river Rhine, the remaining continental rivers and the British rivers. "Old" values were used in chapter 2 for simulations, "new" value were introduced in chapter 3. All values are in Gmol yr^{-1}.

		2001	2002	2003	2004	2005	2006	2007	2008	2009	mean
Ammonium	Elbe old	0.28	0.42	0.35	0.25	0.27	0.31	0.23	0.21	0.20	0.28
	Elbe new	0.04	0.09	0.06	0.04	0.05	0.04	0.06	0.05	0.05	0.05
	Rhine old	0.82	0.73	0.53	0.48	0.33	0.47	0.33	0.38	0.34	0.49
	Rhine new	0.82	0.73	0.53	0.48	0.33	0.47	0.33	0.38	0.34	0.49
	Cont. Rivers old	0.56	0.42	0.40	0.35	0.28	0.33	0.28	0.24	0.29	0.35
	Cont. Rivers new	0.59	0.45	0.42	0.38	0.30	0.35	0.31	0.26	0.30	0.37
	Brit. Rivers old	1.19	1.19	1.19	1.19	1.19	1.19	1.19	1.19	1.19	1.19
	Brit. Rivers new	0.43	0.34	0.26	0.25	0.18	0.24	0.30	0.34	0.24	0.29
Phosphate	Elbe old	0.05	0.09	0.04	0.03	0.04	0.03	0.04	0.03	0.03	0.04
	Elbe new	0.06	0.11	0.05	0.03	0.05	0.04	0.05	0.04	0.04	0.05
	Rhine old	0.17	0.24	0.13	0.14	0.13	0.15	0.19	0.16	0.14	0.16
	Rhine new	0.17	0.24	0.13	0.14	0.13	0.15	0.19	0.16	0.14	0.16
	Cont. Rivers old	0.07	0.09	0.06	0.06	0.05	0.06	0.07	0.04	0.04	0.06
	Cont. Rivers new	0.08	0.10	0.06	0.06	0.05	0.06	0.07	0.05	0.04	0.06
	Brit. Rivers old	0.48	0.48	0.48	0.48	0.48	0.48	0.48	0.48	0.48	0.48
	Brit. Rivers new	0.36	0.34	0.23	0.29	0.20	0.21	0.30	0.28	0.22	0.27
TON	Elbe old	1.46	1.75	0.65	0.61	0.75	0.45	0.80	0.91	0.78	0.91
	Elbe new	1.77	2.12	0.78	0.73	0.91	0.54	0.97	1.10	0.94	1.10
	Rhine old	2.76	3.65	2.76	2.09	2.05	2.09	2.40	1.56	1.83	2.35
	Rhine new	2.76	3.65	2.76	2.09	2.05	2.09	2.40	1.56	1.83	2.35
	Cont. Rivers old	2.81	3.80	2.17	2.65	2.49	1.73	2.45	2.25	1.83	2.46
	Cont. Rivers new	3.00	4.10	2.29	2.80	2.70	1.82	2.57	2.38	1.93	2.62
	Brit. Rivers old	0.73	0.73	0.73	0.73	0.73	0.73	0.73	0.73	0.73	0.73
	Brit. Rivers new	0.73	0.73	0.73	0.73	0.73	0.73	0.73	0.73	0.73	0.73

A9: Modelling of the exchange rates (tidal prisms) between the Wadden Sea and the North Sea

FVCOM is an unstructured-grid, finite-volume, 3-D ocean model (see Chen, 2003). The respective model domain of FVCOM is shown in Fig. A1. The model is solving the integral form of the governing equations for momentum, continuity, temperature, salinity and density on a triangular mesh in the horizontal and a σ-coordinate system with 21 σ-levels in the vertical direction (see manual given by Chen, 2006).

To calculate the horizontal diffusion the Smagorinsky eddy parameterisation method (see Smagorinsky, 1963) and for the parametrisation of the vertical eddy viscosity the Mellor & Yamada (1982) level 2.5 model were applied as turbulence closure schemes.

The resolution of the unstructured-grid mesh ranged from 500 m at the German coast and 6000 m in areas that were located far away from the coast. A section of the modelling area around the islands of Langeoog and Spiekeroog and the unstructured-grid and bathymetry is shown in Fig. A1. The timestep of the hydrodynamic model was 10 s for the simulations. The salinity and the temperature were set to a constant value of 35 PSU and 10° C, respectively. For bottom friction and vertical and horizontal mixing the default values of FVCOM were applied. Hourly data of wind speed, wind direction and pressure provided by the German Weather Service were used as meteorological forcing.

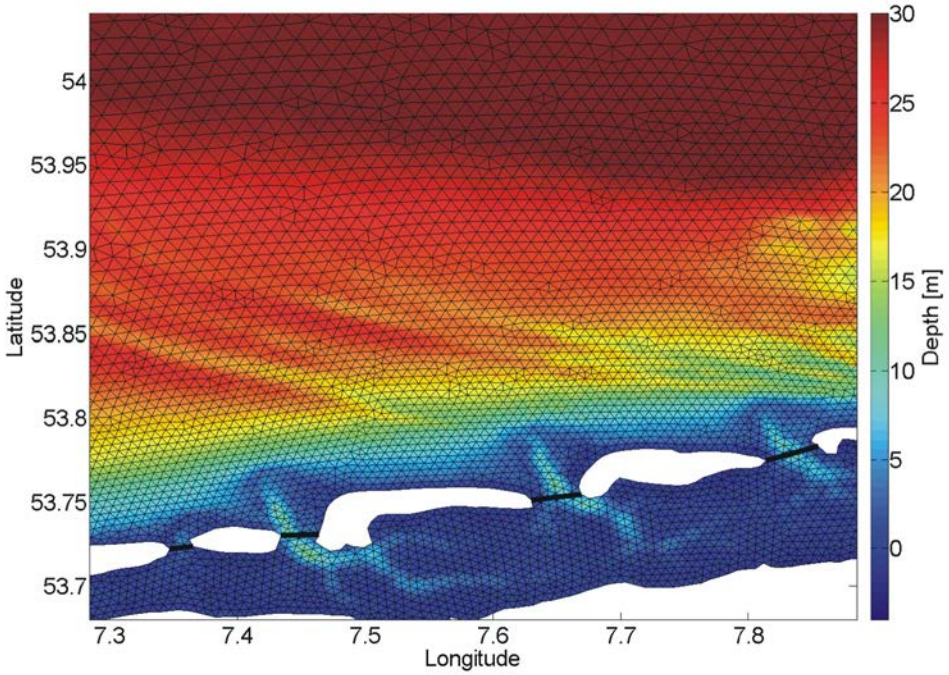

Figure A1: Section of the FVCOM modelling area around the islands of Langeoog and Spiekeroog: unstructured-grid and bathymetry. Black lines indicate positions where *wad_exc* was calculated. This figure is provided by Grashorn (2013).

wad_exc was calculated with FVCOM by adding up the cumulative seaward transport during falling water level (tidal prisms) between the back-barrier islands that were located near the respective ECOHAM cells with adjacent Wadden Sea area. Therefore, model data of a representative period between 13.10.2007 and 15.10.2007 were used that were characterised by a mean significant wave height of 0.75 m, a mean wave direction of 190.6°, a maximum wind speed of 7 m s^{-1} and a mean surface elevation amplitude of approx. 1 m at 54°01'N, 6°35'E. The simulated surface elevation and observed wind speed (FINO 1 station) from 5.10. – 21.10.2007 are shown in Fig. A2. The model results at that position have been validated by Grashorn (2013).

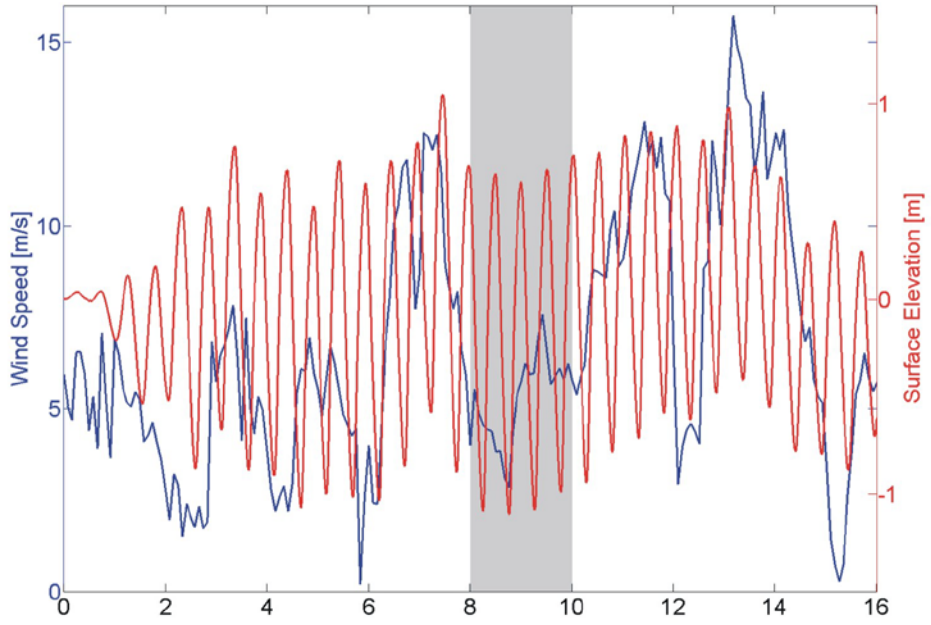

Figure A2: Observed wind speed and simulated surface elevation at FINO1 (54°01'N, 6°35'E). The period that was used for *wad_exc* calculation is highlighted in grey. This figure is provided by Grashorn (2013).

In order to get representative tidal prisms for the Wadden Sea export calculations, a period was chosen that was supposed to represent a usual tidal situation without remarkable strong winds, neap tides or spring tides. Calculations of tidal prisms for every day from 2001 to 2009 were not performed due to high computation time. wad_exc for each ECOHAM cell in the respective export areas are given in Tab. 4.2. The definition of the first cell N1 and the last cell E4 is in accordance to the clockwise order in Fig. 4.1 (right side).

Of course the different timeframes of the modelled exchanged water masses and the conducted measurements of TA and DIC concentrations in the Wadden Sea caused additional uncertainties to the calculated export rates. This is why the timeframe for modelled exchanged water masses was chosen in a way that a representative and normal situation was reproduced that mostly occurred during the course of a year. Except for measurements in the North Frisian Wadden Sea in November 2009, no remarkable strong winds, neap or spring tides were observed during measurements of TA and DIC concentrations in the Wadden Sea. Hence, the above mentioned uncertainties were reduced to a minimum by the selection of the period for water mass exchange simulations.

B Contribution to publications

The following contributions at international conferences were derived from the dissertation:

- F. Schwichtenberg, J. Pätsch, T. Amann, M. Schartau, H. Thomas, V. Winde, O. Dellwig, J. van Beusekom, M. Böttcher, S. Grashorn and L. Salt, Impact of internal and external alkalinity fluxes on the carbonte system in the German Bight / SE North Sea – A model study for the years 2001 – 2009, European Geosciences Union General Assembly 2013, Vienna, Austria, April 2013, poster presentation.
- F. Schwichtenberg, J. Pätsch, I. Lorkowski, T. Amann, M. Schartau, H. Thomas, V. Winde, O. Dellwig, J. van Beusekom, M. Böttcher, Impact of internal and external alkalinity fluxes on the carbonte system of the larger German Bight, European Geosciences Union General Assembly 2012, Vienna, Austria, April 2012, oral presentation.
- F. Schwichtenberg, J. Pätsch, I. Lorkowski, M. Schartau, H. Thomas, V. Winde, O. Dellwig, J. van Beusekom, M. Böttcher, Impact of alkalinity fluxes on the carbon cycle in the southern North Sea, YOUMARES 2.0, Bremerhaven, Germany, September 2011, oral presentation.
- F. Schwichtenberg, J. Pätsch, I. Lorkowski, M. Schartau, H. Thomas, V. Winde, O. Dellwig, J. van Beusekom, M. Böttcher, Impact of alkalinity fluxes on the carbon cycle in the southern North Sea between 1977 and 2009, AMEMR, Plymouth, Great Britain, Juni 2011, poster presentation.
- F. Schwichtenberg, J. Pätsch, I. Lorkowski, M. Schartau, H. Thomas, V. Winde, O. Dellwig, J. van Beusekom, M. Böttcher, Impact of alkalinity fluxes on the carbon cycle in the southern North Sea between 1977 and 2006, European Geosciences Union General Assembly 2011, Vienna, Austria, April 2011, oral presentation.

Bibliography

Amann, T., Weiss, A., Hartmann, J. *Inorganic carbon fluxes in the inner Elbe estuary, Germany*. Submitted to Estuaries & Coasts.

Amann, T., 2013. *Spatio-temporal variability of carbon and silica fluxes through the inner Elbe estuary, Germany*. Dr.rer.nat. thesis, Universität Hamburg.

Artioli, Y., Blackford, J.C., Butenschön, M., Holt, J.T., Wakelin, S.L., Thomas, H., Borges, A.V., Allen, J.I., 2012. *The carbonate system in the North Sea: Sensitivity and model validation.* Journal of Marine Systems, 102-104, 1-13, doi:10.1016/j.jmarsys.2012.04.006.

Backhaus, J.O., 1985. *A three-dimensional model for the simulation of shelf sea dynamics.* Ocean Dynamics, 38(4):165–187.

Backhaus, J.O., Hainbucher, D., 1987. *A finite difference general circulation model for shelf seas and its application to low frequency variability on the North European Shelf.* Elsevier Oceanography Series, 45:221–244.

Berelson, W.M., McManus, J., Coale, K.H., Johnson, K.S., Kilgore, T., Burdige, D., Pilskaln, C., 1996. *Biogenic matter diagenesis on the sea floor: a comparison between two continental margin transects.* Journal of Marine Research, 54, 731–762.

Berelson, W.M., Balch W.M., Najjar R., Feely R.A., Sabine C., Lee K., 2007. *Relating estimates of CaCO3 production, export, and dissolution in the water column to measurements of CaCO3 rain into sediment traps and dissolution on the sea floor: A revised global carbonate budget*. Global Biogeochemical Cycles, 21, GB1024, doi:10.1029/2006GB002803.

Bergemann, M., 2005. *Berechnung des Salzgehaltes der Elbe*, p. 8.

Berner, R.A., Scott, M.R., Thomlinson, C., 1970. *Carbonate alkalinity in the pore waters of anoxic marine sediments*. Limnology & Oceanography, 15, 544–549, doi:10.4319/lo.1970.15.4.0544.

Borges, A.V., 2011. *Present day carbon dioxide fluxes in the coastal ocean and possible feedbacks under global change*, IN *Oceans and the atmospheric carbon content* (P.M. da Silva Duarte & J.M. Santana Casiano Eds), Chapter 3, pp. 47-77.

Brasse, S., Nellen, M., Seifert, R., Michaelis, W., 2002. *The carbon dioxide system in the Elbe estuary*. Biogeochemistry, 59, 25-40.

Brewer, P.G., Goldman, J.C., 1976. *Alkalinity changes generated by phytoplankton growth.* Limnology & Oceanography, 21 (1), 108–117.

Broecker, W.S., Peng, T.-H., 1982. *Tracers in the Sea.* Eldigio Press, New York. (690 pp.).

Brønsted, J.N., 1923. *Einige Bemerkungen über den Begriff der Säuren und Basen.* Recl. Trav. Chim. Pays-Bas, 42, 718–728.

Cadée, G.C., Hegeman, J., 2002. *Phytoplankton in the Marsdiep at the end of the 20th century; 30 years monitoring biomass, primary production, and Phaeocystis blooms*. J. Sea Res. 48, 97e110.

Cai, W.-J., Guo, X., Chen, C.T.A., et al., 2008. *A comparative overview of weathering intensity and HCO3 2_ flux in the world's major rivers with emphasis on the Changjiang, Huanghe, Zhujiang (Pearl) and Mississippi Rivers.* Continental Shelf Research, 28, 1538–1549.

Cai, W.-J., Hu, X., Huang, W.-J., Jiang, L.-Q., Wang, Y., Peng, T.-H., Zhang, X., 2010. *Surface ocean alkalinity distribution in the western North Atlantic Ocean margins*. Journal of Geophysical Research, 115, C08014, doi:10.1029/2009JC005482.

Chambers, R.M., Hollibaugh, J.T., Vink, S.M., 1994. *Sulfate reduction and sediment metabolism in Tomales Bay, California*. Biogeochemistry, 25, 1–18, doi:10.1007/BF00000509.

Chen, C.-T.A., 2002. *Shelf-vs. dissolution-generated alkalinity above the chemical lysocline*. Deep-Sea Research, II 49, 5365–5375.

Chen, C.-T. A., Wang, S.-L., 1999. *Carbon, alkalinity and nutrient budgets on the East China Sea continental shelf*. Journal of Geophysical Research, 104, 20,675–20,686, doi:10.1029/1999JC900055.

Chen, C., Liu, H., Beardsley, R.C., 2003. *An Unstructured Grid, Finite-Volume, Three-Dimensional, Primitive Equations Ocean Model: Application to Coastal Ocean and Estuaries.* J Atmos Oceanic Technol, 20 (1), 159-186

Chen, C., Beardsley, R.C., Cowles, G.W., 2006. *An Unstructured Grid, Finite-Volume Coastal Ocean Model, FVCOM User Manual*, 2nd edn. SMAST/UMASSD Tech. Rep. 060602, 315 pp, School for Marine Science and Technology, University of Massachusetts-Dartmouth, New Bedford, MA

Chung, S.-N., Lee K., Feely R.A., Sabine C.L., Millero F.J., Wanninkhof R., Bullister J.L., Key R.M., Peng T.-H. (2003). *Calcium carbonate budget in the Atlantic Ocean based on water column inorganic carbon chemistry*. Global Biogeochemical Cycles, 17(4), 1093, doi:10.1029/ 2002GB002001.

CPSL, 2005. Coastal protection and sea level rise. Wadden Sea Ecosyst. 21, 1e47.

Dähnke, K., Bahlmann, E., Emeis, K., 2008. *A nitrate sink in estuaries? An assessment by means of stable nitrate isotopes in the Elbe estuary*. Limnology & Oceanography, 53, pp. 1504-1511.

DeBeer, D., Wenzhöfer, F., Ferdelman, T.G., Boehme, S.E., Huettel, M., van Beusekom, J.E.E., Böttcher, M.E., Musat, N., and Dubilier, N., 2005. *Transport and mineralization rates in North Sea sandy intertidal sediments, Sylt-Romo basin, Wadden Sea*. Limnology & Oceanography, 50, 113–127, 2005.

Deek, A., Emeis, K., van Beusekom, J., 2012. Nitrogen removal in coastal sediments of the German Wadden Sea. Biogeochemistry, 108, 467-483.

Deffeyes, K.S. 1965. *Carbonate equilibria: a graphic and algebraic approach.* Limnology & Oceanography, 10:412-426.

Dickson, A.G., 1981. *An exact definition of total alkalinity and a procedure for the estimation of alkalinity and total inorganic carbon from titration data*. Deep-Sea Research, 28A (6), 609–623.

Dickson, A.G., Millero, F.J., 1987. *A comparison of the equilibrium-constants for the dissociation of carbonic-acid in seawater media.* Deep-Sea Research Part AOceanographic Research Papers 34 (10), 1733e1743.

Dickson, A.G., 1992. *The development of the alkalinity concept in marine chemistry.* Marine Chemistry, 40 (1–2), 49–63.

DOE, 1994. *Handbook of methods for the analysis of the various parameters of the carbon dioxide system in sea water.* Version 2. In: Dickson, A.G., Goyet, C. (Eds.), ORNL/CDIAC-74.

Dollar, S.J., Smith, S.V., Vink, S.M., Obrebski, S., Hollibaugh, J.T., 1991. *Annual cycle of benthic nutrient fluxes in Tomales Bay, California, and contribution of the benthos to total ecosystem metabolism.* Marine Ecology Progress Series, 79, 115–125, doi:10.3354/meps079115.

Doney, S.C., Fabry, V.J., Feely, R.A., Kleypas, J.A., 2009. *Ocean acidification: the other CO2 problem.* Annual Review of Marine Scince, 1, 169–192.

Egleston, E.S., Sabine, C.L., Morel,, F.o.M.M., 2010. *Revelle revisited: buffer factors that quantify the response of ocean chemistry to changes in DIC and alkalinity.* Global Biogeochemical Cycles, 24.

Ehlers, J., 1994. *Geomorphologie und Hydrologie des Wattenmeeres.* In: Lozan, J.L., Rachor, E., Von Westernhagen, H., Lenz, W. (Eds.), Warnsignale aus dem Wattenmeer. Blackwell Wissenschaftsverlag, Berlin, pp. 1–11.

Fabry V., Seibel B.A., Feely R.A., Orr J.C. 2008. *Impacts of ocean acidification on marine fauna and ecosystem processes.* ICES Jornal of Marine Science 65, 414-432

Fennel, K., Wilkin, J., Levin, J., Moisan, J., O'Reilly, J., Haidvogel, D., 2006. *Nitrogen cycling in the Middle Atlantic Bight: results from a three-dimensional model and implications for the North Atlantic nitrogen budget.* Global Biogeochemical Cycles 20, 1e14.

Flemming, B.W., Davis, R.A.J., 1994. *Holocene evolution, morphodynamics and sedimentology of the Spiekeroog barrier island system (southern North Sea).* Senckenb. Marit. 25, 117e155.

Frankignoulle, M., Canon, C., Gattuso, J.P., 1994. *Marine calcification as a source of carbon dioxide: positive feedback of increasing atmospheric CO2.* Limnology & Oceanography, 39, 458–462.

Frankignoulle, M., Bourge, I., Wollast, R., 1996. *Atmospheric CO2 fluxes in a highly polluted estuary (the Scheldt)*. Limnology & Oceanography, 41, pp. 365 -369.

Goldman, J.C., Brewer, P.G., 1980. *Effect of nitrogen source and growth rate on phytoplankton mediated changes in alkalinity.* Limnology & Oceanography, 25, 352–357.

Grasshoff, K., Kremling, K., Ehrhardt, M. (Eds.), 1999. *Methods of seawater analysis.* 3rd ed., 600 pp., Wiley-VCH, Weinheim.

Grashorn, S., 2013. *Wave-current interactions in coastal areas*. Dr.rer.nat. thesis, Universität Oldenburg.

Gypens, N., Borges, A.V., Lancelot, C., 2009. *Effect of eutrophication on air-sea CO2 fluxes in the coastal Southern North Sea: a model study of the past 50 years.* Global Change Biology 15, 1040e1056.

Hartmann, J., Moosdorf, N., 2012. *The new global lithological map database GLiM: A representation of rock properties at the Earth surface*. Geochemistry Geophysics Geosystems, 13, DOI: 10.1029/2012gc004370.

HASEC, 2012. *OSPAR Convention for the Protection of the Marine Environment of the North-East Atlantic.* Meeting of the Hazardous Substances and Eutrophication Committee (HASEC), Oslo 27 February – 2 March 2012.

Heath, M.R., Edwards, A.C., Pätsch, J., Turrell,W.R., 2002. *Modelling the behaviour of nutrient in the coastal waters of Scotland*. vol. 10. Report Of the Fisheries Research Services, pp. 1e106.

Hjalmarsson, S., Wesslander, K., Anderson, L.G., Omstedt, A., Perttilä, M., Mintrop, L., 2008. *Distribution, long-term development and mass balance calculation of total alkalinity in the Baltic Sea.* Continental Shelf Research 28, 593–601.

Hu, X., Cai, W.-J., 2011. An assessment of ocean margin anaerobic processes on oceanic alkalinity budget. Global Biogeochemical Cycles, 25, GB3003, doi: 10.1029/2010GB003859.

Hulth, S., Aller, R.C., Canfield, D.E., Dalsgaard, T., Engström, P., Gilbert, F., Sundbäck, K., Thamdrup, B., 2005. *Nitrogen removal in marine environments: Recent findings and future research challenges*. Marine Chemistry, 94, 125–145, doi:10.1016/j.marchem.2004.07.013.

Hoppema, J.M.J, 1990. *The distribution and seasonal variation of alkalinity in the southern bight of the North Sea and in the western Wadden Sea.* Netherlands Journal of Sea Research, 26 (1), 11-23.

Ilyna, T., Zeebe, R., Brewer, P.G. 2010. *Future ocean increasingly transparant to low-frequency sound owing to carbon dioxide emissions.* Nature Geoscience, 3, 18-22.

IPCC. 2001. *Climate Change 2001: Synthesis Report. A contribution of working groups I, II, and III to the Third Assessment Report of the IPCC.* Tech. rept. Cambridge.

Jacobsen, M.Z., 2005. *Studying ocean acidification with conservative, stable numerical schemes for nonequilibrium air-ocean exchange and ocean equilibrium chemistry*. Journal of Geophysical Research – Atmospheres 110: D07302. DOI: 10.1029/2004JD005220.

Jacobsen, O., 1873. *Ueber die Luft des Meerwassers.* Justus Liebig's Ann. Chem. Pharm., 167, 1–38.

Jahnke, R.A., Craven D.B., Gaillard, J.-F. 1994. *The influence of organic matter diagenesis on CaCO3 dissolution at the deep-sea floor*. Geochimica Cosmochimica Acta, 58, 2799–2809, doi:10.1016/0016-7037 (94)90115-5.

Jensen, K.M., Jensen, M.H., Kristensen, E., 1996. *Nitrification and denitrification in Wadden Sea sediments (Konigshafen, Island of Sylt, Germany) as measured by nitrogen isotope pairing and dilution.* Aquat. Microb. Ecol., 11, 181–191.

Johannsen, A., Dahnke, K., Emeis, K., 2008. *Isotopic composition of nitrate in five German rivers discharging into the North Sea.* Organic Geochemistry, 39, 1678-1689.

Kalnay, E., Kanamitsu, M., Kistler, R., Collins, W., Deaven, D., Gandin, L., Iredell, M., Saha S., White, G., Woollen, J., Zhu, Y., Chelliah, M., Ebisuzaki, W., Higgins, W., Janowiak, J., Mo, K.C., Ropelewski, C., Wang, J., Leetmaa, A., Reynolds, R., Jenne, R., Joseph, D., 1996. *The NCEP/NCAR 40-year reanalysis project*. Bulletin Of The American Meteorological Society, 77(3):437–471.

Kleypas, J., Feely, R.A., Fabry, V., Langdon, C., Sabine, C.L., Robbins, L.L. 2006. *Impacts of Ocean Acidification on Coral Reefs and Other Marine Calcifiers: A Guide for Future Research, report of a workshop held* 1820 April 2005, St. Peterburg, FL. Sponsored by NSF, NOAA, and the U.S. Geological Survey, 88 pp.

Kochergin, V.P., 1987. *Three-dimensional prognostic models.* Three-dimensional Coastal Ocean Models, pages 201–208.

Kristensen, E., Bodenbender, J., Jensen, M.H., Rennenberg, H., Jensen, K.M., 2000. *Sulfur Cycling of intertidal Wadden Sea sediments (Konigshafen, Island of Sylt, Germany): sulfate reduction and sulfur gas emission*. Journal of Sea Research, 43, 93–104.

Kroeker, K.J., Kordas, R.L., Crim, R.N., Singh, G.G. 2010. *Meta-analysis reveals negative yet variable effects of ocean acidification on marine organisms.* Ecology Letters, 13, 1419-1434.

Kühn, W., Pätsch, J., Thomas, H., Borges, A.V., Schiettecatte, L.S., Bozec, Y., Prowe, A.E.F., 2010. *Nitrogen and carbon cycling in the North Sea and exchange with the North Atlantic-A model study, Part II: Carbon budget and fluxes*. Continental Shelf Research (30), pp. 1701-1716. DOI: DOI 10.1016/j.csr.2010.07.001.

Lam, P., et al. 2009. *Revising the nitrogen cycle in the Peruvian oxygen minimum zone,* Proc. Natl. Acad. Sci. U. S. A., 106, 4752–4757, doi:10.1073/pnas.0812444106.

Langer, M.R., 2008. *Assessing the contribution of foraminiferan protists to global ocean carbonate production.* The Journal of Eukaryotic Microbiology 55 (3), 163–169.

Lehner, B., Verdin, K., Jarvis, A., 2008. *New global hydrography derived from spaceborne elevation data*. Eos, Transactions, AGU, 89, pp. 93-94.

Lenhart, H.-J., Radach, G., Backhaus, J. O., Pohlmann, T., 1995. *Simulations of the North Sea circulation, its variability, and its implementation as hydrodynamical forcing in ERSEM*, Neth. J. Sea Res., 33, 271–299.

Lenhart, H., Pohlmann, T., 1997. *The ICES-boxes approach in relation to results of a North Sea circulation model.* Tellus, 49A, 139-160.

Lewis, E., Wallace, D.W.R., 1998. Program Developed for CO2 System.

Lorkowski, I., Pätsch, J., Moll, A., Kühn, W., 2012. *Interannual variability of carbon fluxes in the North Sea from 1970 to 2006 – Competing effects of abiotic and biotic drivers on the gas-exchange of CO2.* Estuarine, Coastal and Shelf Science, 100, 38-57, doi:10.1016/j.ecss.2011.11.037.

Ludwig, W., Amiotte-Suchet, P., Probst, J.L., 1996. *River discharges of carbon to the world's oceans: determining local inputs of alkalinity and dissolved and particulate organic carbon.* C.R. Academy of Science, Paris, t. 323, Serie II a, pp. 1007–1014.

Luff, R., Moll, A., 2004. *Seasonal dynamics of the North Sea sediments using a three-dimensional coupled water-sediment model system*. Continental Shelf Research, 24, 1099–1127.

Martin, W.R., Sayles, F.L. 1996. *CaCO3 dissolution in sediments of the Ceara Rise, western equatorial Atlantic.* Geochimica Cosmochimica Acta, 60, 243–263, doi:10.1016/0016-7037(95)00383-5.

McQuatters-Gollop, A., Raitsos, D.E., Edwards, M., Pradhan, Y., Mee, L.D., Lavender, S.J., Attrill, M.J., 2007. *A long-term chlorophyll data set reveals regime shift in North Sea phytoplankton biomass unconnected to nutrient trends.* Limnology & Oceanography, 52, 635e648.

McQuatters-Gollop, A., Vermaat, J.E., 2011. *Covariance among North Sea ecosystem state indicators during the past 50 years e contrasts between coastal and open waters*. Journal of Sea Research, 65, 284e292.

Mehrbach, C., Culberso, C., Hawley, J.E., Pytkowic, R.M., 1973. *Measurement of apparent dissociation-constants of carbonic acid in seawater at atmospheric pressure*. Limnology & Oceanography 18 (6), 897e907.

Mellor, G.L., Yamada, T., 1982. *Development of a Turbulence Closure Model for Geophysical Fluid Problems.* Rev Geophys 20(4): 851-875

Millero, F.J., 2001. *Physical Chemistry of Natural Waters.* Wiley-Interscience Series in Geochemistry. Wiley-Interscience, New York. 654 pp.

Millero, F.J., Graham, T.B., Huang, F., Bustos-Serrano, H., Pierrot, D., 2006. *Dissociation constants of carbonic acid in seawater as a function of salinity and temperature*. Marine Chemistry, 100, pp. 80-94. DOI: 10.1016/j.marchem.2005.12.001.

Milliman, J.D., Troy, P.J., Balch, W.M., Adams, A.K., Li, Y.-H., Mackenzie, F.T., 1999. *Biologically mediated dissolution of calcium carbonate above the chemical lysocline*. Deep Sea Research, Part I, 46, 1653–1669, doi:10.1016/S0967-0637(99)00034-5.

Moll, A., 1998. *Regional distribution of primary production in the North Sea simulated by a three-dimensional model.* Journal of Marine Systems 16, 151–170.

Moore, W.S., Beck, M., Riedel, T., Rutgers van der Loeff, M., Dellwig, O., Shaw, T.J., Schnetger, B., Brumsack, H.-J., 2011. *Radium-based pore water fluxes of silica, alkalinity, manganese, DOC, and uranium: A decade of studies in the German Wadden Sea*. Geochimica et Cosmochimica Acta, 75, 6535 – 6555.

Neal, C., 2002. *Calcite Saturation in eastern UK rivers.* The Science of the Total Environment, 282-283, 311-326.

Neumann, T., 2000. *Towards a 3D-ecosystem model of the Baltic Sea.* Journal of Marine Systems 25, 405e419.

Onken, R., Riethmüller, R., 2010. *Determination of the freshwater budget of tidal flats from measurements near a tidal inlet.* Continental Shelf Research, 30, 924-933, doi: 10.1016/j.csr.2010.02.004.

OSPAR-Commission, 2000. *Quality status report 2000*, volume 3. OSPAR-Commission.

Otto, L., Zimmerman, J.T.F., Furnes, G.K., Mork, M., Saetre, R., Becker, G., 1990. *Review of the physical oceanography of the North Sea.* Netherlands Journal of Sea Research, 26 (2-4):161–238.

Park, K. 1969. *Oceanic CO2 system: an evaluation of ten methods of investigation.* Limnology & Oceanography, 14: 179-186.

Pätsch, J., Kühn, W., 2008. *Nitrogen and carbon cycling in the North Sea and exchange with the North Atlantic – a model study Part I: Nitrogen budget and fluxes*. Continental Shelf Research, 28, 767–787.

Pätsch, J., Lenhart, H.-J., 2008. *Daily Loads of Nutrients, Total Alkalinity, Dissolved Inorganic Carbon and Dissolved Organic Carbon of the European Continental Rivers for the Years 1977–2006.* Berichte aus dem Zentrum für Meeres- und Klimaforschung,

Pätsch, J., Serna, A., Dähnke, K., Schlarbaum, T., Johannsen, A., Emeis, K.-C., 2010. *Nitrogen cycling in the German Bight (SE North Sea) - Clues from modelling stable nitrogen isotopes.* Continental Shelf Research, 30: 203-213.

Pohlmann, T., 1991. *Untersuchung hydro- und thermodynamischer Prozesse in der Nordsee mit einem dreidimensionalen numerischem Modell.* Berichte aus dem Zentrum für Meeres- und Klimaforschung, Reihe B(Nr. 23):1–116.

Pohlmann, T, 1996. *Predicting the thermocline in a circulation model of the North Sea – Part I: model description, calibration and verification.* Continental Shelf Research, 16(2): 131–146.

Provoost, P., van Heuven, S., Soetaert, K., Laane, R.W.P.M., Middelburg, J.J., 2010. Seasonal and long-term changes in pH in the Durch coastal zone. Biogeoscience, 7, 3869-3878.

Quigg, A., Finkel, Z.V., Irwin, A.J., Rosenthal, Y., Ho, T., Reinfelder, J.R., Schofield, O., Morel, F.M.M., Falkowski, P.G., 2003. *The evolutionary inheritance of elemental stoichiometry in marine phytoplankton.* Nature 425, 291e294.

Raaphorst, W., Kloosterhuis H.T., Cramer, A., Bakker, K.J.M., 1990. *Nutrient early diagenesis in the sandy sediments of the Dogger Bank area, North Sea: pore water results.* Neth. J. Sea. Res. 26(1): 25-52.

Rakestraw, N.W., 1949. *The concept of alkalinity or excess base of seawater.* Journal of Marine Research, 8, 14–20.

Raven et al. Royal Society, *Ocean Acidification Due to Increasing Atmospheric Carbon Dioxide* (Policy Document 12/05, Royal Society, London, 2005).

Revelle, R., Suess, H., 1957. *Carbon dioxide exchange between atmosphere and ocean and the question of an increase of atmospheric CO2 during the past decades.* Tellus 9, 18–27.

Sabine, C.L., R.A. Feely, N. Gruber, R.M. Key, K. Lee, J.L. Bullister, R. Wanninkhof, C.S. Wong, D.W.R. Wallace, B. Tilbrook, F.J. Millero, T.-H. Peng, A. Kozyr, T. Ono, and A.F. Rios, 2004. *The Oceanic sink for Anthropogenic CO2*, Science, 305, 367-371.

Sabine, C.L., Tanhua, T., 2010. *Estimation of anthropogenic CO2 inventories in the ocean.* Annual Review of Marine Science, 2, 175–198.

Salt, L., Thomas, H., Prowe, A.E.F., Borges A.V., De Baar, H.J.W., 2012. *Variability of shelf sea pH and CO2 pumping in response to NAO forcing*. submitted to Journal of Geophysical Research.

Seitzinger, S., Giblin, A.E., 1996. *Estimating denitrification in North Atlantic continental shelf sediments.* Biogeochemistry 35, 235–260.

Seitzinger, S.P., Kroeze, C., 1998. *Global distribution of nitrous oxide production and N inputs in freshwater and coastal marine ecosystems*. Global Biogeochemical Cycles, 12, pp. 93-113. DOI: 10.1029/97gb03657.

Seitzinger, S., Harrison, J.A., Bohlke, J.K., Bouwman, A.F., Lowrance, R., Peterson, B., Tobias, C., Drecht, G.V., 2006. *Denitrification across landscapes and waterscapes: A synthesis*. Ecol. Appl., 16, 2064–2090, doi:10.1890/1051-0761(2006)016[2064:DALAWA]2.0.CO;2.

Slater, J.M., Capone, D.G., 1987. *Denitrification in aquifer soils and nearshore marine sediments influenced by groundwater nitrate*. Appl. Environ. Microb., 53, 1292–1297.

Smagorinsky, J., 1963. *General Circulation experiments with the primitive equations I. The basic experiment.* Mon Wea Rev 91(3): 99-164

Smith, S.V., Hollibaugh, J.T., 1993. *Coastal metabolism and the oceanic organic carbon balance*. Reviews of Geophysics, 31, 75–89, doi:10.1029/92RG02584.

Streif, H., 1990. *Das ostfriesische Wattenmeer. Nordsee, Inseln, Watten und Marschen.* Gebrüder Borntraeger, Berlin.

Taylor, K.E., 2001. *Summarizing multiple aspects of model performance in a single diagram.* Journal Geophysical Research, 106 , 7183-7192, 2001

Thomas, H., Bozec, Y., Elkalay, K., de Baar, H.J.W., 2004. *Enhanced open ocean storage of CO2 from shelf sea pumping.* Science 304, 1005e1008.

Thomas, H., Schiettecatte, L.S., Suykens, K., Kone, Y.J.M., Shadwick, E.H., Prowe, A.E.F., Bozec, Y., de Baar, H.J.W., Borges, A.V., 2009. *Enhanced ocean carbon storage from anaerobic alkalinity generation in coastal sediments*. Biogeosciences (6), pp. 267-274.

Turrell, W.R., 1992. *New hypotheses concerning the circulation of the northern North Sea and its relation to North Sea fish stock recruitment*. ICES Journal of Marine Science, 49, 107-123.

Van den Berg, A.J., Ridderinkhof, H., Riegmann, R., Ruardij, P., Lenhart, H., 1996. *Influence of variability in water transport on phytoplankton biomass and composition in the southern North Sea: a modelling approach (FYFY).* Continental Shelf Research, 16, 7, 907-931.

Van Beusekom, J.E.E., Brockmann, U.H., Hesse, K.-J., Hickel, W., Poremba, K., Tillmann, U., 1999. *The importance of sediments in the transformation and turnover of nutrients and organic matter in the Wadden Sea and German Bight.* German Journal Hydrography 51 (2/3), 245–266.

Van Beusekom, J.E.E., de Jonge, V.N., 2002. *Long-term changes in Wadden Sea nutrient cycles: importance of organic matter import from the North Sea*. Hydrobiologica, 475/476, 185–194.

Van Beusekom, J.E.E., Loebl, M., Martens, P., 2009. *Distant riverine nutrient supply and local temperature drive the long-term phytoplankton development in a temperate coastal basin*. J. Sea Res. 61, 26e33.

Van Beusekom, J.E.E., Buschbaum, C., Reise, K., 2012. *Wadden Sea tidal basins and the mediating role of the North Sea in ecological processes: scaling up of management?* Ocean & Coastal Management, 68, 69-78.

Van Goor, M.A., Zitman, T.J.,Wang, Z.B., Stive, M.J.F., 2003. *Impact of sea-level rise on the equilibrium state of tidal inlets*. Mar. Geol. 202, 211e227.

Van Koningsveld, M., Mulder, J.P.M., Stive, M.J.F., Van der Valk, L., Van der Weck, A.W., 2008. *Living with sea-level rise and climate change: a case study of the Netherlands.* J. Coast. Res. 24, 367e379.

Wang, Z.A., Cai, W.-J., 2004. *Carbon dioxide degassing and inorganic carbon export from a marsh-dominated estuary (the Duplin River): A marsh CO2 pump*. Limnology & Oceanography, 49, 341–354, doi:10.4319/lo.2004.49.2.0341.

waterbase.nl, Data-ICT-Dienst Rijkswaterstaat, data obtained on 12.09.2011 – 15.09.2011, http://www.rijkswaterstaat.nl/water/waterdata_waterberichtgeving/

Winde, V., 2013. *Zum Einfluss von benthischen und pelagischen Prozessen auf das Karbonatsystem des Wattenmeeres der Nordsee*. Dr.rer.nat. thesis, EMA Universität Greifswald.

Wolf-Gladrow, D.A., Zeebe, R.E., Klaas, C., Kortzinger, A., Dickson, A.G. (2007). *Total alkalinity: The explicit conservative expression and its application to biogeochemical processes*. Marine Chemistry, 106, 287–300, doi:10.1016/j.marchem.2007.01.006.

Zeebe, R.E., Wolf-Gladrow, D. 2001. *CO2 in seawater: Equilibrium, Kinetics, Isotopes.* 1st edn. ELSEVIER.

Danksagung

Mein besonderer Dank gilt meinem Betreuer Prof. Dr. Kay-Christian Emeis. Seine Ratschläge lenkten meine Arbeit immer wieder auf den rechten Weg zur erfolgreichen Promotion und halfen mir, einen Blick für das Wesentliche zu entwickeln. Durch seine Hilfe war es mir möglich, meine Promotion in der mir zur Verfügung stehenden Zeit zu einem erfolgreichen Abschluss zu bringen. Ich bedanke mich insbesondere bei ihm für die Unterstützung, dass ich meine Arbeit auch im dritten Jahr fortsetzen konnte.

Auch möchte ich mich herzlich bei meinem zweiten Betreuer Dr. Johannes Pätsch bedanken, der mich mit viel Geduld in die Welt der Ökosystemmodellierung eingeführt und meine Fragen beantwortet hat und mir in der täglichen Arbeit hilfsbereit zur Seite stand. Seine Vorarbeiten und die von ihm erstellten Programmstrukturen in bildeten das Grundgerüst meiner Arbeit.

Mein Dank gilt auch Prof. Dr. Carsten Eden, der mir nicht nur in seiner Funktion als Mitglied meines Advisory Panels zur Seite stand, sondern mir auch ermöglichte, meine Arbeit in den letzten drei Monaten zum Abschluss zu bringen.

Ich bedanke mich auch bei Dr. Thomas Pohlmann für seine Ratschläge zum hydrodynamischen Teil der Simulationen und für seine Teilnahme an meiner Prüfungskommission. Ebenfalls bedanke ich mich bei Prof. Dr. Inga Hense für die gewissenhafte Ausübung ihrer Funktion als Vorsitzende meines Advisory Panels sowie ihrer Teilnahme an meiner Prüfungskommission.

Ebenfalls möchte ich mich bei Prof. Dr. Michael Böttcher bedanken für seine Bereitschaft als externes Mitglied an der Prüfungskommission teilzunehmen. Er half mir ebenfalls dabei mein Verständnis der Alkalinität und der biogeochemischen Prozesse im Wattenmeer zu entwickeln. Ich bedanke mich außerdem bei Prof. Dr. Helmuth Thomas, der durch seine Vorarbeit die thematische Grundlage meines Projektes schuf, und auch trotz der großen räumlichen Distanz stets ein offenes Ohr für mich hatte.

Ich bedanke mich auch herzlich bei Dr. Ina Lorkowski, die mir insbesondere in der ersten Phase meiner Arbeit half, mich in der Modellumgebung zurechtzufinden. Ebenfalls möchte ich mich bei Dr. Wilfried Kühn, Dr. Hermann Lenhart, Fabian Große und Dr. Andreas Moll für ihre freundliche Unterstützung und angeregte Diskussionen bedanken.

Ein wesentlicher Bestandteil meiner Arbeit konnte nur durch die Bereitstellung bis dato unveröffentlichter Messdaten und Modellergebnisse realisiert werden. Ich bedanke mich daher besonders für das entgegengebrachte Vertrauen und die Bereitschaft zur Zusammenarbeit bei Vera Winde und Olaf Dellwig, die mir Messdaten aus dem Wattenmeer zur Verfügung gestellt

haben, bei Thorben Amann für Messdaten aus der Elbe und bei Sebastian Grashorn für die simulierten Tidenprismen.

Zu guter Letzt bedanke ich mich bei Dr. Ulrich Callies und Dr. Justus van Beusekom, die mir auch in Zukunft ermöglichen im Bereich der Nordsee und des Wattenmeeres forschen zu können.

Eidesstattliche Versicherung

Ich erkläre hiermit an Eides statt, dass ich die vorliegende Arbeit selbständig angefertigt habe. Die aus fremden Quellen direkt oder indirekt übernommenen Gedanken wurden als solche kenntlich gemacht. Diese Arbeit wurde weder in gleicher noch in ähnlicher Form einer anderen Prüfungsbehörde vorgelegt.

Hamburg, den

Fabian Schwichtenberg